Pharmacological Studies on the Roles of M_1 Muscarinic Acetylcholine Receptors in the Cognitive Function of the Rodent Brain

January 2022

Takao MANDAI

Pharmacological Studies on the Roles of M_1 Muscarinic Acetylcholine Receptors in the Cognitive Function of the Rodent Brain

A Dissertation Submitted to
the Graduate School of Science and Technology,
University of Tsukuba
in Partial Fulfillment of Requirements
for the Degree of Doctor of Philosophy in Science

Doctoral Program in Biology
Degree Programs in Life and Earth Sciences

Takao MANDAI

Table of Contents

Abstract

The neurotransmitter acetylcholine (ACh) is involved in cognitive function. Cholinergic neurotransmission dysfunction has been implicated in cognitive decline in various disorders, such as Alzheimer's disease (AD) and dementia with Lewy bodies (DLB). On the other hand, acetylcholinesterase inhibitors (AChEIs), such as donepezil and rivastigmine, ameliorate cognitive impairment in patients with AD and DLB by increasing ACh levels in the synaptic cleft. In addition, xanomeline, a muscarinic ACh receptor agonist, robustly improved cognitive impairment in patients with AD and schizophrenia. Thus, muscarinic receptors are considered to play a key role in cognitive functions. However, because most muscarinic ACh receptor subtypes are expressed in the brain regions that are critical for cognitive functions, it is unclear which subtypes are important for these functions. Recently, it was reported that knockout of M_1 muscarinic ACh receptor (M_1R) in mice caused cognitive impairment, suggesting that M_1R is mainly involved in the regulation of cognitive functions. To gain further insight into the roles of M_1R in cognitive functions of the rodent brain, an investigation of the impact of selective M_1R activation on cognitive functions is important. In addition, the development of selective M_1R activators can be a new therapeutic agent for the treatment of cognitive deficits associated with cholinergic hypofunction. In the first chapter, I characterized the *in vitro* and *in vivo* profiles of two M_1R positive allosteric modulators (PAMs), T-495 and MK-7622, to confirm whether these compounds are suitable as a tool to investigate the impact of M_1R activation on cognitive functions. Both T-495 and MK-7622 were highly selective M_1R PAMs *in vitro*, and oral administration of T-495 and MK-7622 specifically activated M_1R in the rodent brains. In rats, T-495 ameliorated scopolamine-induced memory deficits at a 100-fold lower dose than that required for the induction of diarrhea. In contrast, MK-7622 showed memory improvement and induction of diarrhea at an equal

dose. Thus, T-495 was an ideal tool to investigate the impact of M_1R activation on cognitive functions. Using T-495, I evaluated the effects of M_1R activation on cognitive deficits in a more disease-relevant model. M_1R activation reversed memory deficits in the contextual fear conditioning test and Y-maze task in a mouse model of DLB and Parkinson's disease with dementia. In the second chapter, to investigate the brain regions activated by muscarinic receptors activators, I assessed c-Fos expression, which has been used widely as a marker of activated neural populations. Surprisingly, donepezil, which improved scopolamine-induced memory deficits, did not increase the number of c-Fos positive cells. On the other hand, xanomeline and TAK-071, a highly selective M_1R PAM, significantly increased the number of c-Fos-positive cells in the brain regions critical for cognitive functions, including cortical areas, hippocampal formation, the amygdala, and nucleus accumbens. In conclusion, the present study found that activation of M_1R enhanced cognitive functions through neural activation in rodents. These findings contribute to an understanding of the roles of M_1R in cognitive functions. In addition, these results demonstrate that highly selective M_1R PAMs can be a novel therapeutic agent for the treatment of cognitive impairment in neurodegenerative and neuropsychiatric diseases, such as AD, DLB, and schizophrenia.

Abbreviations

ACC	anterior cingulate cortex
ACh	acetylcholine
AChE	acetylcholinesterase
AChEI	acetylcholinesterase inhibitor
AD	Alzheimer's disease
ANOVA	analysis of variance
BLA	basolateral nucleus of the amygdala
BSA	bovine serum albumin
CaMKIIα	calcium/calmodulin-dependent protein kinase II α
CEA	central nucleus of the amygdala
CHO	Chinese hamster ovary
CFC	contextual fear conditioning
ChAT	choline acetyltransferase
CLA	claustrum
CPu	caudate putamen
CS	conditioned stimulus
DG	dentate gyrus
DLB	dementia with Lewy bodies
dTg	double transgenic
EC	entorhinal cortex
GAPDH	glyceraldehyde-3-phosphate dehydrogenase
GI	gastrointestinal
HBSS	Hanks' Balanced Salt Solution
ILC	infralimbic cortex

IP inflection point

IP1 inositol 1-phosphate

IP3 inositol 1,4,5-trisphosphate

ITI intertrial interval

LH lateral hypothalamic area

LS lateral septum

KO knockout

Kp brain-to-plasma concentration ratio

LC-MS/MS liquid chromatography–tandem mass spectrometry

LiCl lithium chloride

M_1R M_1 muscarinic acetylcholine receptor

MD mediodorsal thalamic nucleus

METH methamphetamine hydrochloride

MK-801 (5*S*,10*R*)-(+)-5-methyl-10,11-dihydroxy-5*H*-dibenzo[*a,d*]cyclohepten-5,10-imine hydrogen maleate

NAc nucleus accumbens

NDI novelty discrimination index

NMDAR *N*-methyl-D-aspartate receptor

[^{3}H]-NMS [^{3}H]-N-methyl scopolamine

NOR novel object recognition

OC orbital cortex

PAG periaqueductal gray

PAM positive allosteric modulator

PBS phosphate-buffered saline

PBS-TX	PBS containing 0.2% Triton X-100
PDD	Parkinson's disease with dementia
PFA	paraformaldehyde
PH	posterior hypothalamic area
PLC	prelimbic cortex
PPC	posterior parietal cortex
PSD-95	postsynaptic density-95
S1BF	primary somatosensory cortex barrel field
SD	Sprague-Dawley
SUB	subiculum
sTg	single transgenic
tTA	tetracycline-controlled transactivator
TC	temporal cortex
US	unconditioned stimulus
VPM	ventral posteromedial thalamic nucleus
WT	wild-type

General Introduction

Acetylcholine (ACh) is a neurotransmitter, and is implicated in the regulation of various biological functions in both central and peripheral tissues. In the brain, ACh is provided by interneurons and projection neurons and controls neuronal excitability, synaptic transmission, and synaptic plasticity [1]. A part of the projection neurons innervates the cortex and hippocampus critical for cognitive functions. Furthermore, accumulated evidence has indicated that cholinergic neurotransmission plays an important role in cognitive functions. Firstly, scopolamine, an antagonist of ACh receptors, causes cognitive impairment in healthy humans and animals [2]. Secondly, the activity of choline acetyltransferase (ChAT), which is responsible for the synthesis of ACh, is severely reduced in the cortex and hippocampus of patients with Alzheimer's disease (AD), dementia with Lewy bodies (DLB), and Parkinson's disease with dementia (PDD) [3-7]. Furthermore, the reduction of ChAT activity correlates well with the severity of dementia [8-10]. Lastly, acetylcholinesterase inhibitors (AChEIs), such as donepezil and rivastigmine, improve cognitive deficits in patients with AD, DLB, and PDD by increasing ACh levels in the synaptic cleft [11, 12]. Thus, cholinergic neurotransmission is involved in the regulation of cognitive functions and its enhancement would be a valid strategy to treat cognitive dysfunctions in neurodegenerative and neuropsychiatric diseases.

ACh exerts its effects through activation of two distinct types of receptors, ionotropic nicotinic ACh receptors and metabotropic muscarinic ACh receptors. The muscarinic ACh receptors can be further divided into five subtypes, M_1−M_5. It has been reported that antagonists of muscarinic ACh receptors induce cognitive impairment [2]. Conversely, xanomeline, an agonist of muscarinic ACh receptors, improved cognitive functions in patients with AD and schizophrenia [13, 14]. Thus, muscarinic ACh

receptors are considered to play a key role in cognitive functions. However, because most subtypes are expressed in brain regions critical for cognitive functions [15], it is elusive which subtypes are important for cognitive functions. Recently, it was reported that knockout (KO) of M_1 muscarinic acetylcholine receptor (M_1R) in mice caused cognitive impairment, suggesting that M_1R is mainly involved in the regulation of cognitive functions [16, 17]. To further clarify the involvement of M_1R in cognitive functions, findings when M_1R is selectively activated by small molecules are important.

Many academic groups and pharmaceutical companies have developed small molecules that can selectively activate M_1R *in vivo*. However, because these small molecules bound to the orthosteric ACh binding site, which is well conserved among all five subtypes of muscarinic receptors, selective activation of M_1R could not be achieved. Recently, it was reported that M_1R has allosteric sites, which are topographically distinct from the orthosteric ACh binding site and less conserved among five subtypes [18]. Thus, targeting the allosteric site is an attractive approach to achieve highly selective activation of M_1R. Currently, two types of small molecules that can bind to an allosteric site and activate M_1R have been reported: allosteric agonists and positive allosteric modulators (PAMs). Allosteric agonists can directly activate M_1R independently of the presence of ACh. On the other hand, PAMs can activate M_1R by potentiating the actions of ACh; thus, PAMs can exert their effects only in the presence of ACh. One advantage of PAMs is that they can maintain the spatial and temporal actions of ACh [19]. Therefore, M_1R PAMs can be a powerful tool to investigate the impact of physiological M_1R activation on cognitive functions.

The development of M_1R selective PAMs can offer not only an opportunity to investigate the biological roles of M_1R in cognitive functions but also serve as a novel

therapeutic approach for the treatment of cognitive dysfunction. As described above, xanomeline, an orthosteric agonist of muscarinic ACh receptors, reversed cognitive decline in patients with AD and schizophrenia [13, 14]. However, clinical development was discontinued due to severe peripheral cholinergic side effects, such as sweating and gastrointestinal (GI) dysfunction [13, 14]. Furthermore, although AChEIs, such as donepezil and rivastigmine, have been used for the treatment of cognitive impairment in AD and DLB, AChEIs also cause side effects, such as nausea and vomiting, leading to the discontinuation of treatment [20-22]. Since M_2R and M_3R are abundantly expressed in peripheral tissues [23], xanomeline- and AChEIs-induced cholinergic side effects have been considered to occur due to overactivation of M_2R and M_3R in peripheral tissues. Therefore, M_1R selective activation has been expected to improve cognitive impairment without peripheral cholinergic side effects. However, surprisingly, recent studies have shown that even highly selective M_1R activators retain the ability to produce cholinergic side effects such as diarrhea and vomiting in animals [24-26]. My research group previously found that a binding cooperativity factor between ACh and a PAM is positively correlated with ileum contraction and that a low cooperative M_1R PAM improves cognitive impairment without inducing diarrhea [24]. Thus, fine adjustment of cooperativity of an M_1R PAM is key to reducing the liability of GI side effects, leading to the identification of an ideal tool compound for non-clinical studies and a clinical candidate.

In this study, to understand the roles of M_1R in cognitive functions of the rodent brain and ultimately identify a clinical candidate for the treatment of cognitive impairment, I investigated the impact of M_1R activation on cognitive functions using highly selective M_1R PAMs. In the first chapter, I characterized *in vitro* and *in vivo*

profiles of novel highly selective M_1R PAMs to confirm whether these compounds were suitable for assessing cognitive functions in rodents. I next investigated the impact of M_1R selective activation on cognitive functions in rodents. In the second chapter, I investigated the impact of non-selective activation of muscarinic receptors on cognitive functions and then evaluated the effects of non-selective activation of muscarinic receptors and M_1R selective activation on neural activation.

Chapter I:

T-495, a novel low cooperative M_1 receptor positive allosteric modulator, improves memory deficits associated with cholinergic dysfunction and is characterized by low gastrointestinal side effect risk

Abstract

M_1 muscarinic acetylcholine receptor (M_1R) activation can be a new therapeutic approach for the treatment of cognitive deficits associated with cholinergic hypofunction. However, M_1R activation causes gastrointestinal (GI) side effects in animals. I previously found that an M_1R positive allosteric modulator (PAM) with lower cooperativity (α-value) has a limited impact on ileum contraction and can produce a wider margin between cognitive improvement and GI side effects. In fact, TAK-071, a novel M_1R PAM with low cooperativity (α-value of 199), improved scopolamine-induced cognitive deficits with a wider margin against GI side effects than a high cooperative M_1R PAM, T-662 (α-value of 1786), in rats. Here, I describe the pharmacological characteristics of a novel low cooperative M_1R PAM T-495 (α-value of 170), using the clinically tested higher cooperative M_1R PAM MK-7622 (α-value of 511) as a control. In rats, T-495 caused diarrhea at a 100-fold higher dose than that required for the improvement of scopolamine-induced memory deficits. Contrastingly, MK-7622 showed memory improvement and induction of diarrhea at an equal dose. Combination of T-495, but not of MK-7622, and donepezil at each sub-effective dose improved scopolamine-induced memory deficits. Additionally, in mice with reduced acetylcholine levels in the forebrain via overexpression of A53T α-synuclein (i.e., a mouse model of dementia with Lewy bodies and Parkinson's disease with dementia), T-495, like donepezil, reversed the memory deficits in the contextual fear conditioning test and Y-maze task. Thus, low cooperative M_1R PAMs are promising agents for the treatment of memory deficits associated with cholinergic dysfunction.

Introduction

The neurotransmitter acetylcholine (ACh) is involved in synaptic plasticity and cognitive function [27, 28]. Cholinergic neurotransmission dysfunction has been implicated in cognitive decline in various disorders, such as Alzheimer's disease (AD), dementia with Lewy bodies (DLB), and Parkinson's disease with dementia (PDD). The activity of choline acetyltransferase (ChAT), which is responsible for the synthesis of ACh, is severely reduced in the cortex and hippocampus of patients with AD, DLB, and PDD, although postsynaptic muscarinic ACh receptors are preserved [3-7]. Furthermore, the reduction of ChAT activity correlates well with the dementia severity [8-10]. Importantly, acetylcholinesterase inhibitors (AChEIs), such as donepezil and rivastigmine, have provided benefits to patients with AD, DLB, and PDD by increasing ACh levels in the synaptic cleft [11, 12]. However, AChEIs have only modest efficacy and cause side effects, such as nausea and vomiting, leading to discontinuation of treatment [20-22]. Thus, the development of novel therapies with higher efficacy and/or fewer side effects is needed for patients with AD, DLB, and PDD.

M_1 muscarinic acetylcholine receptor (M_1R) is highly expressed in the cerebral cortex and hippocampus, which are critical for cognitive function [15]. Moreover, M_1R deletion in mice led to cognitive impairment [16, 17]. Furthermore, M_1R activators reversed cognitive deficits in various animal models related to AD [29-32]. Importantly, xanomeline, an M_1R/M_4R agonist, produced robust improvement of the cognitive function in patients with AD, although the clinical development of this compound was discontinued due to severe cholinergic side effects, such as sweating and gastrointestinal (GI) dysfunction [13]. Xanomeline-induced cholinergic side effects occur likely due to its lack of selectivity and consequent activation of M_2R and M_3R in peripheral tissues.

Therefore, selective M_1R activation may provide a novel therapeutic strategy for cognitive impairment associated with cholinergic hypofunction.

However, surprisingly, recent studies have shown that even highly selective M_1R activators retain the ability to produce cholinergic side effects such as diarrhea and vomiting in animals [24-26]. Thus, identification of M_1R positive allosteric modulators (PAMs) with better side effect profiles is essential for clinical application. I previously found that cooperativity (α-value) is positively correlated with ileum contraction and that a low cooperative M_1R PAM improves cognitive impairment without inducing diarrhea [24]. These findings led to the hypothesis that fine adjustment of cooperativity of an M_1R PAM is key to reducing the liability of GI side effects. Based on this hypothesis, I discovered a selective low cooperative M_1R PAM, TAK-071 [33]. TAK-071 with a low α-value of 199 exhibited a wider margin between cognitive improvement and diarrhea induction in rats compared with T-662 as a reference M_1R PAM with a high α-value of 1786 [33]. Furthermore, combination of TAK-071, but not T-662, and an AChEI synergistically improved scopolamine-induced cognitive impairment without exacerbating diarrhea [33]. TAK-071 is currently undergoing in clinical trials (ClinicalTrials.gov, Identifier: NCT02769065).

Recently, MK-7622, a first-in-class high cooperative M_1R PAM [34, 35], has shown no effect on cognition as adjunctive therapy with AChEIs in patients with AD [36]. In the present study, to gain more insight into the differences between low and high cooperative M_1R PAMs, I characterized the pharmacological profile of the novel low cooperative M_1R PAM T-495 using MK-7622 as a control M_1R PAM with a higher cooperative value. T-495 exhibited a wider margin between memory improvement and induction of diarrhea than MK-7622 in rats. Combination of T-495, but not of MK-7622,

and donepezil at each sub-effective dose ameliorated scopolamine-induced memory impairment. In addition, in mice with reduced ACh levels in the forebrain due to A53T α-synuclein overexpression (i.e., a mouse model of DLB and PDD), T-495 reversed memory deficits. These results suggest that cooperativity of M_1R PAMs is an important parameter to obtain superior pharmacological profiles.

Materials and Methods

Animals

All procedures involving animals were reviewed and approved by the Institutional Animal Care and Use Committee of Takeda Pharmaceutical Company Limited. All animals were maintained under a 12-hour light/dark cycle, in a room with free access to food and water. Experiments were initiated after acclimation for at least 1 week.

Male ICR and C57BL/6J mice were supplied by CLEA Japan, Inc. (Tokyo, Japan), and Sprague-Dawley (SD) and Long-Evans rats were purchased from Charles River Laboratories Japan, Inc. (Yokohama, Japan) and Japan SLC, Inc. (Shizuoka, Japan), respectively. C57BL/6-*Chrm 1* ^{tm1Stl}/J wild-type (WT) and homozygous knockout (M_1R KO) mice were supplied by the Massachusetts Institute of Technology (Cambridge, MA).

In this study, I used previously generated and characterized mice with overexpressed A53T α-synuclein in the forebrain [37, 38]. To obtain the mice, mice expressing A53T human α-synuclein under the control of a tetO promoter on a B6C3F1 background (tetO-A53T α-synuclein mice) were purchased from The Jackson Laboratory (stock number 016976, Bar Harbor, ME) [37]. In addition, mice expressing tetracycline-controlled transactivator (tTA) under the control of the calcium/calmodulin-dependent protein kinase II α (CaMKIIα) promoter on a C57BL/6J background (CaMKIIα-tTA mice) were purchased from The Jackson Laboratory (stock number 007004) [39] and crossed to C3H/HeN mice (CLEA Japan, Inc.). By crossing tetO-A53T α-synuclein mice and CaMKIIα-tTA mice, non-transgenic, CaMKIIα-tTA single transgenic (CaMKIIα-tTA sTg), tetO-A53T α-synuclein single transgenic (A53T α-syn sTg), and CaMKIIα-tTA; tetO-A53T α-synuclein double transgenic (CaMKIIα-tTA/A53T α-syn dTg) mice were generated. To obtain the CaMKIIα-tTA sTg and CaMKIIα-tTA/A53T α-syn dTg

mice utilized in this study, CaMKIIα-tTA sTg mice were further crossed with A53T α-syn sTg mice. Male mice were used in all experiments. To shut off transgene expression during the embryonic and early postnatal period, pregnant and lactating mice were fed doxycycline-containing chow (200 ppm, Japan SLC, Inc.) from embryo transfer to the first 3 weeks after birth.

Chemical compounds

T-495 (Fig. 1A: 8-chloro-6-((6-chloropyridin-3-yl)methyl)-3-((1*S*,2*S*)-2-hydroxycyclopentyl)-7-methyl-2,3-dihydro-4*H*-1,3-benzoxazin-4-one) and MK-7622 (Fig. 1B: 3-((1*S*,2*S*)-2-hydroxycyclohexyl)-6-((6-methylpyridin-3-yl)methyl)benzo[*h*]quinazolin-4(3*H*)-one) were synthesized by Takeda Pharmaceutical Company Limited. T-495 was synthesized according to the procedure described in the patent (WO2016208775, example 24) [40]. Donepezil hydrochloride was synthesized by Megafine Pharma Limited (Maharashtra, India). Scopolamine hydrobromide and lithium chloride (LiCl) were purchased from Tocris Bioscience (Ellisville, MO) and Wako Pure Chemical Industries Limited (Osaka, Japan), respectively. For in vitro experiments, T-495 and MK-7622 were dissolved in dimethyl sulfoxide (final concentration: 0.3% for Ca^{2+} mobilization assay and [^{3}H]-pirenzepine binding assay and 0.1% for spontaneous ileum contraction assay). For in vivo experiments, T-495 and MK-7622 were suspended in 0.5% methylcellulose in distilled water and administered orally (p.o.). Donepezil hydrochloride was dissolved in distilled water and administered orally. Scopolamine hydrobromide and LiCl were dissolved in saline and injected subcutaneously (s.c.). All compounds were dosed in a volume of 10 mL/kg body weight in mice and 2 mL/kg body weight in rats.

Ca^{2+} mobilization assay in cells expressing M_1R–M_5R

Chinese hamster ovary (CHO)-K1 cells expressing M_1R–M_5R were plated on a 96-well black, clear bottom plate at 30000 cells/well and incubated at 37 °C in an atmosphere of 5% CO_2 for 1 day. On the day of the assay, cells were incubated with calcium dye buffer (Hanks' Balanced Salt Solution (HBSS) containing 20 mM HEPES, 0.1% fatty acid-free bovine serum albumin (BSA), 0.08% pluronic F127 (Dojindo Laboratories, Kumamoto, Japan), 2.5 μg/mL Fluo-4 (Dojindo Laboratories), and 1.25 mM probenecid (Dojindo Laboratories)) for 30 minutes at 37 °C in an atmosphere of 5% CO_2 and then incubated for 30 minutes at room temperature. To measure Ca^{2+} mobilization using CellLux (PerkinElmer, Waltham, MA), cells were stimulated with T-495 or MK-7622 (0.01–1000 nM for PAM activity; 0.3–10000 nM for agonist activity) in assay buffer (HBSS containing 20 mM HEPES and 0.1% fatty acid-free BSA) with or without an EC_{20} concentration of ACh. The inflection point (IP) and EC_{50} values were calculated using the following equation by GraphPad Prism 5 software (GraphPad Software Inc., La Jolla, CA):

$$Y=\text{Bottom}+\frac{(\text{Top-Bottom})}{1+10\text{^}((\text{Log IP or EC50-X})\times\text{HillSlope}))}$$

where X and Y are the log concentration of a compound and the percentage of Ca^{2+} response, respectively, and Top and Bottom are the upper and lower plateaus, respectively.

[^{3}H]-pirenzepine binding assay

Cell membranes from FreeStyle 293 cells transiently expressing human M_1R were incubated with T-495 or MK-7622 (0.1–30 μM), ACh (0.003–3000 μM), and 4 nM [^{3}H]-pirenzepine (PerkinElmer) in assay buffer (20 mM HEPES, 100 mM NaCl, 10 mM $MgCl_2$,

and 0.1% fatty acid free BSA) for 2 hours at room temperature. The binding was terminated by filtration through GF/C filter plates (PerkinElmer) using a cell-harvester (PerkinElmer) and five washed with 300 µL of 50 mM Tris-HCl. The GF/C plates were dried at 42 °C; then, 25 µL of microscint 0 (PerkinElmer) was added. Radioactivity was counted using Topcount (PerkinElmer). Non-specific binding was defined in the presence of 10 µM atropine. To calculate the cooperativity of a PAM, the [^{3}H]-pirenzepine binding assay data were fitted to the allosteric ternary complex model [41], using GraphPad Prism 5 software:

$$Y = \frac{\frac{[C]}{K_C} + \frac{\alpha_{BC}[B][C]}{K_B K_C}}{1 + \frac{[A]}{K_A} + \frac{[B]}{K_B} + \frac{[C]}{K_C} + \frac{\alpha_{AB}[A][B]}{K_A K_B} + \frac{\alpha_{BC}[B][C]}{K_B K_C}}$$

where Y is the fractional specific [^{3}H]-pirenzepine binding; [A], [B], and [C] are the concentrations of ACh, a PAM, and [^{3}H]-pirenzepine, respectively; K_A, K_B, and K_C are the equilibrium dissociation constants of ACh, a PAM, and [^{3}H]-pirenzepine, respectively; and α_{AB} and α_{BC} are the cooperativities between a PAM and ACh or [^{3}H]-pirenzepine, respectively.

[^{3}H]-N-methyl scopolamine ([^{3}H]-NMS) binding assay

Cell membranes from FreeStyle 293 cells transiently expressing human M_1R were incubated with T-495 (0.01–30 µM) and 0.2 nM [^{3}H]-NMS (PerkinElmer) in assay buffer as described above. After 2 hours at room temperature, the binding was terminated by filtration through GF/C filter plates using a cell-harvester and washed 5 times with 300 µl of 50 mM Tris-HCl. GF/C plates were dried at 42°C and then 25 µl of microscint 0 was added. Radioactivity was measured by Topcount.

In vivo inositol 1-phosphate (IP1) assay

Eight-week-old Long-Evans rats, 8- to 9-week-old C57BL/6J mice, and 22- or 29-week old M_1R KO mice and their WT littermates were used in this study. On the day of the experiment, animals were placed in individual cages and acclimated for more than 1 hour. A test compound or vehicle was administered 2 hours before the animals were sacrificed. In the combination study, donepezil was administered 30 minutes after the administration of a test compound. LiCl (10 mmol/kg, s.c.) was injected 1 hour before sacrifice. In the repeated administration study, a test compound was administered to mice once daily for 13 days; on day 14, animals were treated with a test compound and LiCl (10 mmol/kg, s.c.) and then sacrificed. Animals were killed by decapitation, and blood was collected into tubes containing ethylenediaminetetraacetic acid for pharmacokinetic analysis; brains were quickly dissected, frozen on dry ice, and stored at -80°C until analysis. Brain tissues were homogenized in 19 (for rat tissues) or 39 (for mouse tissue) volumes of homogenization buffer (10 mM HEPES pH 7.4, 50 mM LiCl, 150 mM NaCl, and 1% Triton X-100), and the homogenate was incubated on a rotator for 1 hour, followed by centrifugation. The supernatant was diluted with 39 (for rat tissues) or 19 (for mouse tissues) volumes of dilution buffer (10 mM HEPES pH 7.4, 50 mM LiCl, and 150 mM NaCl). IP1 and protein concentrations in the diluted supernatant were measured using IP-One HTRF assay kit (Cisbio Bioassays, Codolet, France) and BCA Protein Assay Kit (Thermo Fisher Scientific Inc, Rockford, IL), respectively, according to the manufacturers' instructions. IP1 production was expressed as the ratio of IP1 to protein concentrations.

ACh quantification

Mice were sacrificed by focused microwave irradiation (MMW-05, Muromachi Kikai Co., Ltd., Tokyo, Japan). The frontal cortex and hippocampus were dissected and stored at -80°C until analysis. Tissues were homogenized with 39 volumes of ice-cold methanol using a ShakeMaster Auto (BioMedical Science, Tokyo, Japan) at 1000 rpm for 2 minutes, followed by centrifugation at 20000 × *g* for 5 minutes at 4°C. The supernatant (100 μL) was mixed with 10 μL of internal standard solution (ACh-d_9, Toronto Research Chemical, Ontario, Canada) and 10 μL of distilled water. It was then centrifuged at 15000 rpm for 5 minutes. Forty microliters of the supernatant was mixed with 60 μL of mobile phase A; subsequently, a 2 μL aliquot was analyzed by a liquid chromatography–tandem mass spectrometry (LC-MS/MS) system consisting of a Prominence 20A LC System (Shimadzu Co., Kyoto, Japan) coupled to a 4000 QTRAP triple quadrupole-mass spectrometer (AB Sciex, Framingham, MA). The chromatographic separation was performed using a LUNA C18(2) column (2 mm × 100 mm, 5 μm particles, Phenomenex, Torrance, CA) at 25°C. The mobile phase was composed of (A) 5 mM heptafluorobutyric acid and 0.1% acetic acid in water and (B) 0.1% acetic acid in acetonitrile. The gradient was started and held at 1% (B) for 0.5 minutes, linearly increased to 100% (B) for over 4 minutes, and maintained at 100% (B) for 2 minutes, at a flow rate of 0.5 mL/minute.

The MS was operated in positive electrospray ionization mode with multiple reaction monitoring. The optimized source parameters for MS analysis were as follows: temperature, 400°C; curtain gas, 50 psi; collision gas, 10 psi; ion source gas 1, 50 psi; ion source gas 2, 50 psi; and ion spray voltage, 3000 V. The following transitions were monitored: *m*/*z* 146 → 87 for ACh and *m*/*z* 155 → 87 for ACh-d_9. The concentration of ACh was determined using a calibration curve constructed by plotting the peak area ratio

of ACh to ACh-d_9 versus the nominal concentration of the analyte.

Automated capillary-based western blot

Mice were sacrificed by decapitation, and their brains were quickly dissected, frozen on dry ice, and stored at -80°C until analysis. Tissues were homogenized and sonicated in 10 volumes of Cell Extraction Buffer (Thermo Fisher Scientific Inc.) supplemented with complete Mini Protease Inhibitor Cocktail (Sigma-Aldrich, St. Louis, MO). The homogenates were incubated for 10 minutes on ice and centrifuged at 15000 rpm for 15 minutes at 4°C. The supernatants were collected, and total protein concentrations were determined using BCA Protein Assay Kit (Thermo Fisher Scientific Inc.). The expression level of target proteins was determined by capillary western blot (Wes, ProteinSimple, San Jose, CA), according to the manufacturer's instructions. Briefly, the supernatants were diluted with 0.1× sample buffer to the appropriate concentration (800 μg/mL for the detection of drebrin, postsynaptic density-95 (PSD-95), M_1R, and synaptophysin; 400 μg/mL for the detection of synapsin I). Additionally, four volumes of the diluted supernatants were mixed with one volume of 5× fluorescent master mix and then incubated at 95°C for 5 minutes (except for the detection of M_1R) or at 37°C for 60 minutes (for the detection of M_1R). The following primary antibodies were used: mouse anti-drebrin (1:50 dilution, catalog no. D029-3, Medical & Biological Laboratories Co., Ltd., Nagoya, Japan), rabbit anti-PSD-95 (1:50 dilution, catalog no. ab18258, Abcam plc, Cambridge, UK), rabbit anti-M_1R (1:10 dilution, catalog no. mAChR-M1-Rb-Af340, Frontier Institute Co. Ltd, Hokkaido, Japan), rabbit anti-synaptophysin (1:25 dilution, catalog no. ab32127, Abcam plc), rabbit anti-synapsin I (1:50 dilution, catalog no. ab64581, Abcam plc), mouse anti-glyceraldehyde-3-phosphate dehydrogenase (GAPDH,

1:100 dilution, catalog no. MAB374, Merck Millipore, Burlington, MA), and rabbit anti-GAPDH (1:100 dilution, catalog no. 2118, Cell Signaling Technology, Inc., Danvers, MA). The prepared samples, antibody diluent 2, primary antibodies, anti-rabbit or anti-mouse secondary antibody, chemiluminescent substrate, and wash buffer were added to the appropriate wells of a prefilled microplate. Separation and detection were performed according to manufacturer's default settings. The peak area of the protein of interest was calculated using Compass software (ProteinSimple). The peak area of the target protein was normalized to that of GAPDH.

Behavioral testing

For all behavioral experiments, animals were acclimated to the experimental room for at least 1 hour before testing.

Novel object recognition (NOR) test

On Day 1, 7-week-old Long-Evans rats were individually placed into the test box fabricated from polyvinyl chloride (40 cm square with 50 cm high walls) without any objects for 10 minutes. On Day 2, a PAM and donepezil were administered 1 hour and 30 minutes prior to the acquisition trial, respectively; furthermore, scopolamine hydrobromide was injected 30 minutes prior to the acquisition trial. In the acquisition trial, each rat was placed in the test box containing two identical objects and allowed to explore them for 3 minutes. After an inter-trial-interval of 4 hours, each rat was again placed in the same test box containing one familiar and one novel objects and allowed to explore both for 3 minutes (retention trial). The behavior of each animal during the acquisition and retention trials was recorded on video, and the time spent exploring each object

(licking, sniffing, or touching the object with the forepaws) was scored manually. Results were presented as novelty discrimination index (NDI) calculated as follows: the exploration time for the novel object / the exploration time for both objects × 100.

Contextual fear conditioning (CFC) test

The CFC test was performed in a clear conditioning chamber (33 cm wide, 25 cm long, and 28 cm high; O'Hara & Co., Ltd., Tokyo, Japan) surrounded by a sound-attenuating box. The illumination in the chamber was maintained at 100 lux. Conditioned stimulus (CS) and unconditioned stimulus (US) were automatically delivered by a tone generator and a shock generator (O'Hara & Co., Ltd.), respectively. On Day 1 (habituation phase), vehicle was orally administered, and mice were placed in the conditioning chamber. They were allowed to freely explore for 120 seconds and then returned to their home cages. On Day 2 (conditioning phase), donepezil and T-495 were orally administered to mice 2 and 1 hour, respectively, prior to conditioning. Mice were placed in the chamber for 120 seconds before the onset of a tone (CS, 60 dB for 30 s). The last 2 seconds of the CS were paired with a foot shock (US, 0.25 mA), and mice were removed and returned to their home cages 180 seconds after the US. On Day 3 (retention phase), donepezil and T-495 were orally administered 2 and 1 hour, respectively, prior to the retention test. Mice were again placed in the same chamber for 180 seconds. Freezing behavior was analyzed using ImageJ FZ4 (O'Hara & Co., Ltd.) during the conditioning and retention phases.

Y-maze task

The Y-maze was fabricated from gray plastic and consisted of three arms (40 cm long, 12 cm high, 3 cm wide at the bottom, and 10 cm wide at the top) with an angle of 120°.

Visual cues were placed outside each arm, and the apparatus was illuminated at 10 lux. Two and one hour after oral administration of donepezil and T-495, respectively, each mouse was placed at the end of one arm and allowed to freely explore the maze for 8 minutes. An arm entry was defined as all four paws of the mouse being in the arm, and the sequence of arm entries was monitored with a video camera and counted manually. An alternation was defined as successive entries into the three arms on overlapping triplet sets [42]. The percentage of alternation was calculated as the ratio of actual to possible alternations (total number of arm entries minus 2) multiplied by 100.

Assessment of cholinergic side effects

Seven- or eight-week-old SD rats were individually placed into observation cages. After an acclimation period of at least 1 hour, a test compound was administered to the rats. In the combination study, donepezil was administered 30 minutes after the administration of a test compound. Cholinergic side effects, including diarrhea, lacrimation, salivation, miosis, and fasciculation, were assessed blindly, as described previously [33], and convulsion was scored using a modified Racine scale [43], as follows: stage 0, normal; stage 1, immobility; stage 2, forelimb and/or tail extension and rigid posture; stage 3, repetitive movements, head nodding, and gnawing; stage 4, rearing and falling; stage 5, continuous rearing and falling; stage 6, severe tonic-clonic seizure with loss of postural control; and stage 7, death in the first 2 hours. The observations were carried out at 15 and 30 minutes and 1, 2, 4, 6, and 8 hours after the administration of T-495 for the study of T-495 alone, at 30 minutes and 1, 2, 4, and 6 hours after the administration of MK-7622 for the study of MK-7622 alone, and at 10 and 30 minutes and 1, 2, 4, and 6 hours after the administration of donepezil for the combination study.

Spontaneous ileum contraction

ICR mice were fasted overnight and sacrificed by decapitation, and the ileum was removed and the luminal contents were gently flushed out with ice-cold modified Krebs buffer (NaCl, 120.7 mM; KCl, 5.9 mM; $NaHCO_3$, 15.5 mM; $MgCl_2$, 1.2 mM; NaH_2PO_4, 1.2 mM; $CaCl_2$, 2.5 mM; glucose, 11.5 mM). The ileum segment (approximately 5 mm in length) was suspended in a 10-mL organ bath filled with oxygenated (95% O_2 and 5% CO_2) modified Krebs buffer at 37°C. One end of the ileum segment was tied to a hook and the other end was secured with a silk thread to an isometric force transducer (MLT050/A, ADInstruments, New South Wales, Australia) connected to a data acquisition system (PowerLab 8/30 ML870 and Octal Bridge Amp ML228, ADInstruments). The ileum segment was subjected to an initial tension of 0.3 to 0.4 g and was allowed to equilibrate for at least 30 minutes. After the equilibration period, spontaneous contractions were measured for 3 minutes (pretreatment) and then increasing concentrations of a test compound (0.01, 0.1, and 1 μM) were cumulatively applied at 3-minute intervals. LabChart software (ADInstruments) was used to analyze the spontaneous contractions. The mean amplitude of spontaneous contractions at each concentration was normalized to that observed at pretreatment.

Statistical analysis

Statistical analysis was performed using EXSUS (CAC EXICARE Corporation, Tokyo, Japan). The statistically significant differences between two groups were determined by Student's t-test (for homogenous data) or Aspin-Welch test (for non-homogenous data), with significance set at $P \leq 0.05$. For dose-response studies, statistical comparison

between vehicle- and drug-treated groups was made by two-tailed Williams' test (for homogenous data) or Shirley-Williams' test (for non-homogenous data), with $P \leq 0.05$ considered a significant difference. Dunnett's test (for homogenous data) or Steel's test (for non-homogenous data) was used to compare multiple independent groups, with significance set at $P \leq 0.05$.

Results

T-495 and MK-7622 were potent and selective M_1R PAMs with different cooperativity.

I first evaluated the PAM activities and selectivity of T-495 (Fig. 1A) and MK-7622 (Fig. 1B) by measuring Ca^{2+} influx in the presence of an EC_{20} concentration of ACh in CHO-K1 cells expressing human M_1R–M_5R. T-495 and MK-7622 potentiated Ca^{2+} influx elicited by an EC_{20} concentration of ACh with IP values of 2.3 and 1.3 nM, respectively, in CHO-K1 cells expressing human M_1R, whereas their IP values for human M_2R–M_5R were > 1,000 nM (Table 1 and Fig. 1C and D). Next, I measured Ca^{2+} influx in the absence of ACh to evaluate their agonist activities. T-495 and MK-7622 showed weak agonist activities with EC_{50} values of 649 and 407 nM, respectively, in CHO-K1 cells expressing human M_1R (Table 1 and Fig. 1E and F).

The selectivity of T-495 at 10 μM against a panel of 106 targets, including receptors, enzymes, ion channels, and transporters, was characterized (Eurofins Panlabs Taiwan Ltd., Taipei, Taiwan). No significant inhibition or stimulation (≥ 50%) was observed, except for two targets: 76% inhibition at the imidazoline I_2 receptor and 58% inhibition at the dopamine transporter (Table 2). Furthermore, MK-7622 was highly selective and exhibited inhibitory activities only against 5-lipoxygenase and phosphodiesterase 4 in a selectivity panel [34].

To evaluate the effects of T-495 on the interaction between scopolamine and M_1R, I conducted a [^{3}H]-NMS binding assay. T-495 concentrations below 30 μM did not inhibit [^{3}H]-NMS binding to M_1R (Fig. 2).

I previously identified cooperativity (α-value) as a key parameter to reduce the risk of M_1R PAMs-induced GI side effects [24]; thus, I assessed cooperativity of T-495

and MK-7622 using a [^{3}H]-pirenzepine binding assay. T-495 and MK-7622 caused a leftward shift in the displacement curve of [^{3}H]-pirenzepine binding by ACh (Fig. 1G and H). The data of T-495 and MK-7622 were fitted to the allosteric ternary complex model, yielding α-values of 170 and 511, respectively (Table 1). These results indicate that T-495 is a potent and selective M_1R PAM with low cooperativity, whereas MK-7622, consistent with previous reports [34, 35], is a potent and selective M_1R PAM with high cooperativity.

T-495 and MK-7622 increased IP1 production mediated by M_1R activation in the rodent brain.

M_1R activation leads to phospholipase C activation and subsequent inositol 1,4,5-trisphosphate (IP3) generation. IP1, a downstream metabolite of IP3, is accumulated in the presence of LiCl, which inhibits IP1 degradation by suppressing inositol monophosphatase [44]. Therefore, IP1 levels can be used to measure the activation levels of Gq protein-coupled receptors, including M_1R [45]. To evaluate the in vivo activation of M_1R by T-495 and MK-7622, IP1 levels after coadministration of T-495 or MK-7622 and LiCl were measured. In the rat hippocampus, T-495 (10 and 30 mg/kg) and MK-7622 (10 mg/kg) significantly increased IP1 production (Fig. 3A and B). Under these experimental conditions, the brain-to-plasma concentration ratios (Kp) of T-495 and MK-7622 were 1.0–1.4 and 0.1–0.2, respectively (Table 3 and 4). In the mouse hippocampus, T-495 and MK-7622 significantly increased IP1 production with a minimum effective dose of 10 mg/kg (Fig. 3C and D).

To investigate whether the increases in IP1 production by T-495 and MK-7622 are mediated by M_1R activation, I examined IP1 production in the mouse forebrain (hippocampus, prefrontal cortex, and striatum) and brainstem, where the expression

levels of M_1R are high and low, respectively [15]. T-495 at 10 mg/kg significantly increased IP1 production in the hippocampus, prefrontal cortex, and striatum, but not in the brainstem, of wild-type mice (Fig. 3E). MK-7622 at 20 mg/kg increased and slightly reduced the IP1 production in the forebrain and brainstem of wild-type mice (Fig. 3F), respectively. In addition, T-495 and MK-7622 did not cause a significant increase in IP1 production in the hippocampus, prefrontal cortex, and striatum of M_1R KO mice (Fig. 3E and F). Concentrations of T-495 and MK-7622 in the plasma and brain of M_1R KO mice were comparable to those observed in wild-type mice (Table 5). These results indicate that T-495 and MK-7622 stimulate IP1 production through M_1R activation. In contrast, MK-7622 led to a slight reduction in IP1 production in the brainstem of both wild-type and M_1R KO mice, indicating that MK-7622 may modulate molecular targets other than M_1R.

M_1R activation and signal transduction are strictly controlled by multiple molecular mechanisms such as the receptor internalization and downregulation [46]. Persistent M_1R activation by orthosteric agonists causes receptor internalization and downregulation in vitro [47, 48]. To examine the effect of repeated administration of T-495 or MK-7622 on M_1R signal transduction, I evaluated IP1 levels in the mouse hippocampus after 13 days of pretreatment with T-495 at 10 mg/kg or MK-7622 at 10 mg/kg. The magnitudes of the increase after pretreatment with T-495 or MK-7622 were comparable to those after single administration of T-495 or MK-7622 (Fig. 3G and H). Basal IP1 levels and concentrations of T-495 and MK-7622 in the plasma and brain after 13 days of pretreatment were comparable with those after single administration (Table 6–9). These results suggest that repeated administration of T-495 and MK-7622 does not cause M_1R desensitization.

T-495 and MK-7622 improved scopolamine-induced memory impairment in a rat NOR test.

Scopolamine has been used to induce cholinergic dysfunction-related cognitive deficits in healthy humans and animals [2]. To evaluate the effects of T-495 and MK-7622 on object recognition memory, rats pretreated with scopolamine were used. In the retention trial, scopolamine significantly reduced NDI; T-495 (1 and 3 mg/kg) and MK-7622 (3 and 10 mg/kg) significantly reversed the scopolamine-induced NDI reduction (Fig. 4A and B). These data suggest that T-495 and MK-7622 have the potential to ameliorate cholinergic dysfunction-related memory deficits.

T-495 exhibited a wider margin than MK-7622 between memory improvement and diarrhea induction in rats.

I previously found that an M_1R PAM with lower cooperativity had a lower impact on ileum contraction and a wider margin between memory improvement and diarrhea induction in rodents [24]. To confirm these findings, the effects of T-495 and MK-7622 on ileum contraction were evaluated. T-495 increased spontaneous ileum contraction at 1 μM, whereas MK-7622 increased that even at the lowest concentration tested (0.01 μM; Fig. 5A), suggesting that T-495 has a lower impact on ileum motility.

Next, I characterized the cholinergic side effects induced by T-495 (1–100 mg/kg) and MK-7622 (3–30 mg/kg) in rats. T-495 did not elicit any cholinergic side effects at doses up to 30 mg/kg (Table 10). However, T-495 at 100 mg/kg significantly increased diarrhea score (Fig. 5B) and incidence of diarrhea (Table 10) and caused convulsion and salivation in one of six rats (Table 10). MK-7622 at 3 mg/kg tended to increase diarrhea

score ($P = 0.07$; Fig. 5C) and incidence of diarrhea (Table 11). Thus, T-495 and MK-7622 had 100-fold and 1-fold dose differences, respectively, between memory improvement and induction of cholinergic side effects, including diarrhea, in rats.

Combining sub-effective doses of T-495, but not of MK-7622, with donepezil improved scopolamine-induced memory impairment without exacerbating cholinergic side effects in rats.

Combination of an M_1R PAM with an AChEI is expected to produce synergistic effects. In fact, additive or synergistic effects of an M_1R PAM and an AChEI have been shown in behavioral paradigms and on M_1R downstream signaling [31, 33, 49]. Importantly, contrary to the low cooperative M_1R PAM TAK-071, the combination of T-662, an M_1R PAM with high cooperativity, and donepezil did not produce any additive or synergistic effects against scopolamine-induced cognitive deficits [33].

I evaluated the effects of combination of T-495 or MK-7622 and donepezil on scopolamine-induced memory deficits in a rat NOR test. To avoid a ceiling effect, sub-effective doses of T-495 (0.3 mg/kg; Fig. 4A), MK-7622 (1 mg/kg; Fig. 4B), and donepezil (0.1 mg/kg [33]) were used in this study. In the retention trial, similar to TAK-071 [33], the combination of T-495 and donepezil significantly improved scopolamine-induced reduction in NDI (Fig. 6A). When T-495 (0.3 mg/kg) was combined with donepezil (0.1 mg/kg), no cholinergic side effects were observed (Table 12). In agreement with previous observations using T-662, the combination of MK-7622 and donepezil could not reverse scopolamine-induced reduction in NDI (Fig. 6B).

These results suggest that combination of T-495, but not MK-7622, and an AChEI have a potential to synergistically improve cholinergic dysfunction-related memory

deficits.

Validation of the CaMKIIα-tTA/A53T α-syn dTg mice as an animal model of DLB and PDD

Finally, to evaluate the efficacy of T-495 on memory deficits in a disease-relevant model, I used a recently reported mouse model of DLB and PDD (CaMKIIα-tTA/A53T α-syn dTg mice). Critical pathogenesis of DLB and PDD involves α-synuclein accumulation. In the CaMKIIα-tTA/A53T α-syn dTg mice, A53T human α-synuclein, which is an aggregation-prone mutant, was specifically expressed in the forebrain, the region involved in cognitive functions, using the Tet-off system and the CaMKIIα promoter [37]. From 4 to 20 months of age, abnormal α-synuclein accumulation was detected, which became progressively more profound [38]. At 8 and 12 months of age, the mice exhibited cognitive deficits in the CFC test [38]. Thus, in the current study, 12-month-old mice were used, and age-matched CaMKIIα-tTA sTg mice were utilized as a control for CaMKIIα-tTA/A53T α-syn dTg mice.

ACh content and synaptic protein levels in the frontal cortex and hippocampus of the CaMKIIα-tTA/A53T α-syn dTg mice

To investigate the impact of abnormal α-synuclein accumulation on the cholinergic system, I evaluated ACh levels in the frontal cortex and hippocampus, where marked reduction in ChAT activity has been observed in patients with DLB and PDD [4, 5, 7]. ACh levels in the frontal cortex, but not in the hippocampus, of the CaMKIIα-tTA/A53T α-syn dTg mice were significantly lower than those of the CaMKIIα-tTA sTg mice (Fig. 7A).

In the brains of patients with DLB and PDD, most α-synuclein aggregates are located in the presynaptic terminals and cause synaptic dysfunction via significant reduction of pre- and postsynaptic proteins, such as synaptophysin and drebrin [50-52]. To quantitatively evaluate the effects of abnormal α-synuclein accumulation on synaptic proteins in the frontal cortex and hippocampus, I assessed synaptophysin and synapsin I levels as presynaptic markers and drebrin and PSD-95 levels as postsynaptic markers using capillary western blot. In the frontal cortex of the CaMKIIα-tTA/A53T α-syn dTg mice, synaptophysin and synapsin I levels were significantly reduced by 24% and 35%, respectively, whereas no significant drebrin and PSD-95 reduction was observed compared to the CaMKIIα-tTA sTg mice (Fig. 7B). In the hippocampus of the CaMKIIα-tTA/A53T α-syn dTg mice, 42% and 43% reduction of synaptophysin and synapsin I, respectively, and 26% and 15% reduction of drebrin and PSD-95, respectively, were observed (Fig. 7C). I also evaluated the expression levels of M_1R in the CaMKIIα-tTA/A53T α-syn dTg mice. Although the M_1R levels were unaltered in the frontal cortex (Fig. 7B), a 20% reduction in M_1R levels was observed in the hippocampus of the CaMKIIα-tTA/A53T α-syn dTg mice (Fig. 7C).

Memory deficits in the CaMKIIα-tTA/A53T α-syn dTg mice and efficacy of donepezil

Next, I assessed the memory function of the CaMKIIα-tTA/A53T α-syn dTg mice. First, the CFC test was used to measure associative learning in the CaMKIIα-tTA/A53T α-syn dTg mice. No significant difference in the level of freezing behavior during the conditioning phase between the CaMKIIα-tTA sTg and CaMKIIα-tTA/A53T α-syn dTg mice was observed (Fig. 8A). In contrast, consistent with a previous report [38], the CaMKIIα-tTA/A53T α-syn dTg mice exhibited a significantly reduced level of freezing

behavior during the retention phase compared to the CaMKIIα-tTA sTg mice (Fig. 8A); these results suggest that associative learning is impaired in the CaMKIIα-tTA/A53T α-syn dTg mice. Cognitive deficits observed in patients with DLB and PDD include impairment of working memory [53-55]. Thus, I also evaluated spatial working memory in CaMKIIα-tTA/A53T α-syn dTg mice using the Y-maze task. The percentage of alternations in the CaMKIIα-tTA/A53T α-syn dTg mice was significantly reduced compared to that in the CaMKIIα-tTA sTg mice (Fig. 8B), suggesting that working memory was impaired in the CaMKIIα-tTA/A53T α-syn dTg mice.

I then evaluated whether donepezil, which improves cognitive decline in patients with DLB and PDD [56, 57], can reverse the memory deficits observed in the CaMKIIα-tTA/A53T α-syn dTg mice. Donepezil at 1 mg/kg improves memory deficits in a mouse model of AD [58, 59]; thus, a dose of 1 mg/kg was used in this study. In the CFC test, donepezil treatment (1 mg/kg) before both the conditioning and retention phases significantly reversed the reduced level of freezing behavior during the retention phase in the CaMKIIα-tTA/A53T α-syn dTg mice; however, donepezil did not affect the level of freezing behavior during the conditioning phase (Fig. 8A). Furthermore, in the Y-maze task, donepezil treatment (1 mg/kg) tended to reverse the reduced percentage of alternations in the CaMKIIα-tTA/A53T α-syn dTg mice ($P = 0.12$; Fig. 8B).

Together with the results of a previous study [38], our data imply that CaMKIIα-tTA/A53T α-syn dTg mice, the recently reported mouse model of DLB and PDD, replicate multiple key features of DLB and PDD. Therefore, CaMKIIα-tTA/A53T α-syn dTg mice are a good animal model for DLB and PDD.

T-495 reversed the memory impairment observed in the CaMKIIα-tTA/A53T α-syn

dTg mice

I evaluated the effects of T-495 on memory deficits in CaMKIIα-tTA/A53T α-syn dTg mice. T-495 at 1 and 3 mg/kg significantly improved scopolamine-induced memory impairment in a rat NOR test (Fig. 4). Furthermore, hippocampal IP1 production was significantly increased at the same dose in rats and mice (Fig. 3A and B). Thus, I decided to use a dose of 3 mg/kg.

In this cohort, the level of freezing behavior during the retention phase in the CFC test and the percentage of alternations in the Y-maze task were significantly reduced in the CaMKIIα-tTA/A53T α-syn dTg mice compared to the CaMKIIα-tTA sTg mice (Fig. 9A and B). In the CFC test, T-495 treatment (3 mg/kg) before both conditioning and retention phases significantly reversed the reduced level of freezing behavior during the retention phase in the CaMKIIα-tTA/A53T α-syn dTg mice; however, T-495 did not change the level of freezing behavior during the conditioning phase (Fig. 9A). Moreover, in the Y-maze task, T-495 (3 mg/kg) significantly reversed the reduced percentage of alternations in the CaMKIIα-tTA/A53T α-syn dTg mice (Fig. 9B).

Discussion

M_1R activation may be a promising therapeutic approach to improve cognitive impairment associated with cholinergic dysfunction [60]. However, highly selective M_1R PAMs have been reported to induce cholinergic side effects, particularly GI side effects such as diarrhea, in animals [24-26]. In fact, in a recently published phase 2 clinical trial of MK-7622 in patients with AD, diarrhea was the most common adverse effect associated with MK-7622 treatment at the estimated effective dose, affecting 15% of the patients [36]. Therefore, the identification of M_1R PAMs with minimal GI side effects is needed to improve the clinical utility of this drug class.

I have previously determined that fine-tuning of cooperativity is essential to identify M_1R PAMs with a wider safety margin [24]. Using this approach, I identified the low cooperative M_1R PAM TAK-071 (α-value of 199) [33]. In rats, TAK-071 exhibited a 33-fold difference between doses improving cognitive function and doses inducing diarrhea, whereas the high cooperative M_1R PAM T-662 (α-value of 1786) showed no dose difference between the two effects [33]. Furthermore, interestingly, combination of sub-effective doses of TAK-071, but not T-662, and an AChEI currently used for the treatment of AD synergistically improved scopolamine-induced cognitive deficits detected in the NOR test [33]. Here, using the novel low cooperative M_1R PAM T-495 (α-value of 170) and the clinically tested high cooperative M_1R PAM MK-7622 (α-value of 511) (Fig. 1), I further investigated the pharmacological differences between low and high cooperative M_1R PAMs. Consistent with previous observations using TAK-071 and T-662, T-495 elicited cholinergic side effects, including diarrhea, at a 100-fold higher dose than that required for the improvement of scopolamine-induced memory deficits in the NOR test (Table 10 and Fig. 4A and 5B), whereas MK-7622 showed memory

improvement and diarrhea induction at an equal dose (Table 11 and Fig. 4B and 5C). Furthermore, potential efficacy was observed with the combination of T-495, but not of MK-7622, and donepezil when a sub-effective dose of each drug was used (Fig. 6A and B); however, combination studies using multiple doses of each drug could not be conducted owing to a potential "ceiling effect" in memory enhancement. Notably, MK-7622 did not improve cognition as adjunctive therapy with AChEIs in patients with AD [36]. ACh release is spatiotemporally controlled in tissues, and an appropriate coordinated cholinergic system activation in the brain would be required for cognitive performance [61, 62]. Unlike M_1R agonists, M_1R PAMs are expected to boost the action of ACh and maintain its spatiotemporal characteristics. However, high cooperative M_1R PAMs may disrupt the spatiotemporally controlled manner of M_1R activation via a robust increase of the binding affinity of ACh to M_1R, especially when the ACh levels are high by coadministration of an AChEI.

Recent studies have implicated the association of M_1R PAM agonism with cholinergic side effects [63, 64]. Both T-495 and MK-7622 showed agonist activity in CHO-K1 cells expressing human M_1R. The margins between PAM and agonist activities of T-495 (282-fold) and MK-7622 (313-fold) were comparable (Fig. 1C–F). Therefore, cooperativity, but not agonist activity, of M_1R PAMs may contribute to the improved and superior pharmacological profile. However, to more precisely quantify agonist activity, physiological receptors in brain slices and primary cells, rather than cell lines, should be used, because agonist activity is greatly affected by various factors including the degree of receptor reserve [65]. Unfortunately, only low-throughout electrophysiological assays using brain slices are available for characterization of the agonist activity of M_1R PAMs. Further efforts to establish higher throughput assays for the discovery of a variety of

potent M_1R PAMs with a wider margin between PAM activity and agonist activity would be needed.

To evaluate the procognitive efficacy of T-495 and MK-7622, scopolamine-induced memory deficits in a NOR test were used. Both compounds have a potential to improve scopolamine-induced memory deficits by directly inhibiting scopolamine binding to M_1R. I previously showed that other low and high cooperative M_1R PAMs, TAK-071 and T-662, did not inhibit the binding of scopolamine to M_1R at concentrations required for their procognitive efficacy [33]. In this study, I observed that T-495 did not inhibit [^{3}H]-NMS binding to M_1R at up to 100-fold higher concentration than that required for the procognitive efficacy (Table 3 and Fig. 2). Thus, the inhibition of binding between scopolamine and M_1R by M_1R PAMs may not contribute to their memory enhancing effects in the rat NOR test.

To model α-synuclein-associated diseases, including DLB and PDD, multiple transgenic animals overexpressing wild-type or mutant α-synuclein under the control of various promoters have been generated [66]. However, in these mice, α-synuclein is broadly expressed in central nervous system neurons, including regions not affected in DLB and PDD. Recently, an interesting novel transgenic mouse associated with DLB and PDD (CaMKIIα-tTA/A53T α-syn dTg mice) has been generated using the Tet-off system and the CaMKIIα promoter [37, 38]. CaMKIIα-tTA/A53T α-syn dTg mice express A53T human α-synuclein in the neurons of the forebrain, the region involved in cognitive function, and exhibit cognitive deficits accompanied by α-synuclein pathology [37, 38]. To determine whether the CaMKIIα-tTA/A53T α-syn dTg mice are a valid animal model of DLB and PDD, I further characterized their behavioral, molecular, and pharmacological phenotypes. CaMKIIα-tTA/A53T α-syn dTg mice replicate the

following key features of DLB and PDD: 1) α-synuclein pathology [38]; 2) cholinergic deficit in the cerebral cortex (Fig. 7A); 3) reduction in pre- and postsynaptic proteins (Fig. 7B and C); 4) cerebral and hippocampal atrophy [38]; 5) memory deficits (Fig. 8) [38]; and 6) amelioration of memory deficits by donepezil (Fig. 8). Thus, the CaMKIIα-tTA/A53T α-syn dTg mice are a good animal model for DLB and PDD and may assist in elucidating the molecular mechanisms underlying DLB and PDD and testing new therapeutic agents.

Cognitive deficits observed in the CaMKIIα-tTA/A53T α-syn dTg mice were correlated with α-synuclein pathology in the hippocampus [38]; however, the underlying molecular mechanism remains unknown. In the hippocampus of the CaMKIIα-tTA/A53T α-syn dTg mice, the expression levels of M_1R and other postsynaptic proteins, such as drebrin and PSD-95, were reduced (Fig. 7C). In M_1R KO mice, cognitive deficits were observed [16, 17]. Thus, reduced M_1R signaling in the hippocampus may contribute to memory deficits in the CaMKIIα-tTA/A53T α-syn dTg mice. T-495 treatment may improve memory deficits via restoration of the reduced M_1R signaling in the CaMKIIα-tTA/A53T α-syn dTg mice (Fig. 9), but further studies are required to confirm this.

In summary, together with our previous findings [33], the present data demonstrate that low and high cooperative M_1R PAMs exhibit different pharmacological profiles with regards to a safety margin between memory improvement and cholinergic side effects and combination efficacy with AChEIs. Therefore, fine-tuning of M_1R PAM cooperativity is key to achieving superior pharmacological profiles. Low cooperative M_1R PAMs, such as TAK-071 and T-495, may represent a novel therapeutic agent for memory deficits associated with cholinergic hypofunction.

Tables and Figures

Table 1. Summary of PAM activity, agonist activity, and cooperativity of T-495 and MK-7622

	PAM activity		Agonist activity		Cooperativity	
	pIP	IP (nM)	pEC_{50}	EC_{50} (nM)	Log α	α
T-495	8.64 (8.34–8.93)	2.3	6.19 (6.12–6.25)	649	2.23 (2.07–2.40)	170
MK-7622	8.88 (8.72–9.05)	1.3	6.39 (6.30–6.49)	407	2.71 (2.48–2.94)	511

95% confidence intervals are shown in parentheses.

Table 2. in vitro selectivity of T-495 at 10 μM

Enzyme, receptor, or ion channel	% inhibition at 10 μM	Enzyme, receptor, or ion channel	% inhibition at 10 μM	Enzyme, receptor, or ion channel	% inhibition at 10 μM
ATPase, Ca^{2+}, Skeletal Muscle	0	Adrenergic β_2	15	Histamine H_1	2
ATPase, Na^+/K^+, Heart	4	Adrenergic β_3	7	Histamine H_2	22
Carbonic anhydrase II	-9	Androgen (testosterone)	3	Imidazoline I_2, central	76
Catechol-O-Methyl Transferase (COMT)	2	Angiotensin AT_1	23	Insulin	-10
Choline esterase, acetyl, ACES	-2	Angiotensin AT_2	0	IP (PGI2)	16
Cyclooxygenase-1 (COX-1)	-14	Bradykinin B_1	2	Melatonin MT_1	29
Cyclooxygenase-2 (COX-2)	31	Bradykinin B_2	-4	Muscarinic M_1	15
HMG-CoA reductase	-10	Calcium channel L-type, benzothiazepine	-5	Muscarinic M_2	8
Lipoxygenase (5-LO)	15	Calcium channel L-type, dihydropyridine	27	Muscarinic M_3	20
Monoamine oxidase A (MAO-A)	36	Calcium channel L-type, phenylalkylamine	19	Nicotinic acetylcholine	-4
Monoamine oxidase B (MAO-B)	6	Calcium channel N-type	0	Opiate δ_1 (OP1, DOP)	4
Nitric oxide synthase, inducible (iNOS)	0	Cannabinoid CB_1	14	Opiate κ (OP2, KOP)	14
Nitric oxide synthase, neuronal (nNOS)	5	Cannabinoid CB_2	12	Opiate μ (OP3, MOP)	12
Peptidase, factor Xa	-2	Cholecystokinin CCK_1 (CCK_A)	2	Potassium channel (K_{ATP})	2
Matrix metalloproteinase-1 (MMP-1)	5	Cholecystokinin CCK_2 (CCK_B)	10	Potassium channel (SK_{CA})	1
Matrix metalloproteinase-7 (MMP-7)	3	Dopamine D_1	-7	Progesterone PR-B	21
Matrix metalloproteinase-13 (MMP-13)	-26	Dopamine D_{2L}	4	Serotonin 5-HT_{1A}	8
Metalloproteinase, Neutral Endopeptidase	10	Dopamine D_{2S}	15	Serotonin 5-HT_{2A}	20
Phosphodiesterase PDE3	2	Dopamine D_3	-3	Serotonin 5-HT_{2B}	28
Phosphodiesterase PDE4	22	Dopamine $D_{4.2}$	3	Serotonin 5-HT_{2C}	10
Phosphodiesterase PDE4D2	2	Endothelin ET_A	-4	Serotonin 5-HT_3	-3
Phosphodiesterase PDE5	48	Estrogen Receptor (non-selective)	5	Serotonin 5-HT_4	22
Phosphodiesterase PDE6	6	$GABA_A$, chloride channel	45	Sigma, non-selective	25
Phosphodiesterase PDE10A2	5	$GABA_A$, flunitrazepam, central	12	Sodium channel, Site 2	1
Protein kinase C (PKC), non-selective	0	$GABA_A$, muscimol, central	-1	Tachykinin NK_1	-2
Protein kinase A (PKA)	-4	$GABA_B$, non-selective	4	Tachykinin NK_2	-20
Protein kinase, ROCK1	-22	$GABA_{B1A}$	5	Tachykinin NK_3	5
Protein tyrosine kinase, EGF receptor	9	$GABA_{B1B}$	6	Transporter, dopamine (DAT)	58
Steroid 5α-reductase	2	Glucocorticoid	25	Transporter, GABA	-7
Xanthine oxidase	7	Glutamate, AMPA	20	Transporter, norepinephrine (NET)	17
Adenosine A_1	15	Glutamate, kainate	13	Transporter, serotonin (SERT)	17
Adenosine A_{2A}	-4	Glutamate, NMDA	14	Transporter, vesicular monoamine (non-selective)	12
Adenosine A_{2B}	7	Glutamate, NMDA, glycine	15	Vasopressin V_{1A}	7
Adrenergic α_1, non-selective	11	Glutamate, NMDA, phencyclidine	3	Vasopressin V2	-7
Adrenergic α_2, non-selective	26	Glycine, strychnine-sensitive	9		
Adrenergic β_1	4	Growth hormone secretagogue (ghrelin)	8		

Table 3. Concentrations of T-495 in rat plasma and brain

Dose (mg/kg, p.o.)	3	10	30
Plasma (ng/mL)	49.6 ± 14.5	298.0 ± 75.2	1045.5 ± 357.5
Brain (ng/g)	66.2 ± 18.5	304.1 ± 82.8	1005.0 ± 329.5
Kp	1.4 ± 0.1	1.0 ± 0.1	1.0 ± 0.1

Data are presented as the mean ± SD (n = 6). Concentration of T-495 in the hippocampus was regarded as the concentrations in the brain.

Table 4. Concentrations of MK-7622 in rat plasma and brain

Dose (mg/kg, p.o.)	1	3	10
Plasma (ng/mL)	99.2 ± 27.4	217.9 ± 42.9	944.4 ± 246.3
Brain (ng/g)	14.5 ± 6.3	39.3 ± 5.6	220.4 ± 72.2
Kp	0.14 ± 0.04	0.19 ± 0.04	0.23 ± 0.02

Data are presented as the mean ± SD (n = 6). Concentration of MK-7622 in the hippocampus was regarded as the concentration in the brain.

Table 5. Concentrations of T-495 and MK-7622 in the plasma and brain of wild-type and M_1R KO mice

	T-495 (10 mg/kg, p.o.)		MK-7622 (20 mg/kg, p.o.)	
	Wild-type	M_1R KO	Wild-type	M_1R KO
Plasma (ng/mL)	1689.9 ± 280.4	1593.4 ± 265.7	2235.1 ± 376.5	2194.6 ± 311.8
Brain (ng/g)	1026.5 ± 145.2	856.0 ± 78.4	582.1 ± 132.9	456.1 ± 85.8
Kp	0.62 ± 0.10	0.55 ± 0.09	0.26 ± 0.06	0.21 ± 0.03

Data are presented as the mean ± SD (n = 10). Concentrations of T-495 and MK-7622 in the hippocampus were regarded as the concentration in the brain.

Table 6. Basal IP1 levels in the mouse hippocampus after repeated T-495 treatment for 13 days

Pretreatment	IP1 level (nmol/mg protein)
Vehicle	1.05 ± 0.04
T-495 (10 mg/kg, p.o.)	1.09 ± 0.03

Data are presented as the mean ± SEM (n = 10).

Table 7. Basal IP1 levels in the mouse hippocampus after repeated MK-7622 treatment for 13 days

Pretreatment	IP1 level (nmol/mg protein)
Vehicle	0.93 ± 0.03
MK-7622 (10 mg/kg, p.o.)	0.99 ± 0.05

Data are presented as the mean ± SEM (n = 10).

Table 8. Concentrations of T-495 in mouse plasma and brain after single and repeated treatment for 13 days

	Vehicle-pretreated		T-495 (10 mg/kg, p.o.)-pretreated	
	T-495 (10 mg/kg, p.o.)	T-495 (30 mg/kg, p.o.)	T-495 (10 mg/kg, p.o.)	T-495 (30 mg/kg, p.o.)
Plasma (ng/mL)	1148.2 ± 214.6	4894.9 ± 923.4	1299.8 ± 337.8	5422.1 ± 1745.5
Brain (ng/g)	955.7 ± 122.2	3654.0 ± 744.2	878.9 ± 158.8	4089.3 ± 599.2

Data are presented as the mean ± SD (n = 10). Concentration of T-495 in the hippocampus was regarded as the concentration in the brain.

Table 9. Concentrations of MK-7622 in mouse plasma and brain after single and repeated treatment for 13 days

	Vehicle-pretreated		MK-7622 (10 mg/kg, p.o.)-pretreated	
	MK-7622 (10 mg/kg, p.o.)	MK-7622 (30 mg/kg, p.o.)	MK-7622 (10 mg/kg, p.o.)	MK-7622 (30 mg/kg, p.o.)
Plasma (ng/mL)	624.0 ± 61.4	2342.4 ± 517.7	489.9 ± 86.4	2430.4 ± 550.5
Brain (ng/g)	136.6 ± 23.1	787.0 ± 284.1	126.0 ± 28.7	813.1 ± 262.0

Data are presented as the mean ± SD (n = 10). Concentration of MK-7622 in the hippocampus was regarded as the concentration in the brain.

Table 10. Observed side effects after oral administration of T-495 in rats

Drug	Dose (mg/kg)	Loose or mucous stool or diarrhea	Convulsion	Lacrimation	Salivation	Miosis	Fasciculation
Vehicle	-	0/6	0/6	0/6	0/6	0/6	0/6
T-495	1	0/6	0/6	0/6	0/6	0/6	0/6
T-495	3	0/6	0/6	0/6	0/6	0/6	0/6
T-495	10	0/6	0/6	0/6	0/6	0/6	0/6
T-495	30	0/6	0/6	0/6	0/6	0/6	0/6
T-495	100	5/6	1/6	0/6	1/6	0/6	0/6

Observations were carried out at 15 and 30 minutes and 1, 2, 4, 6, and 8 hours after drug administration. The data are presented as the ratio of rats exhibiting side effects to the total number of rats (n = 6).

Table 11. Observed side effects after oral administration of MK-7622 in rats

Drug	Dose (mg/kg)	Loose or mucous stool or diarrhea	Convulsion	Lacrimation	Salivation	Miosis	Fasciculation
Vehicle	-	0/6	0/6	0/6	0/6	0/6	0/6
MK-7622	3	2/6	0/6	0/6	0/6	0/6	0/6
MK-7622	10	3/6	0/6	0/6	0/6	0/6	0/6
MK-7622	30	6/6	0/6	0/6	0/6	0/6	0/6

Observations were carried out at 30 minutes and 1, 2, 4, and 6 hours after drug administration. The data are presented as the ratio of rats exhibiting side effects to the total number of rats (n = 6).

Table 12. Side effects observed after oral administration of T-495 in combination with donepezil in rats

Group (dose, mg/kg, p.o.)	Loose, mucous stool, or diarrhea	Convulsion	Lacrimation	Salivation	Myosis	Fasciculation
Vehicle	0/6	0/6	0/6	0/6	0/6	0/6
Donepezil (0.1)	0/6	0/6	0/6	0/6	0/6	0/6
T-495 (0.3)	0/6	0/6	0/6	0/6	0/6	0/6
Donepezil (0.1) + T-495 (0.3)	0/6	0/6	0/6	0/6	0/6	0/6

T-495 (0.3 mg/kg, p.o.) was administered to rats 30 minutes before the administration of donepezil (0.1 mg/kg, p.o.). Observations were carried out at 10 and 30 minutes and 1, 2, 4, and 6 hours after the administration of donepezil. The data are presented as the ratio of rats exhibiting side effects to the total number of rats (n = 6).

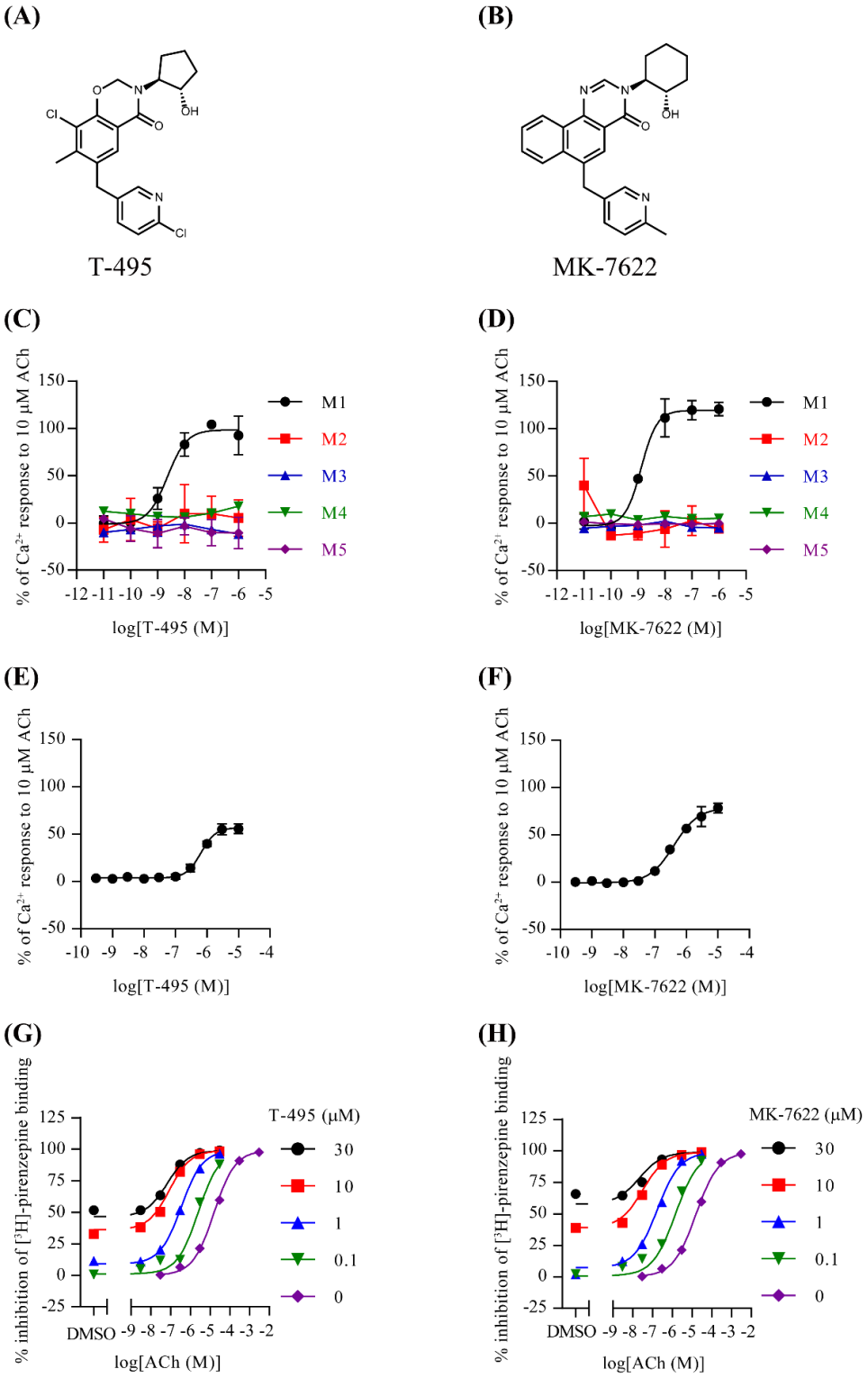

Figure 1. T-495 and MK-7622 selectively potentiate M_1R with low and high cooperativity, respectively. (A and B) Chemical structures of T-495 (A) and MK-7622 (B). (C and D) Potentiation of ACh-mediated Ca^{2+} mobilization by T-495 (C) or MK-

7622 (D) in CHO-K1 cells expressing human M_1R-M_5R. The response to an EC_{20} concentration and 10 μM of ACh was set as the 0% and 100% response, respectively. Data are presented as the mean ± SD (n = 3). (E and F) Effect of T-495 (E) or MK-7622 (F) on Ca^{2+} mobilization in the absence of ACh in CHO-K1 cells expressing human M_1R. The response to solvent and 10 μM of ACh was set as the 0% and 100% response, respectively. Data are presented as the mean ± SD (n = 4). (G and H) Effect of T-495 (G) or MK-7622 (H) on [^{3}H]-pirenzepine binding in cell membranes from human M_1R-expressing cells (n = 2). Nonspecific binding was defined in the presence of 10 μM atropine.

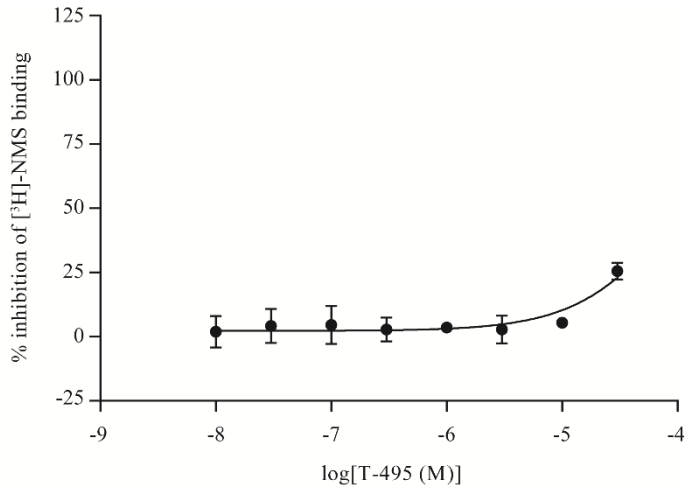

Figure 2. Effects of T-495 on [^{3}H]NMS binding in cell membranes from human M_1R-expressing cells.

Nonspecific binding was defined in the presence of 10 μM atropine. Data are presented as the mean ± SD (n = 3).

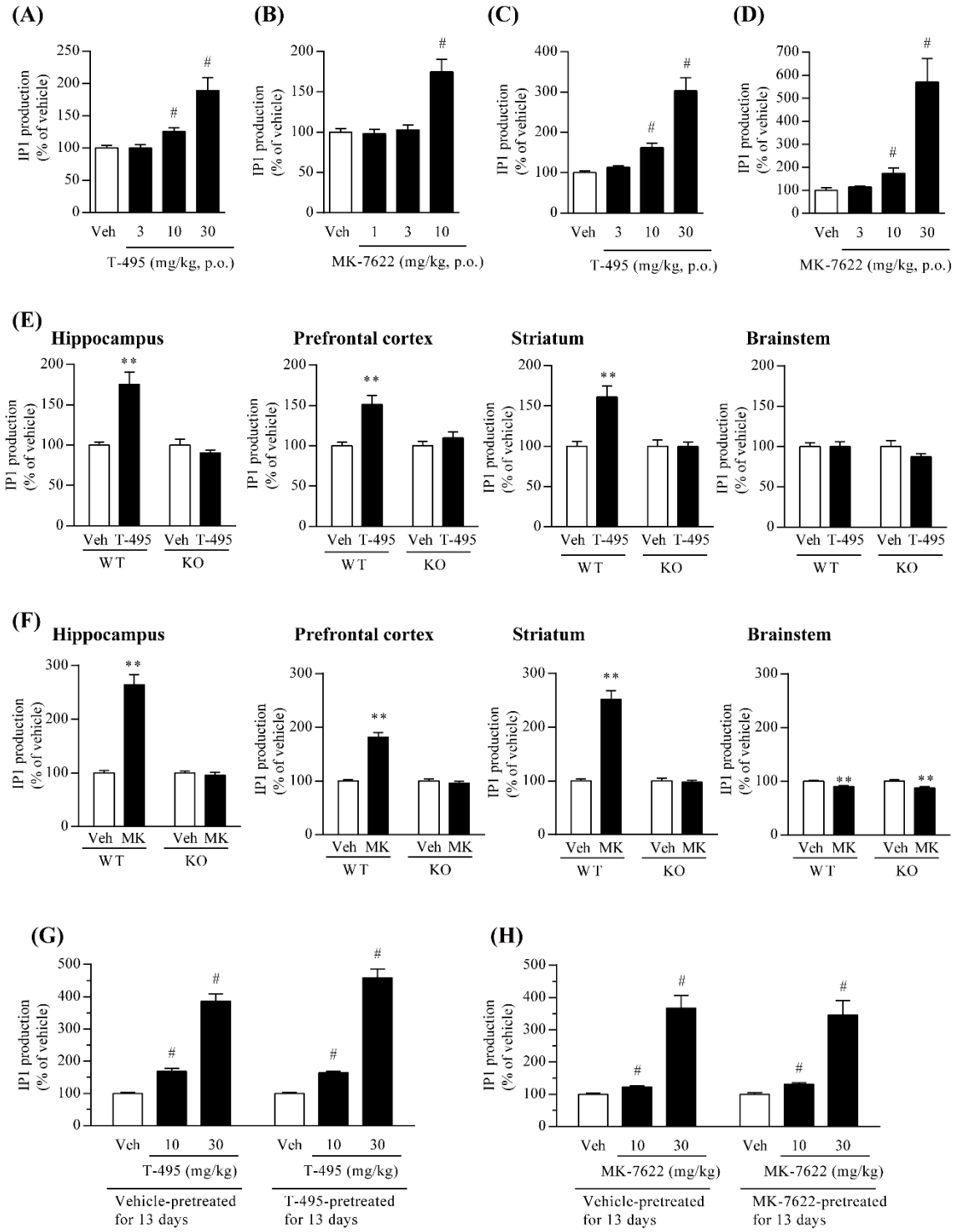

Figure 3. T-495 and MK-7622 increase IP1 production mediated by M_1R activation in the rodent brain. (A and B) Effects of T-495 (A) or MK-7622 (B) on IP1 production in the rat hippocampus. One hour after oral administration of vehicle (Veh) or a test

compound (T-495: 3, 10, and 30 mg/kg; MK-7622: 1, 3, and 10 mg/kg), animals were injected with LiCl (10 mmol/kg, s.c.). One hour after the LiCl injection, animals were sacrificed to collect the hippocampus. Concentrations of T-495 and MK-7622 in rat plasma and hippocampus are presented in Tables 3 and 4, respectively. Data are presented as the mean + SEM (n = 6). (C and D) Effects of T-495 (C) or MK-7622 (D) on IP1 production in the mouse hippocampus. One hour after oral administration of vehicle or a test compound (3, 10, and 30 mg/kg), animals were injected with LiCl (10 mmol/kg, s.c.). One hour after LiCl injection, animals were sacrificed to collect the hippocampus. Data are presented as the mean + SEM (n = 6). (E and F) Effects of T-495 (E) or MK-7622 (F) on IP1 production in the hippocampus, prefrontal cortex, striatum, and brainstem of wild-type and M_1R KO mice. One hour after oral administration of vehicle or a test compound (T-495: 10 mg/kg; MK-7622 (MK): 20 mg/kg), mice were injected with LiCl (10 mmol/kg, s.c.). One hour after the LiCl injection, brain tissues were collected. Concentrations of T-495 and MK-7622 in the plasma and hippocampus of wild-type and M_1R KO mice are shown in Table 5. Data are presented as the mean + SEM (n = 10). (G and H) Effects of repeated treatment with T-495 (G) or MK-7622 (H) for 13 days on IP1 production in the mouse hippocampus. Vehicle or a test compound (10 mg/kg, p.o.) was administered to mice once daily for 13 days. On the 14th day, 1 hour after the administration of vehicle or a test compound (10 and 30 mg/kg, p.o.), mice were injected with LiCl (10 mmol/kg, s.c.). One hour after the LiCl injection, mice were sacrificed to collect the hippocampus. Basal IP1 levels in the mouse hippocampus after repeated treatment with vehicle or a test compound for 13 days are shown in Table 6 (T-495) and 7 (MK-7622). Concentrations of T-495 and MK-7622 in the plasma and hippocampus of mice pretreated with vehicle or a test compound are shown in Table 8 and 9, respectively.

Data are presented as the mean + SEM (n = 10). $^{\#}P \leq 0.05$ versus vehicle-treated group by two-tailed Shirley-Williams' test. $^{**}P \leq 0.01$ versus vehicle-treated group by Student's t-test or Aspin-Welch t-test.

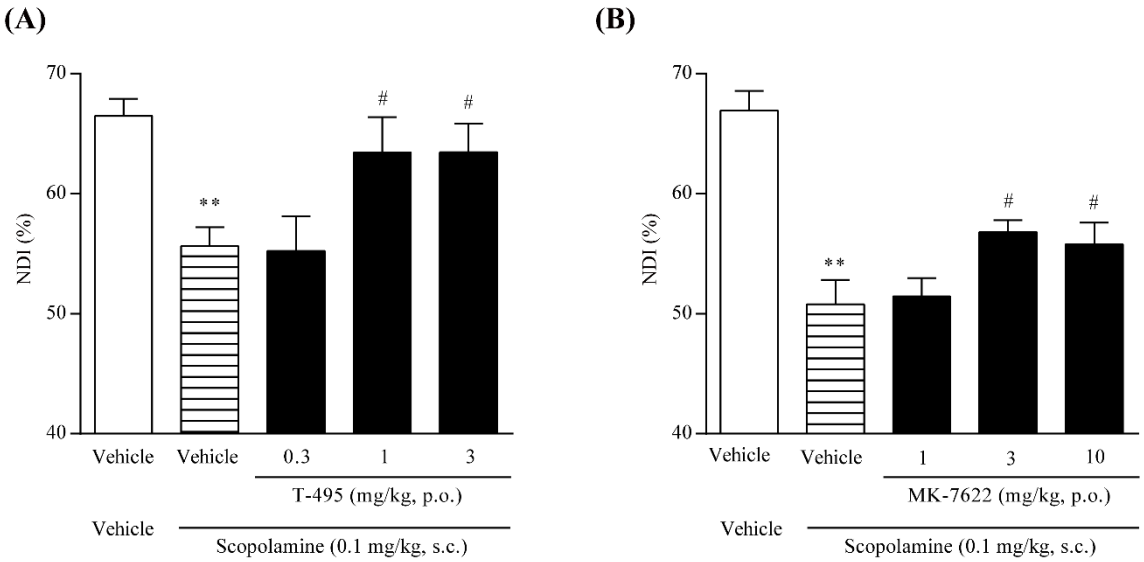

Figure 4. T-495 and MK-7622 improve scopolamine-induced memory impairment in a rat NOR test. A test compound (T-495 (A): 0.3, 1, and 3 mg/kg, p.o.; MK-7622 (B): 1, 3, and 10 mg/kg, p.o.) and scopolamine (0.1 mg/kg, s.c.) were administered to rats 1 hour and 30 minutes prior to the acquisition trial, respectively. Data are presented as the mean + SEM (n = 6–8). $^{**}P \leq 0.01$ versus vehicle-vehicle-treated group by Student's t-test. $^{\#}P \leq 0.05$ versus vehicle-scopolamine-treated group by two-tailed Williams' test.

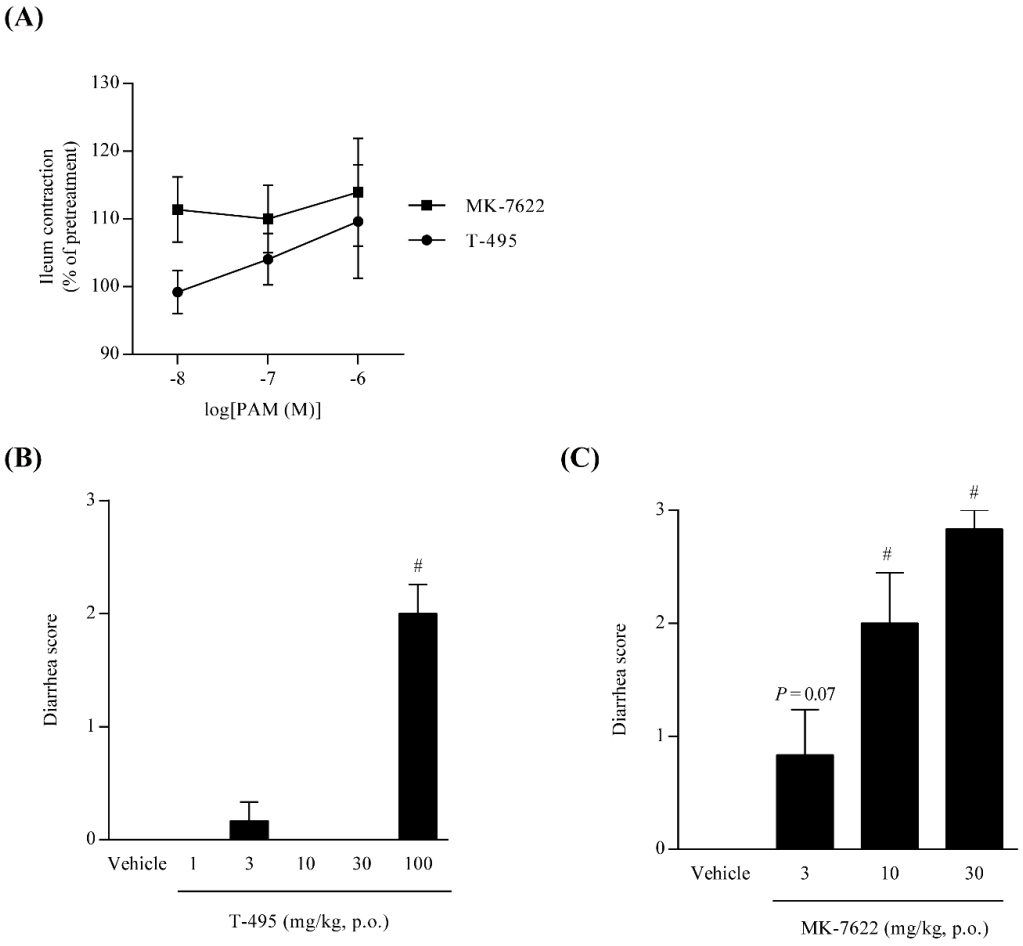

Figure 5. Effects of T-495 and MK-7622 on spontaneous ileum contraction and diarrhea score. (A) Effects of T-495 and MK-7622 on spontaneous ileum contraction. The mean amplitude of spontaneous contractions at each concentration was normalized to that at pretreatment. Data are presented as the mean ± SEM (n = 7–10). (B and C) Diarrhea score. T-495 (B; 1, 3, 10, 30, and 100 mg/kg, p.o.) or MK-7622 (C; 3, 10, and 30 mg/kg, p.o.) was administered to rats, and the severity of diarrhea was scored. The highest score during the observation period was used for analysis. Data are presented as the mean + SEM (n = 6). $^{\#}P \leq 0.05$ versus vehicle-treated group by two-tailed Williams' test.

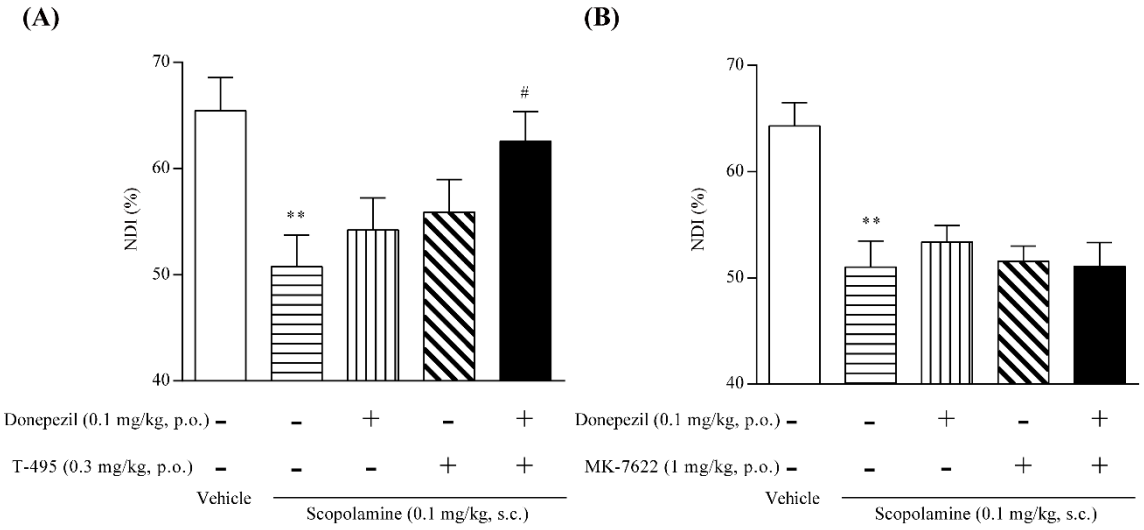

Figure 6. Effects of T-495 or MK-7622 in combination with donepezil on scopolamine-induced memory impairment in a rat NOR test. A test compound (T-495 at 0.3 mg/kg (A) or MK-7622 at 1 mg/kg (B)), donepezil (0.1 mg/kg, p.o.), and scopolamine (0.1 mg/kg, s.c.) were administered 1, 0.5, and 0.5 hours, respectively, prior to the acquisition trial. Data are presented as the mean + SEM (n = 7–8). $^{**}P \leq 0.01$ versus vehicle-vehicle-vehicle-treated group by Student's t-test. $^{\#}P \leq 0.05$ versus vehicle-vehicle-scopolamine-treated group by Dunnett's test.

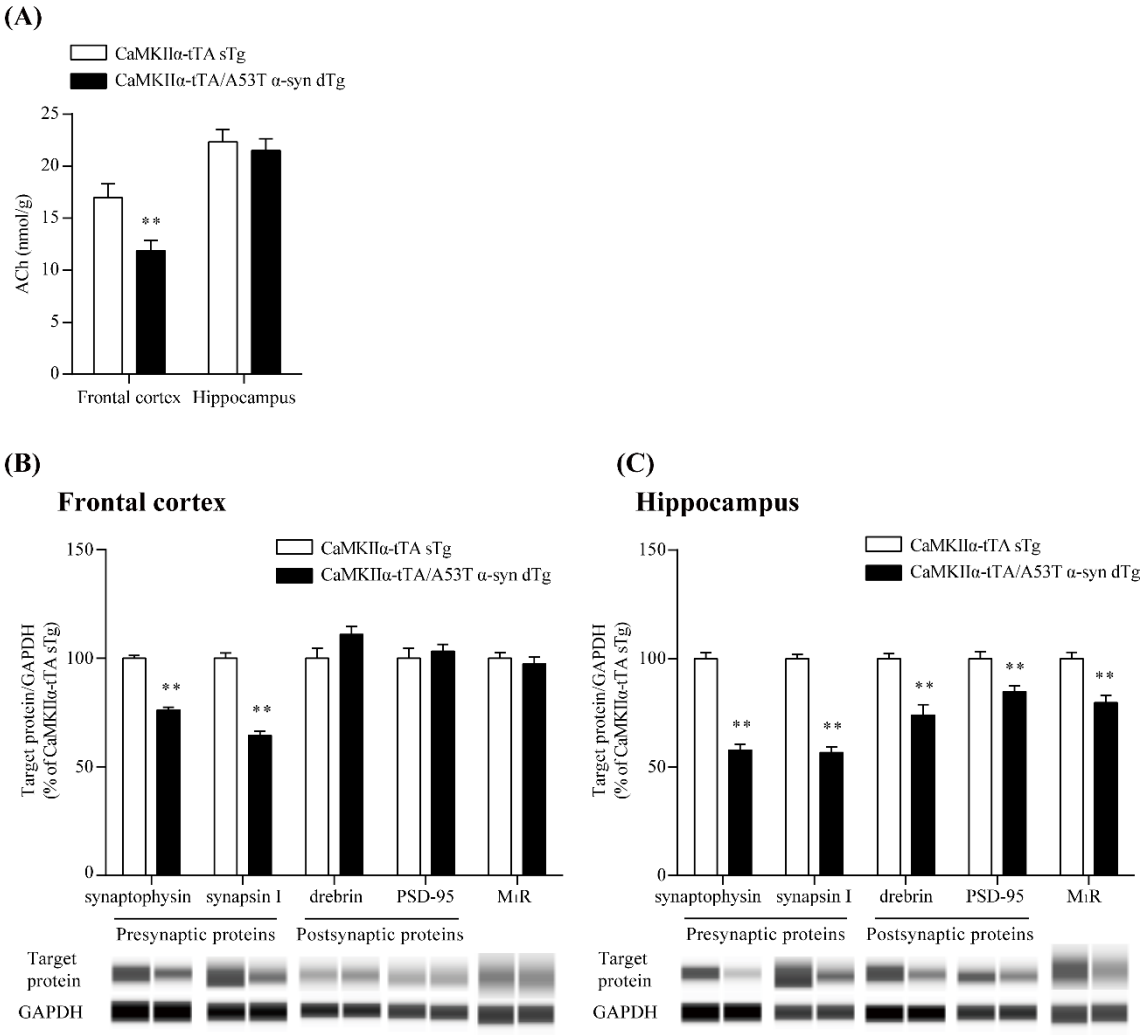

Figure 7. ACh content and synaptic protein and M_1R levels in the frontal cortex and hippocampus of the CaMKIIα-tTA/A53T α-syn dTg mice. The frontal cortex and hippocampus were dissected from 12-month-old mice. (A) The ACh content in the tissues was measured by LC-MS/MS. Data are presented as the mean + SEM (n = 21–24), and statistical significance of the differences between the CaMKIIα-tTA sTg and CaMKIIα-tTA/A53T α-syn dTg mice was determined using Student's t-test (**$P \leq 0.01$). (B and C) Presynaptic and postsynaptic proteins in the frontal cortical (B) and hippocampal (C) lysates from the CaMKIIα-tTA sTg and CaMKIIα-tTA/A53T α-syn dTg mice were determined by an automated capillary western blot system. Synaptic protein levels were

normalized to the levels of GAPDH, which was a loading control. Results are expressed as percentages of the values obtained from age-matched CaMKIIα-tTA sTg mice and are presented as the mean + SEM (n = 10). The statistical significance of the difference between the CaMKIIα-tTA sTg and CaMKIIα-tTA/A53T α-syn dTg mice was determined using Student's t-test or Aspin-Welch test (**$P \leq 0.01$). Representative images of capillary western blot are shown below the quantified results in panels B and C.

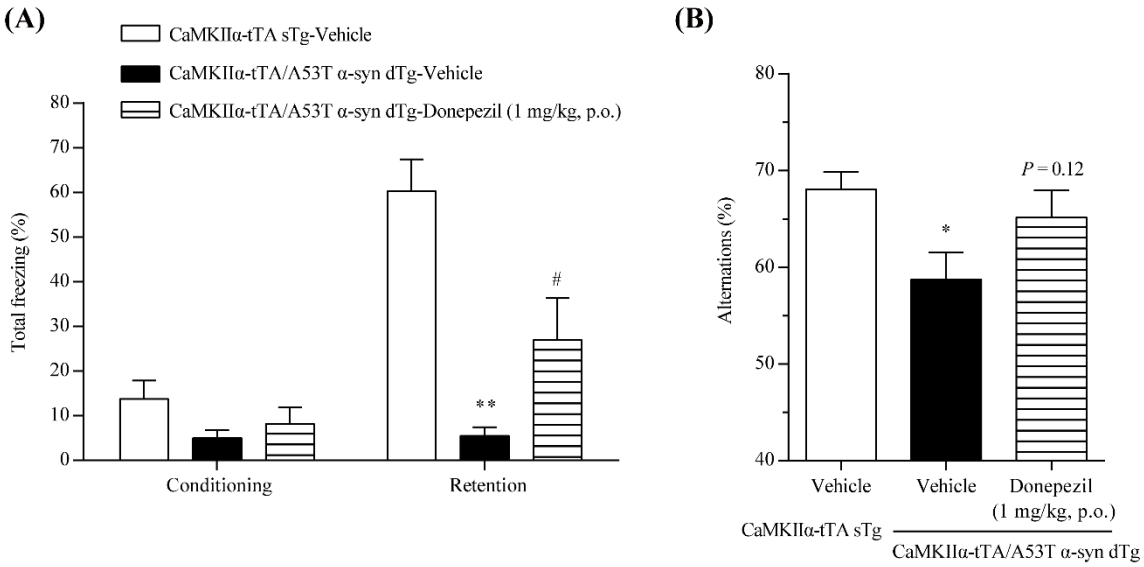

Figure 8. Effects of donepezil on the memory deficits in the CaMKIIα-tTA/A53T α-syn dTg mice. (A) The CFC test was performed to evaluate associative learning of 12-month-old CaMKIIα-tTA sTg and CaMKIIα-tTA/A53T dTg mice. The percentage of freezing behavior was analyzed during the conditioning and retention phases. Vehicle or donepezil (1 mg/kg) was orally administered 2 hours prior to both the conditioning and retention phases. (B) The Y-maze task was performed to evaluate spatial working memory of 12-month-old CaMKIIα-tTA sTg and CaMKIIα-tTA/A53T dTg mice. The percentage of alternations was measured. Vehicle or donepezil (1 mg/kg) was orally administered 2 hours prior to the test. Data are presented as the mean + SEM (n = 10); statistical significance between the vehicle-treated CaMKIIα-tTA sTg and CaMKIIα-tTA/A53T α-syn dTg mice was determined using Student's t-test or Aspin-Welch test (*$P \leq 0.05$; **$P \leq 0.01$). Significant differences between vehicle- and donepezil-treated CaMKIIα-tTA/A53T α-syn dTg mice were determined by Student's t-test or Aspin-Welch test (#$P \leq 0.05$).

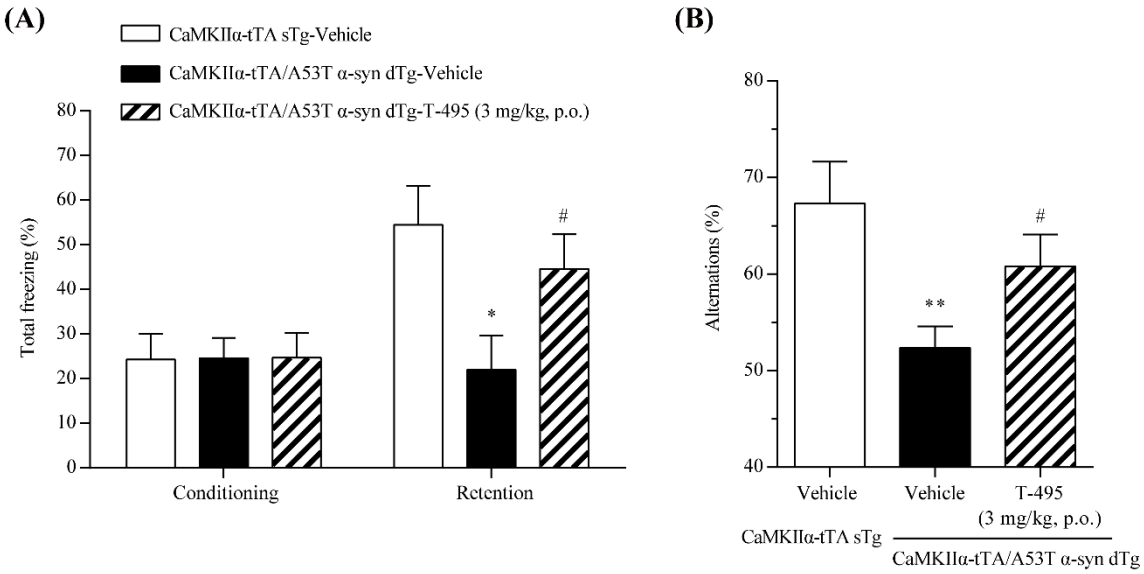

Figure 9. Effects of T-495 on the memory deficits in the CaMKIIα-tTA/A53T α-syn dTg mice. (A) The CFC test was performed at 12 months of age. The percentage of freezing behavior was analyzed during the conditioning and retention phases. Vehicle or T-495 (3 mg/kg) was administered orally 1 hour prior to both the conditioning and retention phases. (B) The Y-maze task was performed at 12 months of age. The percentage of alternations was measured. Vehicle or T-495 (3 mg/kg) was orally administered 1 hour prior to the test. Data are presented as the mean + SEM (n = 10–15), and statistical significance between the vehicle-treated CaMKIIα-tTA sTg and CaMKIIα-tTA/A53T α-syn dTg mice was determined using Student's t-test or Aspin-Welch test (*$P \leq 0.05$; **$P \leq 0.01$). Significant differences between vehicle- and T-495-treated CaMKIIα-tTA/A53T α-syn dTg mice were determined by Student's t-test or Aspin-Welch test (#$P \leq 0.05$).

Chapter II:

In vivo pharmacological comparison of TAK-071, a positive allosteric modulator of muscarinic M_1 receptor, and xanomeline, an agonist of muscarinic M_1/M_4 receptor, in rodents

Abstract

Activation of the M_1 muscarinic acetylcholine receptor (M_1R) may be an effective therapeutic approach for Alzheimer's disease (AD), dementia with Lewy bodies, and schizophrenia. Previously, the M_1R/M_4R agonist xanomeline was shown to improve cognitive function and exert antipsychotic effects in patients with AD and schizophrenia. However, its clinical development was discontinued because of its cholinomimetic side effects. I compared in vivo pharmacological profiles of a novel M_1R-selective positive allosteric modulator, TAK-071, and xanomeline in rodents. Xanomeline suppressed both methamphetamine- and MK-801-induced hyperlocomotion in mice, whereas TAK-071 suppressed only MK-801-induced hyperlocomotion. In a previous study, I showed that TAK-071 improved scopolamine-induced cognitive deficits in a rat novel object recognition task (NORT) with 33-fold margins versus cholinergic side effects (diarrhea). Xanomeline also improved scopolamine-induced cognitive impairments in a NORT; however, it had no margin versus cholinergic side effects (e.g., diarrhea, salivation, and hypoactivity) in rats. These side effects were observed even in M_1R knockout mice. Evaluation of c-Fos expression as a marker of neural activation revealed that xanomeline increased the number of c-Fos-positive cells in several cortical areas, the hippocampal formation, amygdala, and nucleus accumbens. Other than in the orbital cortex and claustrum, TAK-071 induced similar c-Fos expression patterns. When donepezil was co-administered to increase the levels of acetylcholine, the number of TAK-071-induced c-Fos-positive cells in these brain regions was increased. TAK-071, through induction of similar neural activation as that seen with xanomeline, may produce procognitive and antipsychotic effects with improved cholinergic side effects.

Introduction

Cognitive impairment is one of the major disabling features in Alzheimer's disease (AD), dementia with Lewy bodies (DLB), and schizophrenia. However, currently available pharmacological treatments have limited efficacy for the treatment of cognitive impairment in these diseases. Therefore, the development of new drugs with better efficacy is warranted. Cholinergic neurotransmission in the cerebral cortex and hippocampus is a key mediator of learning and memory [67], and cholinergic dysfunction is commonly reported in patients with AD, DLB, and schizophrenia. In AD and DLB, the basal forebrain cholinergic neurons that innervate the cerebral cortex and hippocampus are selectively degenerated [68, 69]. The activity of choline acetyltransferase, the enzyme that synthesizes acetylcholine, is also reduced in these brain areas in patients with AD and DLB [5, 6]. In patients with schizophrenia, the expression levels of muscarinic acetylcholine receptors, such as M_1 muscarinic acetylcholine receptor (M_1R) and M_4 muscarinic acetylcholine receptor (M_4R), in the same brain regions are reduced, while the basal forebrain cholinergic neurons and activity of choline acetyltransferase are unaffected [70-74]. Therefore, enhancing cholinergic neurotransmission in the cerebral cortex and hippocampus might be a promising treatment strategy in these disorders.

Of the acetylcholine receptors, the M_1R is one of the most promising targets for improving cognition. The M_1R is highly expressed in the brain regions that mediate cognition, including the cerebral cortex and hippocampus [15], and M_1R knockout (KO) mice exhibit cognitive impairment [16]. At the clinical level, the M_1R/M_4R agonist xanomeline was reported to improve cognitive function in patients with AD [13]. However, other muscarinic receptor agonists, such as alvameline, milameline, and talsaclidine, have shown a lack of efficacy against cognitive decline in patients with AD

[75-77]. Furthermore, xanomeline showed a significant improvement in cognitive deficits as well as positive and negative symptoms in patients with schizophrenia [14]. Xanomeline has limited selectivity for M_1R and M_4R. It activates all other muscarinic subtypes [78] and has an agonistic effect on 5-HT_{1A} and 5-HT_{1B} receptors and an antagonistic effect on the 5-HT_2 receptor [79]. However, antipsychotic-like effects of xanomeline were partially reduced in M_1R KO mice and completely abolished in M_4R KO mice [80]. In addition, it has been reported that recent selective M_1R positive allosteric modulators (PAMs), such as PQCA, MK-7622, and VU0453595, reverse cognitive impairment in multiple rodent and monkey models of AD and schizophrenia [29-31, 34, 81]. Thus, M_1R and M_4R appear to primarily contribute to the efficacy of xanomeline.

Unfortunately, the clinical development of xanomeline was discontinued because of its side effects, including sweating and gastrointestinal (GI) dysfunction [13]. These side effects have been suggested to result from activation of M_2R and M_3R in the peripheral tissues. However, recent studies have revealed that M_1R-selective activation may also be associated with GI dysfunction in animals [24-26]. To discover novel M_1R PAMs with a reduced risk of GI side effects, I characterized the parameters of M_1R PAMs and their GI side effects and cognitive effects. As a result, I found that a M_1R PAM with a low α-value (a binding cooperativity factor between acetylcholine and a PAM) improved cognitive impairment with a wide therapeutic margin in rodents [24, 33]. TAK-071 (4-fluoro-2-[(3*S*,4*S*)-4-hydroxytetrahydro-2*H*-pyran-3-yl]-5-methyl-6-[4-(1*H*-pyrazol-1-yl)benzyl]-2,3-dihydro-1*H*-isoindol-1-one) is a novel M_1R PAM with a low α-value that was discovered using this approach and reversed scopolamine-induced cognitive impairment with a substantially decreased risk of GI side effects in rats [33].

A detailed comparison of the pharmacological profiles of TAK-071 and xanomeline would be effective in determining the therapeutic potential of TAK-071 in human patients. In this study, using the same experimental protocols, I first compared the antipsychotic-like activity, procognitive efficacy, and cholinergic side effects. In addition, to compare the brain regions activated by TAK-071 and xanomeline, I evaluated c-Fos expression, which has been used widely as a marker of activated neural populations.

Materials and methods

Animals

Male ICR and C57BL/6J mice were purchased from CLEA Japan Inc. (Tokyo, Japan), and Sprague-Dawley (SD) and Long-Evans rats were purchased from Charles River Laboratories Japan, Inc. (Yokohama, Japan) and Japan SLC, Inc. (Shizuoka, Japan), respectively. C57BL/6-*Chrm1*^{tm1Stl}/J wild-type (WT) and homozygous KO mice were obtained from the Massachusetts Institute of Technology (Cambridge, MA). The animals were housed in a light-controlled room (12-h light/dark cycle with lights on at 7:00 AM) and allowed free access to food and water. The animals were acclimated for at least 1 week before the experiments. The care and use of the animals and experimental protocols used in this study were approved by the Experimental Animal Care and Use Committee of Takeda Pharmaceutical Company Limited.

Chemical compounds

TAK-071 was synthesized by Takeda Pharmaceutical Company Limited, and donepezil hydrochloride was synthesized by Megafine Pharma Ltd. (Maharashtra, India). Xanomeline oxalate, methamphetamine hydrochloride (METH), (5*S*,10*R*)-(+)-5-methyl-10,11-dihydroxy-5*H*-dibenzo[*a,d*]cyclohepten-5,10-imine hydrogen maleate (MK-801), and scopolamine hydrobromide were purchased from Metina AB (Lund, Sweden), Sumitomo Dainippon Pharma Co., Ltd. (Osaka, Japan), Sigma-Aldrich (St. Louis, MO), and Tocris Bioscience (Ellisville, MO), respectively. For oral administration (p.o.), TAK-071 was suspended in a vehicle (0.5% methylcellulose in distilled water), and donepezil hydrochloride was dissolved in a vehicle (distilled water). In a combination study of TAK-071 with donepezil, each compound was individually administered to animals.

Xanomeline oxalate was dissolved in a vehicle (saline) and injected intraperitoneally (i.p.) or subcutaneously (s.c.). METH, MK-801, and scopolamine were dissolved in a vehicle (saline) and injected s.c. All compounds were given in a volume of 10 mL/kg body weight in mice and 2 mL/kg body weight in rats.

Measurements of locomotor activity

Seven-week-old ICR mice were placed in the test chamber alone for over 1 h to habituate to the experimental conditions. For xanomeline, METH (2 mg/kg s.c.) or MK-801 (0.3 mg/kg s.c.) was coadministered with xanomeline (s.c.). For TAK-071, METH (2 mg/kg s.c.) or MK-801 (0.3 mg/kg s.c.) was administered 2 h after oral administration of TAK-071. Locomotion was recorded in 1-min intervals for 60 min after drug administration using the MDC system (Brain Science Idea Co., Ltd., Osaka, Japan). The sum of the activity counts during the 60-min period was calculated in the analysis of the total activity counts.

Novel object recognition (NOR) task

The details of the NOR task are described elsewhere [33]. In brief, seven-week-old Long-Evans rats were injected with vehicle or xanomeline (i.p.) 30 min before the acquisition trial. For scopolamine-induced amnesia, the rats were injected with vehicle or scopolamine (s.c.) 30 min before the acquisition trial. For the acquisition trial, each rat was placed in a test box containing two identical objects that the rat was allowed to explore for 3 min. For the retention trials conducted 4 h (scopolamine-induced amnesia) and 1 and 48 h (natural forgetting) later, each rat was placed in the same test box containing one familiar and one novel object that the rat was allowed to explore for 3 min.

During the acquisition and retention trials, the time spent exploring each object was scored manually. The results were presented as novelty discrimination index (NDI) calculated as follows: the exploration time of the novel object ⁄ the exploration time of both objects × 100.

Evaluation of the cholinergic side effects

Six-week-old SD rats, 8-week-old C57BL/6J mice, and 8-week-old *Chrm1* WT and KO mice were placed in observation cages alone and habituated for at least 1 h. The animals were treated with vehicle or xanomeline, and cholinergic side effects (loose stools and diarrhea, lacrimation, salivation, and hypoactivity) were assessed 10 and 30 min and 1, 2, and 4 h later. The number of animals with observable side effects was counted. For loose stools and diarrhea, the number of animals with moist and soft stools, mucous stools, and/or watery unformed stools was counted. For lacrimation, the number of animals showing considerable moisture around the eyes was counted. For salivation, the number of animals with considerable moisture around the mouth, throat, and/or neck was counted. For hypoactivity, the number of animals with obviously reduced or absent motor activity was counted.

Immunohistochemical detection of c-Fos expression

Immunohistochemistry

After 4 days of isolation and habituation to the vehicle injections, eight-week-old male ICR mice were treated with TAK-071 (p.o.), donepezil (p.o.), or xanomeline (s.c.) on Day 5. The mice were anesthetized with an i.p. injection of pentobarbital 10 min before the transcardial perfusion. At 3 h (TAK-071 and donepezil) or 1.25 h (xanomeline) after the

drug administration, the transcardial perfusion was performed with saline solution containing 0.5% heparin, which was followed by phosphate-buffered saline (PBS) containing 4% paraformaldehyde (PFA). The brains were dissected out immediately after the perfusion. The dissection was performed between 12:00 and 17:00. Because c-Fos expression appears 30 min and peaks 1–2 h after the stimulation and then lasts for a few hours [82, 83], the brains were dissected out within 1–3 h of the time that each drug reached its maximum plasma concentration (Tmax).

The collected brain samples were stored in 25 mL of 4% PFA in PBS overnight at 4°C and then moved to and stored in 25 mL of a 30% sucrose solution in PBS at 4°C at least until the brain samples sank to the bottom of the tubes. The brains were sliced into 40-µm-thick coronal sections using a Leica CM3050S Cryostat (Leica Microsystems GmbH, Wetzlar, Germany). The brain sections were stored in antifreeze solution (PBS containing 30% glycerol and 30% ethylene glycol) at -30°C until immunostaining was performed. The sections were washed once with PBS for 5 min and twice with PBS containing 0.2% Triton X-100 (PBS-TX) for 5 min each and then incubated in blocking solution (3% bovine serum albumin in PBS-TX) for 1 h at room temperature on a shaker. After washing once with PBS-TX for 5 min, the sections were incubated with a rabbit anti-c-Fos monoclonal primary antibody (catalog number 2250S, lot number 6, Cell Signaling Technology Inc., Danvers, MA) at a 1:1000 dilution (antibody:blocking solution) overnight at 4°C on a shaker. This anti-c-Fos monoclonal primary antibody does not recognize other Fos family proteins, including FosB, FRA1, and FRA2 (https://www.cellsignal.com/products/primary-antibodies/c-fos-9f6-rabbit-mab/2250). After incubation with the primary antibody, the sections were washed three times with PBS-TX for 5 min each and then incubated with biotinylated goat anti-rabbit IgG (catalog

number 711-065-152, Jackson ImmunoResearch Laboratories, Inc., West Grove, PA) at a 1:200 dilution (antibody:blocking solution) for 1 h at room temperature on a shaker. After washing three times with PBS-TX for 5 min each, the sections were incubated with blocking solution containing Alexa Fluor 488-conjugated streptavidin (10 μg/mL; Thermo Fisher Scientific Inc., Waltham, MA) and propidium iodide (1 μg/mL; Thermo Fisher Scientific) for 1 h at room temperature on a shaker. After washing twice with PBS-TX for 5 min each and once with PBS for 5 min, the sections were mounted on Platinum-coated glass slides (Matsunami Glass Ind., Ltd., Osaka, Japan), allowed to dry, and then sealed with PermaFluor aqueous mounting medium (Thermo Fisher Scientific Inc.) and a cover glass.

Quantification of c-Fos-positive cells

Images of the slides were taken with IN Cell Analyzer 2000 (GE Healthcare Life Sciences, Little Chalfont, UK) and montaged into an image of the entire slide using NIS-Elements imaging software (Nikon Corporation, Tokyo, Japan). To identify and count c-Fos-positive cells within the regions of interest of predefined size, WinROOF 2015 imaging software (Mitani Corporation, Fukui, Japan) was used. For all regions analyzed, contrast was adjusted using a fixed value, followed by background and noise subtraction using constant values. A threshold, determined by the darkest signal in each area, was applied to create a binary image. A size filter was then applied to exclude objects other than c-Fos-positive nuclei for all regions. Quantification was performed in random order. The size of the region of interest was 0.278 mm × 0.278 mm, except in the dentate gyrus (DG) (0.555 mm × 0.278 mm) and CA3 and CA1 (0.555 mm × 0.139 mm). The following brain regions were analyzed: the anterior cingulate cortex (ACC), prelimbic cortex (PLC),

infralimbic cortex (ILC), orbital cortex (OC), posterior parietal cortex (PPC), primary somatosensory cortex barrel field (S1BF), temporal cortex (TC), DG, CA3, CA1, subiculum (SUB), entorhinal cortex (EC), central nucleus of the amygdala (CEA), basolateral nucleus of the amygdala (BLA), nucleus accumbens (NAc), caudate putamen (CPu), claustrum (CLA), lateral septum (LS), mediodorsal thalamic nucleus (MD), ventral posteromedial thalamic nucleus (VPM), lateral hypothalamic area (LH), posterior hypothalamic area (PH), and periaqueductal gray (PAG). The exact same area was identified using the Allen Mouse Brain Atlas (©2004 Allen Institute for Brain Science; http://mouse.brain-map.org) [84], and the areas analyzed are illustrated in Figure 10. The numbers of c-Fos-positive cells in the left and right hemispheres of one section were averaged and used in the statistical analyses.

In vivo myo-inositol 1-phosphate (IP1) assay

An i*n vivo* IP1 assay was performed as previously described [33]. Briefly, eight-week-old Long-Evans rats and ICR mice were treated with vehicle or xanomeline (i.p. and s.c., respectively). Thirty min later, the rats were administered lithium chloride (LiCl; 10 mmol/kg s.c.). The mice were administered LiCl at the same time as the xanomeline injection. One hour after the LiCl injections, the animals were sacrificed, and their hippocampi were isolated immediately. The dissected tissues were homogenized, incubated on a rotator for 1 h at 4°C, and centrifuged. The concentrations of IP1 and total protein in the supernatant were measured using IP-One HTRF assay kit (Cisbio Bioassays, Codolet, France) and BCA Protein Assay Kit (Thermo Fisher Scientific Inc.), respectively, according to the manufacturers' instructions. The IP1 levels were expressed as a ratio of the IP1 concentration to the total protein concentration.

Pharmacokinetic studies

Eight-week-old C57BL/6J mice were used in this study. TAK-071 was administered to mice, and blood samples were collected into tubes containing EDTA from the tail vein at 0.5, 1, 2, 4, and 6 h postdose. The concentrations of TAK-071 were determined using high-performance liquid chromatography with tandem mass spectrometry.

Statistical analyses

The statistical analyses were performed using SAS EXSUS software (CAC Croit Corporation, Tokyo, Japan). For the dose-response studies, the statistical comparisons were made between the vehicle- and drug-treated groups using the two-tailed Williams' test (homogeneous data) or two-tailed Shirley-Williams' test (nonhomogeneous data) with $P \leq 0.05$ set as the level of significance. Statistical analyses between two groups were performed using Student's t-tests (homogeneous data) or Aspin–Welch tests (nonhomogeneous data), and P values less than or equal to 0.05 indicated statistical significance. For the TAK-071 and donepezil coadministration study, a two-way analysis of variance (ANOVA) was used to determine if the combined treatment had synergistic effects, which were indicated by significant interactions ($P \leq 0.05$). Following the two-way ANOVAs, Dunnett's *post-hoc* multiple comparison tests were performed with the level of statistical significance set at $P \leq 0.05$.

Results

Effects of xanomeline and TAK-071 on psychostimulants-induced hyperlocomotion in mice

Hyperlocomotion induced by psychostimulants, including METH and MK-801, has been widely used to characterize the antipsychotic-like effects of drugs [85]. Xanomeline at 3 mg/kg s.c. suppressed both METH-induced hyperlocomotion ($P \leq 0.05$; Fig. 11A) and MK-801-induced hyperlocomotion ($P \leq 0.05$; Fig. 11B), although it also suppressed spontaneous locomotor activity at ≥0.3 or 1 mg/kg s.c. ($P \leq 0.05$; Fig. 11A and B). TAK-071 at 1 mg/kg p.o. did not suppress METH-induced hyperlocomotion ($P > 0.05$; Fig. 11C), but produced a significant suppression of MK-801-induced hyperlocomotion ($P \leq 0.05$; Fig. 11D) with no effect on spontaneous locomotion ($P > 0.05$; Fig. 11C and D). These results suggest that, like xanomeline, TAK-071 may have antipsychotic-like effects.

Effects of xanomeline on scopolamine-induced amnesia and natural forgetting in the NOR task in rats

I investigated the procognitive effects of xanomeline on scopolamine-induced amnesia and natural forgetting using a NOR task; however, I could not establish scopolamine-induced cognitive deficits in mice. Therefore, I used rats to evaluate the procognitive effects of xanomeline. Similar to TAK-071 and donepezil [33], xanomeline (1 mg/kg i.p.) significantly reversed the NDI reduction induced by scopolamine ($P \leq 0.05$; Fig. 12A) but did not improve the delay-dependent NDI reduction ($P > 0.05$; Fig. 12B).

Side effects profiles of xanomeline in mice and rats

I previously evaluated cholinergic side effects, including diarrhea, salivation, and

lacrimation, in rats after oral administration of TAK-071 [33]. TAK-071 elicited only diarrhea at a 33-fold higher dose than that required for cognitive improvement [33]. On the other hand, xanomeline caused loose stools and diarrhea and salivation at the same dose as the procognitive dose (i.e., 1 mg/kg i.p.) and hypoactivity at ≥10 mg/kg i.p. in rats (Table 13). These side effects other than loose stools and diarrhea were replicated in mice treated with xanomeline (Table 14). Xanomeline caused these side effects even in *Chrm1*-KO mice, in which the gene encoding for M_1R is deleted (Table 15).

Dose selection for c-Fos studies

To investigate the neural activation related to the procognitive and antipsychotic-like efficacy of xanomeline and TAK-071, I evaluated the number of c-Fos-positive cells at the efficacious doses. TAK-071 showed antipsychotic-like activity at 1 mg/kg p.o. in mice. Unfortunately, I could not investigate the procognitive effects of TAK-071 in mice because of a technical limitation. Thus, I translated the procognitive doses in rats to mice using pharmacokinetic and pharmacodynamic parameters. The plasma concentration of TAK-071 in mice (Table 16) was comparable to that in rats [33]. In addition, IP1 production, a pharmacodynamic marker to monitor activation level of Gq-coupled receptors including M_1R [86], was significantly increased at the same dose in rats and mice [33]; thus, the procognitive doses were estimated to be comparable in rats and mice. Because TAK-071 at 0.3, 1, and 3 mg/kg p.o. significantly improved scopolamine-induced cognitive impairment in rats [33], I estimated that the doses of 0.3, 1, and 3 mg/kg p.o. were also sufficient procognitive doses in mice. Thus, in the c-Fos studies, I decided to use 0.3, 1, and 3 mg/kg p.o. as the effective doses, as well as 0.1 mg/kg p.o. as an ineffective dose, in the mouse model.

Like TAK-071, xanomeline also increased IP1 production at the same dose in rats (Fig. 13A) and mice (Fig. 13B); thus, procognitive doses were estimated to be comparable in rats and mice. In rats, xanomeline significantly improved scopolamine-induced cognitive impairment at 1 mg/kg i.p. (Fig. 12A) and 1 and 3 mg/kg i.p. [87]; I estimated that the doses of 1 and 3 mg/kg were also procognitive doses in mice. In addition, xanomeline produced antipsychotic-like efficacy at 3 mg/kg s.c. in mice. Thus, I decided to use 3 mg/kg of xanomeline in the c-Fos study.

Induction of c-Fos expression by xanomeline

The number of c-Fos-positive cells was counted in 17 brain regions where M_1R is highly expressed (e.g., cortical areas and hippocampal formation) and 6 brain regions where M_1R is weakly expressed (e.g., thalamus and hypothalamus) (Fig. 10).

Xanomeline (3 mg/kg s.c.) significantly increased the number of c-Fos-positive cells in the cortical areas, including the ACC ($P \leq 0.05$), PLC ($P \leq 0.01$), ILC ($P \leq 0.01$), PPC ($P \leq 0.05$), S1BF ($P \leq 0.01$), and TC ($P \leq 0.05$), but not in the OC ($P = 0.49$; Fig. 14A and B). The magnitudes of the increases reached 168%, 216%, 234%, 278%, 253%, and 361% that of the vehicle-treated group in the ACC, PLC, ILC, PPC, S1BF, and TC, respectively (Fig. 14B). Xanomeline significantly increased the number of c-Fos-positive cells in the hippocampal formation, including the CA3, CA1, SUB, and EC ($P \leq 0.05$), and a clear trend for an increase was observed in the DG ($P = 0.07$; Fig. 14C and D). The magnitudes of the increases reached 151%, 149%, 268%, 286%, and 250% that of the vehicle-treated group in the DG, CA3, CA1, SUB, and EC, respectively (Fig. 14D). Xanomeline also increased the number of c-Fos-positive cells in subcortical areas, including the amygdala and NAc ($P \leq 0.01$), but not in the CPu ($P = 0.33$) and CLA ($P =$

0.57; Fig. 14E and F). The magnitudes of the increases reached 232%, 215%, and 587% that of the vehicle-treated group in the CEA, BLA, and NAc, respectively (Fig. 14F). On the other hand, there were no significant increase in the number of c-Fos-positive cells in the LS, thalamus, hypothalamus, and PAG ($P > 0.05$; Fig. 14G and H).

Induction of c-Fos expression by TAK-071

As the first experiment (Experiment 1), I evaluated the effects of TAK-071 at 0.1–1 mg/kg p.o. on c-Fos expression. TAK-071 (1 mg/kg p.o.) significantly increased the number of c-Fos-positive cells in the cortical areas, including the ACC, PLC, ILC, OC, PPC, S1BF, and TC ($P \leq 0.05$; Fig. 15A and B). These increases reached 199%, 218%, 216%, 458%, 237%, 280%, and 1029% that of the vehicle-treated group in the ACC, PLC, ILC, OC, PPC, S1BF, and TC, respectively (Fig. 15B). TAK-071 (1 mg/kg p.o.) also increased the number of c-Fos-positive cells in the hippocampal formation, including the DG, CA3, CA1, SUB, and EC ($P \leq 0.05$; Fig. 15C and D). The magnitudes of the increases reached 189%, 210%, 286%, 623%, and 269% that of vehicle-treated group in the DG, CA3, CA1, SUB, and EC, respectively (Fig. 15D). TAK-071 (1 mg/kg p.o.) significantly increased the number of c-Fos-positive cells in subcortical areas, including the amygdala, NAc, and CLA ($P \leq 0.05$), but not in the CPu ($P = 0.76$; Fig. 15E and F). The magnitudes of the increases reached 258%, 186%, 201%, and 225% that of the vehicle-treated group in the CEA, BLA, NAc, and CLA, respectively (Fig. 15F). On the other hand, TAK-071 did not increase the number of c-Fos-positive cells in the LS, thalamus, hypothalamus, and PAG ($P > 0.05$; Fig. 15G and H).

As the second experiment (Experiment 2), to confirm dose-dependency of the TAK-071-induced c-Fos expression, the induction of c-Fos expression by TAK-071 was

further assessed at a higher dose (3 mg/kg p.o.). TAK-071 at 1 and 3 mg/kg p.o. produced dose-dependent increases in the number of c-Fos-positive cells in the cortical areas, hippocampal formation, amygdala, NAc, and CLA ($P \leq 0.05$; Fig. 15A–F), and no increase was observed in the number of c-Fos-positive cells in the CPu, LS, thalamus, hypothalamus, and PAG even at 3 mg/kg ($P > 0.05$; Fig. 15F–H).

Overall, TAK-071 induced neural activation in all cortical areas and hippocampal formation examined and in the amygdala, NAc, and CLA.

Induction of c-Fos expression by TAK-071 in combination with donepezil

I evaluated c-Fos induction when TAK-071 was co-administered with donepezil (3 mg/kg p.o.), an acetylcholinesterase (AChE) inhibitor. Donepezil has been reported to inhibit approximately 30–40% of the AChE activity at 3 mg/kg p.o. in the mouse brain and improve cognitive impairment in mice at 0.1 mg/kg p.o. or more [58, 88-90].

In all cortical areas analyzed, donepezil (3 mg/kg p.o.) did not increase the number of c-Fos-positive cells ($P > 0.05$; Fig. 16A and B). The magnitudes of the increases by TAK-071 alone reached 180%, 207%, 205%, 182%, 275%, 517%, and 213% that of the vehicle-treated group in the ACC, PLC, ILC, OC, PPC, S1BF, and TC, respectively (Fig. 16B). The coadministration of TAK-071 (1 mg/kg p.o.) and donepezil (3 mg/kg p.o.) significantly increased the number of c-Fos-positive cells in all cortical areas ($P \leq 0.01$; Fig. 16A and B). The magnitudes of the increases reached 339%, 441%, 296%, 436%, 436%, 1206%, and 743% that of the vehicle-treated group in the ACC, PLC, ILC, OC, PPC, S1BF, and TC, respectively (Fig. 16B). A two-way ANOVA showed significant interactive effects of TAK-071 and donepezil on c-Fos expression in the OC ($P \leq 0.05$) and TC ($P \leq 0.05$) and trends for interactions in the ACC ($P = 0.09$), PLC (P

= 0.07), ILC ($P = 0.22$), PPC ($P = 0.18$), and S1BF ($P = 0.12$).

In all hippocampal subregions analyzed, donepezil did not increase the number of c-Fos-positive cells ($P > 0.05$; Fig. 16C and D). The magnitudes of the increases by TAK-071 alone reached 145%, 227%, 378%, 200%, and 292% that of the vehicle-treated group in the DG, CA3, CA1, SUB, and EC, respectively (Fig. 16D). The coadministration of TAK-071 and donepezil significantly increased the number of c-Fos-positive cells in all subregions of the hippocampal formation ($P \leq 0.01$; Fig. 16C and D). The magnitudes of the increases reached 180%, 378%, 761%, 814%, and 518% that of the vehicle-treated group in the DG, CA3, CA1, SUB, and EC, respectively (Fig. 16D). A two-way ANOVA demonstrated a significant interactive effect of TAK-071 and donepezil on c-Fos expression in the SUB ($P \leq 0.05$) and trends toward significant interactions in the CA1 ($P = 0.11$) and CA3 ($P = 0.07$).

In all subcortical areas examined, donepezil did not increase the number of c-Fos-positive cells ($P > 0.05$; Fig. 16E and F). The magnitudes of the increases by TAK-071 reached 179%, 171%, 200%, and 213% that of the vehicle-treated group in the CEA, BLA, NAc, and CLA, respectively (Fig. 16F). The coadministration of TAK-071 and donepezil significantly increased the number of c-Fos-positive cells in the amygdala, NAc, and CLA ($P \leq 0.01$; Fig. 16E and F). The magnitudes of the increases reached 269%, 287%, 399%, and 607% that of the vehicle-treated group in the CEA, BLA, NAc, and CLA, respectively (Fig. 16F). A two-way ANOVA showed a significant interactive effect of TAK-071 and donepezil on c-Fos expression in the CLA ($P \leq 0.05$) and trends towards significant interactions in the BLA ($P = 0.13$) and NAc ($P = 0.11$). In contrast, c-Fos induction was not observed in the CPu when TAK-071 was administered alone ($P = 0.97$) or in combination with donepezil ($P = 0.83$; Fig. 16F).

In the LS, thalamus, hypothalamus, and PAG, either donepezil or TAK-071 alone did not increase the number of c-Fos-positive cells ($P > 0.05$; Fig. 16G and H). In addition, the combination of TAK-071 and donepezil also did not change the number of c-Fos-positive cells ($P > 0.05$; Fig. 16G and H).

Taken together, the coadministration of TAK-071 and an AChE inhibitor increased c-Fos expression more robustly than the administration of TAK-071 alone in the brain regions where TAK-071 alone increased c-Fos expression.

Discussion

TAK-071 is a novel M_1R PAM that improves scopolamine-induced cognitive impairment with a wide therapeutic margin in rats [33]. To assess the therapeutic potential of TAK-071 in human patients, I compared in vivo pharmacological profiles of TAK-071 and the clinically effective M_1R activator xanomeline in rodents.

A direct comparison of c-Fos expression patterns induced by TAK-071 and xanomeline should be made using the same administration route, as well as at the same time point after drug administration. However, because the pharmacokinetic profile of xanomeline was quite different from that of TAK-071, the administration route and time point of brain collection were adjusted for each drug. Xanomeline has poor oral bioavailability [91], contrary to TAK-071, which is orally bioavailable in rodents [33]. Thus, xanomeline and TAK-071 were administered s.c. and p.o., respectively. The numbers of c-Fos-positive cells after oral and subcutaneous administration of vehicle were comparable in most brain areas analyzed, except for some areas such as ACC and OC (Fig. 14–16). In the exceptional areas such as ACC and OC, the difference of the number of c-Fos-positive cells in the vehicle group between experiments might affect the c-Fos induction. In addition, because c-Fos expression is known to peak 1–2 h after stimulation and last for a few hours [82, 83], the mouse brains were collected within 1–2 h of the time that each drug reached its maximum plasma concentration. Therefore, differences in the route of administration and the time point of brain collection would be unlikely to affect c-Fos expression patterns induced by TAK-071 and xanomeline.

Xanomeline has been reported to induce c-Fos expression in the medial prefrontal cortex and NAc, but not in the CPu, of rats [92]. Consistently, I found that xanomeline increased the number of c-Fos-positive cells in the prefrontal cortex and NAc, but not in

the CPu, of mice (Fig. 14). In addition, xanomeline increased the number of c-Fos-positive cells in the mouse parietal, somatosensory, and temporal cortex, hippocampal formation, and amygdala in this study. Xanomeline mainly activates the M_1R and M_4R, with similar levels of potency and efficacy [78]. However, the selective activation of only the M_4R did not induce c-Fos expression in the prefrontal areas and NAc [93], even though *Chrm4* is highly expressed in these areas (©2004 Allen Institute for Brain Science. Available from: http://mouse.brain-map.org) [84]. Thus, the contribution of M_4R activation in the induction of c-Fos expression by xanomeline might be limited.

TAK-071 at 1 and 3 mg/kg p.o. dose-dependently increased c-Fos expression in the cortical areas, hippocampal formation, amygdala, NAc, and CLA, but not in the CPu, LS, thalamus, hypothalamus, and PAG (Fig. 15). However, an observer counted the number of c-Fos-positive cells in an unblinded manner; this is a limitation of this study. I independently evaluated the effects of TAK-071 at 1 mg/kg p.o. on c-Fos expression thrice (Experiments 1 and 2 in Fig. 15 and TAK-071 alone group in Fig. 16), and observed c-Fos induction in the same brain areas for all three experiments. Therefore, it is evident that TAK-071 induced c-Fos expression in the cortical areas, hippocampal formation, amygdala, NAc, and CLA, but not in the CPu, LS, thalamus, hypothalamus, and PAG. The TAK-071-induced c-Fos expression pattern was similar to that induced by xanomeline. Both TAK-071 and xanomeline induced c-Fos expression in the brain regions where *Chrm1* was highly expressed, but these compounds did not induce expressions in the regions where *Chrm1* was weakly expressed (Allen Mouse Brain Atlas) [84]. Thus, it appears that these compounds induce c-Fos expression specifically in the areas with high expression levels of *Chrm1*.

Donepezil can increase ACh levels; therefore, with a higher concentration of ACh,

TAK-071 could more robustly activate M_1R and potently induce c-Fos expression in combination with donepezil (Fig. 16). The synergistic effect of an M_1R PAM and donepezil on c-Fos expression is consistent with the IP1 assay and behavioral study results when TAK-071 was combined with donepezil [33]. However, because xanomeline is an M_1R agonist, its efficacy is not dependent on the ACh concentration. Thus, a combination of xanomeline with donepezil may not be able to produce synergistic efficacy although further studies are needed.

TAK-071 and xanomeline at their efficacious doses induced c-Fos expression in the brain regions that are related to procognitive and antipsychotic-like efficacy, such as the cortical areas, hippocampal formation, and NAc. Thus, neural activation in these regions might contribute to their efficacy. However, xanomeline elicited salivation and hypoactivity at the dose used in the c-Fos study (Table 14). Although the brain regions where c-Fos induction was observed, such as cortical areas and hippocampal formation, are not related to salivation and hypoactivity, these side effects may indirectly affect c-Fos expression induced by xanomeline. Thus, c-Fos induction by xanomeline should be carefully interpreted.

In patients with AD, xanomeline robustly improved cognitive function [13]. Magnetic resonance imaging analyses have revealed that the atrophy of the hippocampus, EC, and amygdala is consistently observed in patients with AD and the volumes of these areas correlate with the severity of dementia [94-96]. Furthermore, positron emission tomography studies have revealed that regional glucose metabolism, a marker of synaptic activity, is markedly reduced in these brain regions [97, 98]. Both xanomeline and TAK-071 induced neural activation in these severely affected areas in mice (Fig. 14 and 15). In addition, xanomeline and TAK-071 restored the scopolamine-induced cognitive

impairment, which are often used as a preclinical model of the cognitive impairment associated with cholinergic hypofunction in patients with AD (Fig. 12A) [33]. Furthermore, the coadministration of TAK-071 and an AChE inhibitor synergistically induced neural activation in the same brain regions (Fig. 16) and improved the scopolamine-induced cognitive impairment without exacerbating the side effects [33]. Thus, like xanomeline, TAK-071 alone or the combination of TAK-071 and an AChE inhibitor might activate the brain regions that mediate cognitive function and in turn show efficacy on the cognitive impairment in patients with AD.

In patients with schizophrenia, xanomeline attenuates cognitive deficits, particularly working memory and verbal learning deficits [14]. The prefrontal areas are the key brain areas for these cognitive domains [99, 100]. In these areas, like xanomeline, TAK-071 induced neural activation (Fig. 14 and 15). Furthermore, recent studies have reported that selective M_1R PAMs, VU0453595 and VU6004256, reverse impaired long-term depression and improve prefrontal-dependent cognitive deficits in novel object recognition and cued fear conditioning tasks in two animal models of schizophrenia, the NR1 subunit of the *N*-methyl-D-aspartate receptor knockdown mice and mice repeatedly treated with phencyclidine [81, 101]. Thus, TAK-071 might improve prefrontal-dependent cognitive impairment through the activation of prefrontal areas. The effectiveness of TAK-071 on these impairments should be investigated in our future studies.

The ability of antipsychotics to induce c-Fos expression in the NAc is associated with their antipsychotic efficacy [102]. Similar to antipsychotics, xanomeline and TAK-071 increased c-Fos expression in the NAc, but not in the CPu, of mice (Fig. 14 and 15). As expected, xanomeline produced antipsychotic-like effects in multiple rodent models

(Fig. 11A and B) [103, 104] and showed a significant improvement in the positive symptoms of schizophrenia [14]. Interestingly, TAK-071 suppressed only MK-801-induced hyperlocomotion, while xanomeline suppressed both METH- and MK-801-induced hyperlocomotion (Fig. 11). The suppression of amphetamine-induced hyperlocomotion by xanomeline was partially reduced in M_1R KO mice and completely abolished in M_4R KO mice [80]. This suggests that pharmacological efficacy is mediated predominantly through M_4R, but also partially through M_1R. Furthermore, an increase in the c-Fos expression in the NAc by TAK-071 was attenuated compared to that induced by xanomeline at the dose that produced antipsychotic-like effects (2.0–3.0-fold vs. 5.9-fold; Fig. 14F and 15F). Thus, activation of M_1R alone might be insufficient to induce the neural activation required for producing robust antipsychotic-like effects.

I previously reported that TAK-071 causes diarrhea at a dose that is 33-fold higher than its procognitive dose in rats [33]. Conversely, as shown in the present study and other studies, xanomeline causes diarrhea as well as salivation and hypoactivity at equal or lower doses than those required to elicit antipsychotic-like and procognitive effects in rodents and monkeys (Tables 13 and 14 and Fig. 11 and 12) [49, 91]. Notably, salivation and hypoactivity were present even in the *Chrm1*-KO mice (Table 15). Thus, it appears that the contribution of M_1R is limited to salivation and hypoactivity. However, diarrhea induced by M_1R PAMs, such as TAK-071 and benzyl quinolone carboxylic acid, has been suggested to be mediated by M_1R [24, 33]. Furthermore, I previously showed that high cooperative M_1R PAMs enhance ileum contraction in an *in vitro* assay. Thus, I hypothesized that M_1R PAM-induced diarrhea is caused by the activation of M_1R in GI tissues. To verify our hypothesis, it would be interesting in future studies to evaluate the number of c-Fos-positive cells in the brain regions involved in the regulation of GI

functions, such as the nucleus tractus solitarius.

Unlike xanomeline, TAK-071 induced c-Fos expression in the OC and CLA (Fig. 14 and 15). The OC has been implicated in various brain functions, such as sensory integration, reward processing, and decision making [105], and OC abnormalities have been reported in patients with schizophrenia [106, 107]. The CLA is reciprocally connected with various cortical areas, the hippocampus, and subcortical areas, and the CLA is thought to mediate sensory integration [108], although its exact function remains unclear. Neuronal loss and neurofibrillary tangles have been reported in the CLA of patients with AD [109]. Contrary to TAK-071, xanomeline shows limited selectivity for M_1R. Neural activation by stimulation of M_1R may be canceled by either activating or inhibiting other receptors, such as M_4R and 5-HT_2 receptor, in the relevant areas. Therefore, c-Fos expression may not be induced by xanomeline in the OC and CLA, although further studies are needed. Overall, the activation of these additional areas by TAK-071 suggests that TAK-071 may potentially provide additional effects compared with xanomeline in the treatment of patients with AD and schizophrenia.

In this study, I used male mice to characterize c-Fos expression patterns induced by TAK-071 and xanomeline. However, in some cases, differences in c-Fos expression patterns have been observed between male and female mice [110, 111]. Thus, it may be worthwhile to also compare c-Fos expression patterns induced by these compounds in female mice. In addition, although I analyzed c-Fos induction in only a limited number of brain areas in this study, there are many other interesting brain areas that could be assessed. For example, distinct c-Fos expression patterns are induced by some drugs, such as olanzapine and clozapine, in the CA2 [112, 113]. The CA2 area is impacted in patients with schizophrenia and plays a pivotal role in social memory, when compared to the other

hippocampal subregions [114, 115]. Thus, the evaluation of c-Fos expression induced by xanomeline and TAK-071, not only in the CA1, CA3, and DG but also in the CA2, would be interesting. Furthermore, in the relatively large regions of the brain, such as the hippocampus and OC, effects of xanomeline and TAK-071 on c-Fos induction may be different depending on the sub-area analyzed. Although it is strenuous to count the number of c-Fos-positive cells in all brain areas using immunohistochemical techniques, recently reported automated c-Fos expression analysis, using c-Fos-GFP mice and serial two-photon tomography, would enable comprehensively mapping of c-Fos expression [116].

In summary, together with our previous report [33], the present study shows that TAK-071 had a 33-fold difference between the dose that induced cognitive improvement and the dose that induced cholinergic side effects, while xanomeline showed cognitive improvement and antipsychotic-like effects at equal or higher doses than those required to elicit cholinergic side effects in rodents. Furthermore, TAK-071 and xanomeline induced similar neural activation patterns in the brain areas that are related to procognitive and antipsychotic-like efficacy. Thus, TAK-071 may have the potential to induce procognitive and antipsychotic-like effects with minimal cholinergic side effects. Clinical studies of TAK-071 are currently ongoing (ClinicalTrials.gov Identifier: NCT02769065).

Tables and Figures

Table 13. Side effects induced by xanomeline in rats.

Xanomeline (mg/kg i.p.)	Loose stools and diarrhea	Lacrimation	Salivation	Hypoactivity
Vehicle	0/6	0/6	0/6	0/6
1	1/6	0/6	1/6	0/6
3	2/6	0/6	1/6	0/6
10	2/6	0/6	3/6	1/6
30	3/6	0/6	2/6	3/6

The data are presented as the number of animals showing side effects over the total number of animals tested.

Table 14. Side effects induced by xanomeline in mice.

Xanomeline (mg/kg s.c.)	Loose stools and diarrhea	Lacrimation	Salivation	Hypoactivity
Vehicle	0/6	0/6	0/6	0/6
0.3	0/6	0/6	0/6	0/6
1	0/6	0/6	0/6	2/6
3	0/6	0/6	2/6	5/6
10	0/6	0/6	4/6	6/6

The data are presented as the number of animals showing side effects over the total number of animals tested.

Table 15. Side effects induced by xanomeline in *Chrm1* WT and KO mice.

Genotype	Xanomeline (mg/kg s.c.)	Loose stools and diarrhea	Lacrimation	Salivation	Hypoactivity
WT	Vehicle	0/6	0/6	0/6	0/6
	10	0/6	0/6	6/6	6/6
KO	Vehicle	0/6	0/6	0/6	0/6
	10	0/6	0/6	6/6	6/6

The data are presented as the number of animals showing side effects over the total number of animals tested.

Table 16. Pharmacokinetics of TAK-071 in mice

TAK-071 (mg/kg p.o.)	0.03	0.1	0.3	1	3
Cmax (ng/mL)	52 ± 7	164 ± 14	472 ± 57	1728 ± 196	4514 ± 256
Tmax (h)	0.8 ± 0.3	0.8 ± 0.3	0.7 ± 0.3	0.8 ± 0.3	1.0 ± 0.0

Blood samples were collected at 0.5, 1, 2, 4, and 6 h after oral administration of TAK-071.

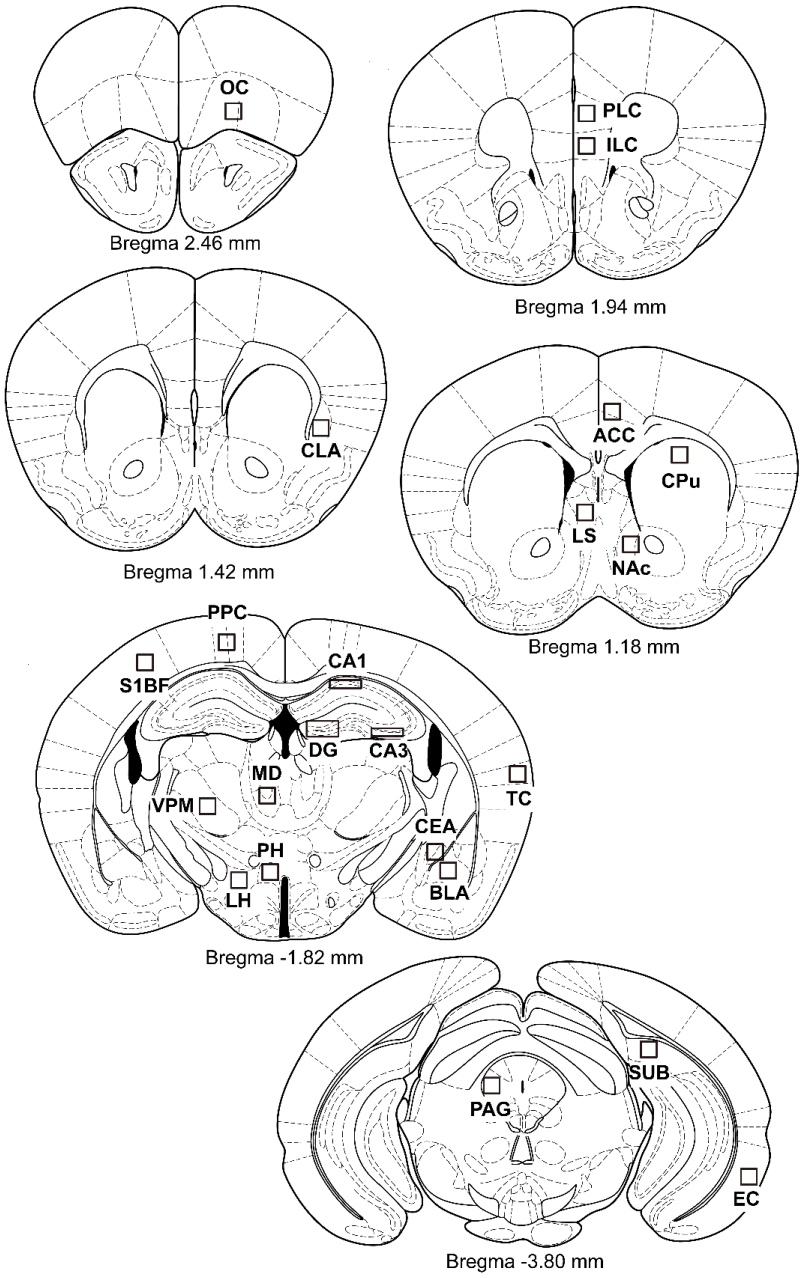

Figure 10. Schematic diagrams of coronal sections modified from the mouse brain atlas [117]. The squares indicate the areas where c-Fos-positive cells were counted. Abbreviations: ACC, anterior cingulate cortex; BLA, basolateral nucleus of the amygdala; CEA, central nucleus of the amygdala; CLA, claustrum; CPu, caudate putamen; DG, dentate gyrus; EC, entorhinal cortex; ILC, infralimbic cortex; LH, lateral hypothalamic area; LS, lateral septum; MD, mediodorsal thalamic nucleus; NAc, nucleus

accumbens; OC, orbital cortex; PAG, periaqueductal gray; PH, posterior hypothalamic area; PLC, prelimbic cortex; PPC, posterior parietal cortex; S1BF, primary somatosensory cortex barrel field; SUB, subiculum; TC, temporal cortex; VPM, ventral posteromedial thalamic nucleus.

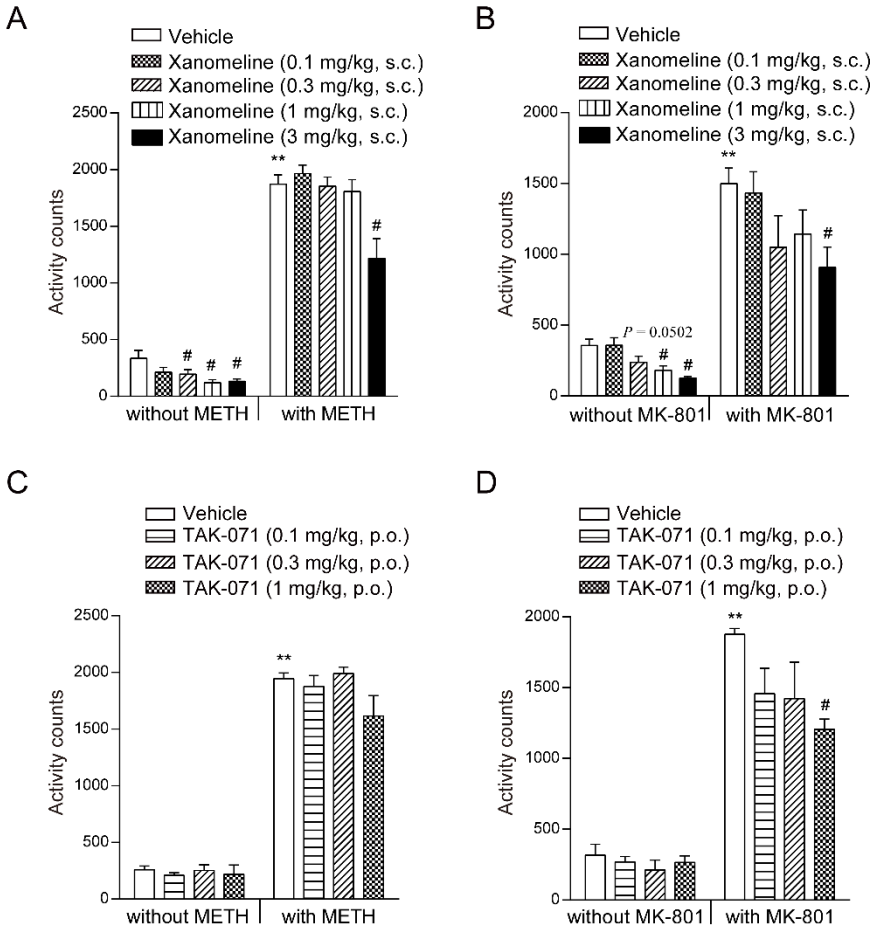

Figure 11. Effects of xanomeline and TAK-071 with/without psychostimulants on locomotion in mice. METH (A; 2 mg/kg s.c.) or MK-801 (B; 0.3 mg/kg s.c.) was coadministered with xanomeline. METH (C; 2 mg/kg s.c.) or MK-801 (D; 0.3 mg/kg s.c.) was administered 120 min after oral administration of TAK-071. After the drug treatment, locomotion was measured for 60 min. The cumulative locomotion during the 60-min test session is shown as the mean ± S.E.M. (n = 5–6 in each treatment group). #$P \leq 0.05$ compared with the vehicle-treated group using two-tailed Williams' test (homogenous data) or two-tailed Shirley-Williams' test (nonhomogenous data). **$P \leq 0.01$ compared between the vehicle-treated group and vehicle + psychostimulants-treated group using Student's t-test (homogenous data) or Aspin-Welch test (nonhomogenous data).

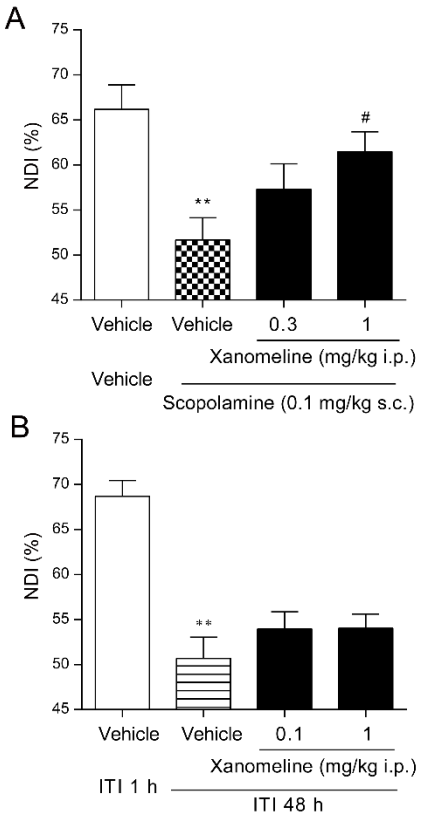

Figure 12. Effects of xanomeline on scopolamine-induced cognitive impairment (A) and natural forgetting (B) in a rat NOR task. (A) Scopolamine hydrobromide (0.1 mg/kg s.c.) and xanomeline (i.p.) were injected 30 min before the acquisition trial. The retention trial was performed 4 h after the acquisition trial. (B) Xanomeline (i.p.) was injected 30 min before the acquisition trial. The retention trial was performed 1 and 48 h after the acquisition trial. The novel discrimination index (NDI) was calculated as the ratio of the total time spent exploring the novel object to the total time spent exploring both objects. The results are presented as the mean ± S.E.M. (n = 10 in each treatment group). $^{**}P \leq 0.01$ compared with the vehicle-treated group (A) and between the intertrial interval (ITI) of 1 and 48 h in the vehicle-treated group (B) in Student's *t*-test. $\#P \leq 0.05$ versus vehicle + scopolamine group in two-tailed Williams' test.

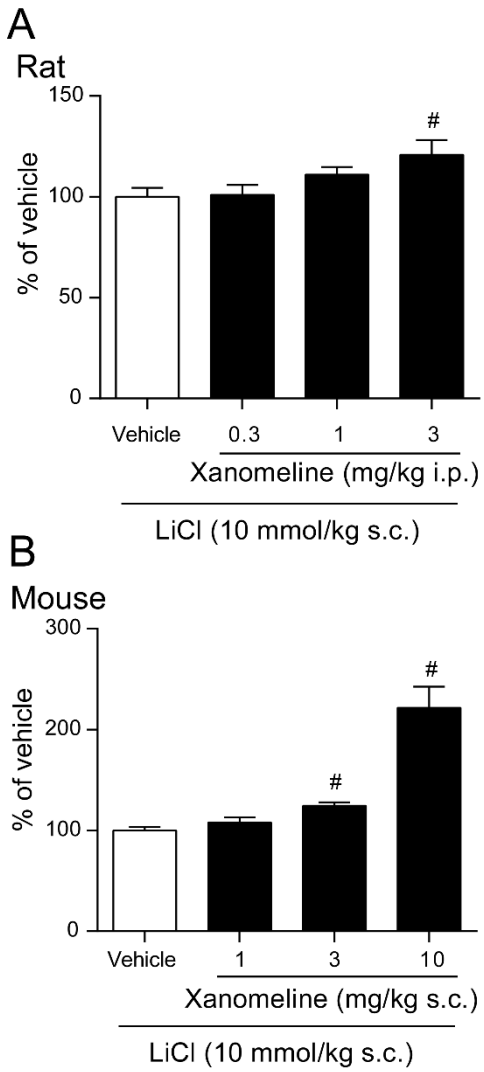

Figure 13. Effects of xanomeline on IP1 production in the hippocampus of rats (A) and mice (B). (A) Thirty min after the i.p. administration of xanomeline, rats were injected s.c. with LiCl (10 mmol/kg). (B) Xanomeline and LiCl (10 mmol/kg) were injected s.c. at the same time in the mice. One h after the LiCl injections, the animals were sacrificed to collect the hippocampus. The data are presented as the mean ± S.E.M. (n = 6 in each treatment group). #$P \leq 0.05$ compared with the vehicle-treated group using two-tailed Williams' test (homogenous data) or two-tailed Shirley-Williams' test (nonhomogenous data).

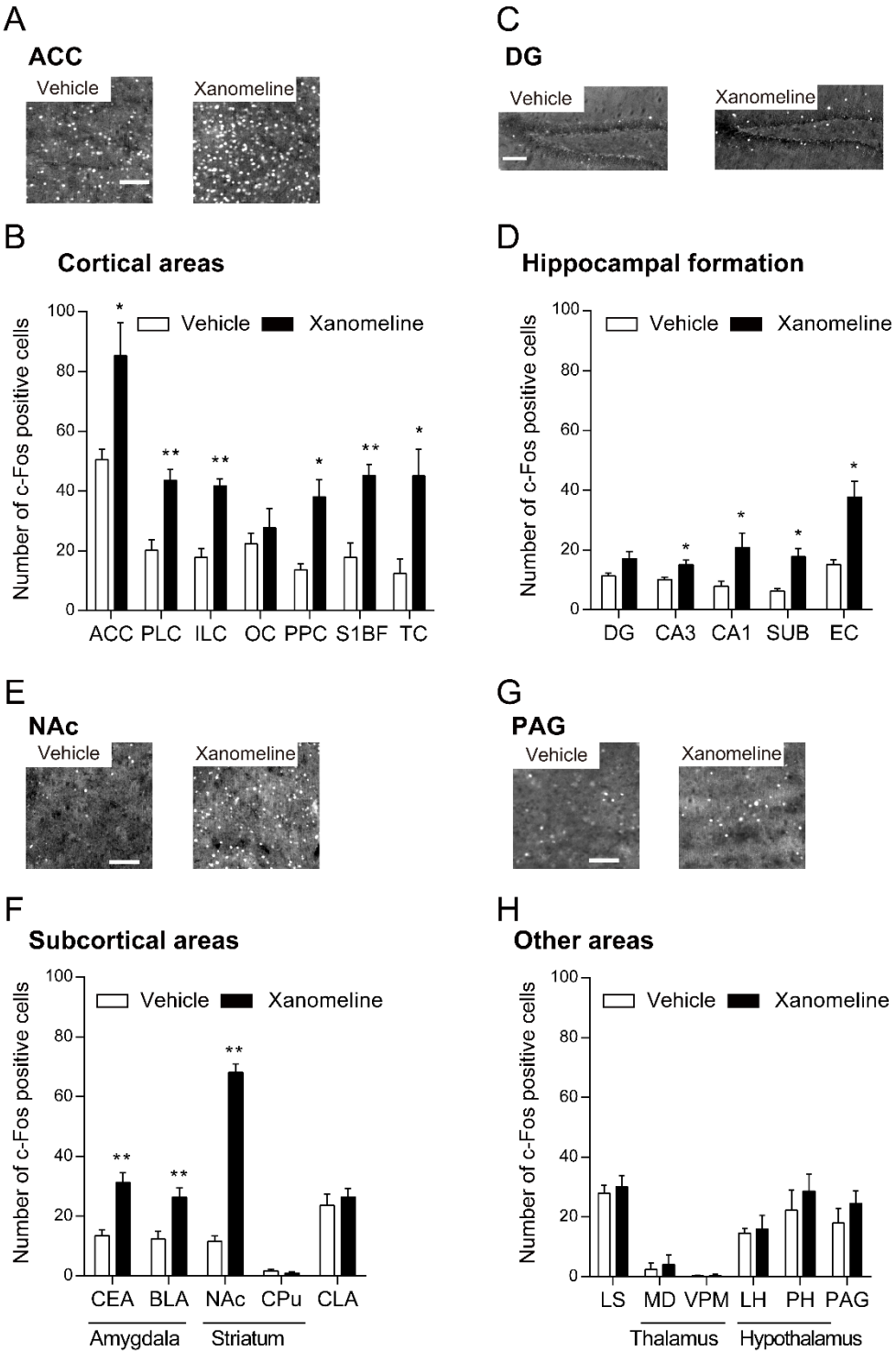

Figure 14. Effects of xanomeline on c-Fos expression in the cortical areas, hippocampal formation, subcortical areas, and other areas. Xanomeline (3 mg/kg s.c.) was injected 1.25 h before the brain collection. (A, C, E, G) Representative images

of c-Fos immunoreactivity in the ACC (A), DG (C), NAc (E), and PAG (G). Scale bars = 100 μm. (B, D, F, H) The number of c-Fos-positive cells in the cortical areas (B), hippocampal formation (D), subcortical areas (F), other areas (H). The data are presented as the mean ± S.E.M. (n = 5 in each treatment group). *$P \leq 0.05$ and **$P \leq 0.01$ compared with the vehicle-treated group using Student's t-test (homogenous data) or Aspin-Welch test (nonhomogenous data).

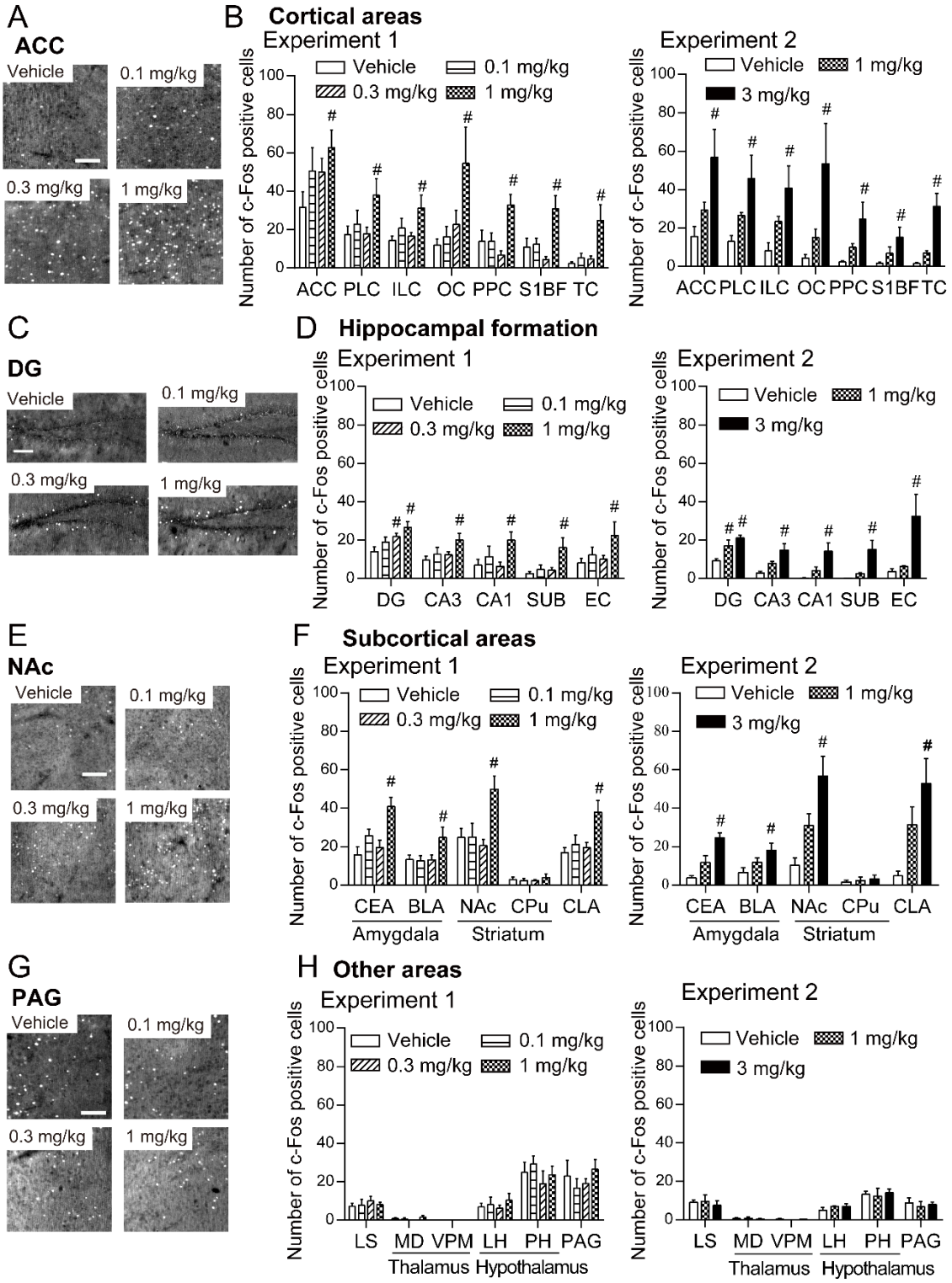

Figure 15. Effects of TAK-071 on c-Fos expression in the cortical areas, hippocampal formation, subcortical areas, and other areas. In experiment 1, TAK-071 was orally administered at 0.1, 0.3, and 1 mg/kg. In experiment 2, TAK-071 was orally administered

at 1 and 3 mg/kg. Brains were collected 3 h after administration. (A, C, E, G) Representative images of c-Fos immunoreactivity in the ACC (A), DG (C), NAc (E), and PAG (G). Scale bars = 100 μm. (B, D, F, H) The number of c-Fos-positive cells in the cortical areas (B), hippocampal formation (D), subcortical areas (F), and other areas (H). The data are presented as the mean ± S.E.M. (n = 5 and n = 4 in each treatment group of Experiment 1 and Experiment 2, respectively). #$P \leq 0.05$ compared with the vehicle-treated group using two-tailed Williams' test.

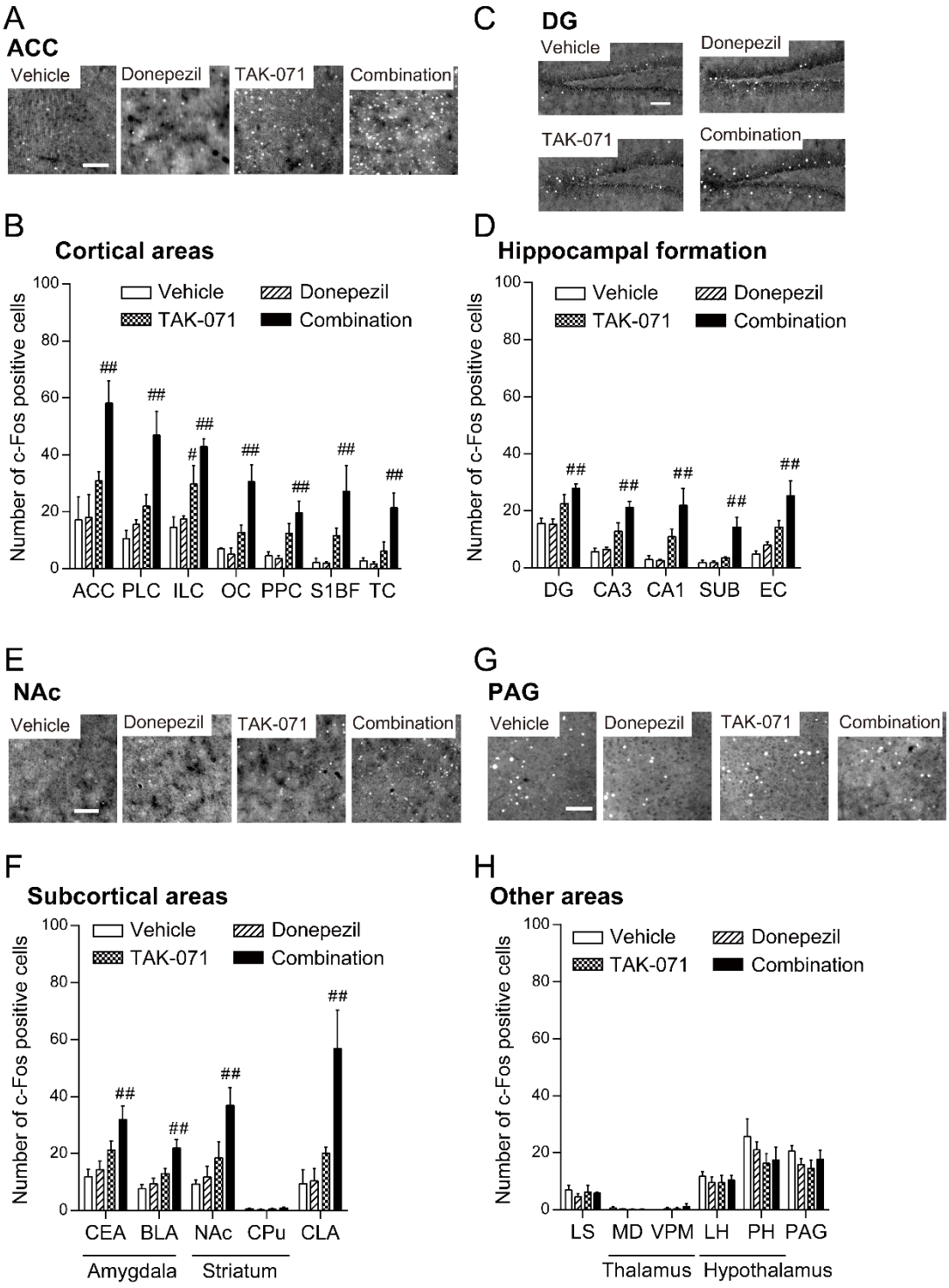

Figure 16. Effects of the combination of TAK-071 and donepezil on c-Fos expression in the cortical areas, hippocampal formation, subcortical areas, and other areas. Three h after the oral administration of TAK-071 (1 mg/kg), donepezil (3 mg/kg), or their

combination, c-Fos expression was detected by immunohistochemistry. (A, C, E, G) Representative images of c-Fos immunoreactivity in the ACC (A), DG (C), NAc (E), and PAG (G). Scale bars = 100 μm. (B, D, F, H) The number of c-Fos-positive cells in the cortical areas (B), hippocampal formation (D), subcortical areas (F), and other areas (H). The data are shown as the mean ± S.E.M. (n = 4 in each treatment group). #$P \leq 0.05$ and ##$P \leq 0.01$ compared with the vehicle-treated group using Dunnett's test.

General Discussion

ACh plays an important role in the regulation of cognitive functions [1]. However, it is unclear through which receptors ACh controls cognitive functions. Recently, it was reported that M_1R deletion in mice led to cognitive impairment, suggesting that M_1R contributes to the control of cognitive functions via ACh [16, 17]. In this study, to obtain additional insight into the roles of M_1R in cognitive functions of the rodent brain, I investigated the impact of M_1R selective activation on cognitive functions using highly selective M_1R PAMs. Furthermore, since dysfunction of cholinergic neurotransmission is implicated in cognitive impairment in neurodegenerative and neuropsychiatric diseases such as AD and schizophrenia, elucidating the importance of M_1R in cognitive functions may lead to the development of a novel therapy for the treatment of cognitive impairment.

Behavioral studies have been used to evaluate cognitive functions in rodents. Behavioral studies can be affected by various factors such as the environment and side effects. In particular, side effects caused by a compound of interest can severely affect the interpretation of results of behavioral studies. Thus, a compound that does not cause side effects is needed as a tool to precisely evaluate cognitive functions. Although multiple highly selective M_1R PAMs have recently been reported, these compounds induced side effects, such as convulsion and GI dysfunction, even at low doses [24-26]. Thus, it was difficult to precisely evaluate the impact of M_1R selective activation on cognitive functions. In this study, I selected two M_1R PAMs, T-495 and MK-7622. T-495 was discovered by Takeda Pharmaceutical Company Limited based on Takeda's original screening strategy to reduce the liability of side effects [24, 33]. MK-7622 was discovered by Merck & Co., Inc. and its phase II clinical study was conducted [34-36]. Firstly, I confirmed whether these compounds were suitable for the evaluation of cognitive

functions. Both compounds were highly selective for M_1R and activated M_1R in the rodent brain after oral administration (Fig. 1 and 3). While T-495 ameliorated scopolamine-induced cognitive deficits in rats at a 100-fold lower dose than that required for the induction of diarrhea, MK-7622 showed cognitive improvement and induction of diarrhea at an equal dose (Fig. 4 and 5). Thus, I found that T-495 is an ideal tool to evaluate the impact of M_1R selective activation on cognitive functions. It is unclear why T-495 had a wider margin between cognitive improvement and GI side effects than MK-7622. My research group previously found that fine adjustment of cooperativity of an M_1R PAM is key to reducing the liability of GI side effects although detailed mechanisms are still unclear [24, 33]. Recently, high-resolution structures of muscarinic receptors bound to agonists, antagonists, or PAMs have been reported [118, 119]. If high-resolution structures of M_1R bound to T-495 or MK-7622 are resolved, M_1R PAMs with a wide margin between cognitive improvement and GI side effects are efficiently identified by *in silico* approaches.

Donepezil, an AChEI, increases ACh at the synaptic cleft by suppressing the degradation of ACh, leading to the activation of all ACh receptors at the synaptic cleft. Thus, in this study, I used donepezil as a tool to non-selectively activate ACh receptors. Xanomeline is a muscarinic ACh receptor agonist with limited selectivity for M_1R. Thus, I used xanomeline as a tool to non-selectively activate muscarinic ACh receptors. Similar to T-495, both donepezil and xanomeline improved scopolamine-induced cognitive deficits in rats (Fig. 4 and 12) [33]. Furthermore, donepezil reversed memory deficits also in a disease-relevant model (CaMKIIα-tTA/A53T α-syn dTg mice) as did T-495 (Fig. 8 and 9). Since selective activation of M_1R produced the same efficacy as the activation of non-selective ACh receptors and non-selective muscarinic ACh receptors, the

improvement of cognitive deficits is suggested to be caused mainly by the activation of M_1R. A limitation of this study is that the efficacy of each compound was evaluated in independent tests. Thus, in a future study, a head-to-head comparison should be conducted. Although there is a limitation, selective activators of M_1R can provide a novel treatment for patients with cognitive impairment.

Combining the studies using M_1R KO mice [16, 17] and this study using an M_1R PAM (Fig. 4 and 9), clearly show that M_1R is mainly involved in the control of cognitive functions in rodents. To increase the success rate of M_1R activators in clinical trials, evidence not only in rodents but also in monkeys and humans is needed. Recently, it was reported that M_1R PAMs can restore scopolamine-induced cognitive deficits in monkeys [29, 49]. Furthermore, a study using single photon emission computed tomography with ^{123}I-IDEX, an M_1R antagonist, as a radio tracer showed that reduced M_1R levels in the dorsolateral prefrontal cortex were correlated with worsened performances in verbal learning and memory in humans with psychosis [120]. Therefore, M_1R activation might also improve cognitive impairment in humans.

The molecular mechanisms by which M_1R activation can enhance cognitive functions remain unclear. It has been reported that M_1R activation potentiates *N*-methyl-D-aspartate receptor (NMDAR) currents, leading to neural activation and synaptic plasticity [16, 81, 121]. In line with this evidence, TAK-071 reversed hyperactivity induced by MK-801, an NMDAR antagonist (Fig. 11). In addition, TAK-071 significantly increased c-Fos expression, a marker of neural activation, in several brain regions (Fig. 15). It is well known that synaptic plasticity, long-term potentiation and long-term depression, are critical for cognitive functions. Therefore, M_1R activation enhances cognitive functions probably through the enhancement of NMDAR and the subsequent

neural activation and facilitation of synaptic plasticity, although further studies are needed to confirm this.

In this study, I used the NOR test, CFC test, and Y-maze task to evaluate cognitive functions. The NOR test, CFC test, and Y-maze task can measure recognition memory, associative learning, and spatial working memory, respectively. Cognitive functions include not only learning and memory but also attention and executive function. Furthermore, learning and memory are divided into various categories. Thus, assessment of the impact of M_1R activation on attention and executive function and other categories of learning and memory using behavioral tests will further provide biological insights into the contribution of M_1R in the regulation of cognitive functions.

To understand *in vivo* functional roles of a protein, genetic approaches such as knockdown and KO of a gene encoding the target protein are useful. However, genetic approaches have some disadvantages: 1) knockdown or KO of a target gene during the prenatal period has the potential to inhibit normal development, thus affecting the phenotypes observed in the adult stage; 2) it is difficult to investigate the impact on phenotypes when the target protein is activated. Thus, as in this study, pharmacological approaches using small molecules that can selectively activate or inhibit the target protein can further provide insight into *in vivo* functional roles of the target protein. While M_1R is highly expressed in the brain, such as the cortex and hippocampus, it is also highly expressed in the salivary glands and prostate [15, 23, 122]. A study using M_1R KO mice suggested that M_1R facilitates the secretion of saliva in salivary glands [123]. In contrast, there are no reports investigating the roles of M_1R in the prostate. Therefore, highly selective M_1R PAMs may provide opportunities to understand the functions of M_1R in the salivary glands and prostate.

In conclusion, the present study found that activation of M_1R enhances cognitive functions through neural activation in rodents. This finding contributes to an understanding of the roles of M_1R in cognitive functions. In addition, these results demonstrate that an M_1R PAM can be a novel therapeutic agent for the treatment of cognitive impairment in neurodegenerative and neuropsychiatric diseases, such as AD, DLB, and schizophrenia.

Acknowledgements

I am deeply grateful to Professor Chikafumi Chiba of the University of Tsukuba for supervising my work and for providing valuable discussion throughout my doctoral program. I am also grateful to Professor Kazuto Nakada, Professor Kentaro Nakano, and Associate Professor Ryuhei Harada of the University of Tsukuba for guiding my work and for providing valuable discussion throughout my doctoral program.

Chapter I:

I would like to thank the following employees of Takeda Pharmaceutical Company Limited: Tomohiro Ohashi, Jinichi Yonemori, Tomohiro Okawa, Hideo Suzuki, Hitoaki Nishikawa, and Shoutarou Miura for providing T-495; Toshihiro Imaeda for supplying MK-7622; Takahiro Sugimoto, Shinkichi Suzuki, Takuto Kojima, Kenichiro Shimokawa, Masataka Murakami, Hiroki Sakamoto, Masami Yamada, and Makoto Kamata for providing valuable advice and participating in discussions on the identification of T-495; Noriko Suzuki and Yuichi Arakawa for conducting the NOR test; Motohisa Suzuki for helpful discussions regarding the NOR test; and Yasuyuki Debori for performing pharmacokinetic studies. I also thank the following employees of Axcelead Drug Discovery Partners, Inc.: Naoya Nishimura and Michiyasu Takeyama for generating transgenic animals and Chisato Takahara, Takeo Moriya, and Tomohiro Andou for quantifying ACh.

Chapter II:

I thank Dr. Noriko Suzuki for performing the NOR task and Dr. Masami Yamada for providing the chemical compounds.

References

1. Picciotto, M. R., Higley, M. J. & Mineur, Y. S. (2012) Acetylcholine as a neuromodulator: cholinergic signaling shapes nervous system function and behavior, *Neuron.* **76**, 116-29.

2. Klinkenberg, I. & Blokland, A. (2010) The validity of scopolamine as a pharmacological model for cognitive impairment: a review of animal behavioral studies, *Neurosci Biobehav Rev.* **34**, 1307-50.

3. Shiozaki, K., Iseki, E., Uchiyama, H., Watanabe, Y., Haga, T., Kameyama, K., Ikeda, T., Yamamoto, T. & Kosaka, K. (1999) Alterations of muscarinic acetylcholine receptor subtypes in diffuse lewy body disease: relation to Alzheimer's disease, *J Neurol Neurosurg Psychiatry.* **67**, 209-13.

4. Tiraboschi, P., Hansen, L. A., Alford, M., Sabbagh, M. N., Schoos, B., Masliah, E., Thal, L. J. & Corey-Bloom, J. (2000) Cholinergic dysfunction in diseases with Lewy bodies, *Neurology.* **54**, 407-11.

5. Ballard, C., Piggott, M., Johnson, M., Cairns, N., Perry, R., McKeith, I., Jaros, E., O'Brien, J., Holmes, C. & Perry, E. (2000) Delusions associated with elevated muscarinic binding in dementia with Lewy bodies, *Ann Neurol.* **48**, 868-76.

6. Bartus, R. T., Dean, R. L., 3rd, Beer, B. & Lippa, A. S. (1982) The cholinergic hypothesis of geriatric memory dysfunction, *Science.* **217**, 408-14.

7. Hall, H., Reyes, S., Landeck, N., Bye, C., Leanza, G., Double, K., Thompson, L., Halliday, G. & Kirik, D. (2014) Hippocampal Lewy pathology and cholinergic dysfunction are associated with dementia in Parkinson's disease, *Brain.* **137**, 2493-508.

8. Samuel, W., Alford, M., Hofstetter, C. R. & Hansen, L. (1997) Dementia with Lewy bodies versus pure Alzheimer disease: differences in cognition, neuropathology, cholinergic dysfunction, and synapse density, *J Neuropathol Exp Neurol.* **56**, 499-508.

9. Tiraboschi, P., Hansen, L. A., Alford, M., Merdes, A., Masliah, E., Thal, L. J. & Corey-Bloom, J. (2002) Early and widespread cholinergic losses differentiate dementia with Lewy bodies from Alzheimer disease, *Arch Gen Psychiatry.* **59**, 946-51.

10. Bierer, L. M., Haroutunian, V., Gabriel, S., Knott, P. J., Carlin, L. S., Purohit, D. P., Perl, D. P., Schmeidler, J., Kanof, P. & Davis, K. L. (1995) Neurochemical correlates of dementia severity in Alzheimer's disease: relative importance of the cholinergic deficits, *J Neurochem.* **64**, 749-60.

11. Rolinski, M., Fox, C., Maidment, I. & McShane, R. (2012) Cholinesterase inhibitors

for dementia with Lewy bodies, Parkinson's disease dementia and cognitive impairment in Parkinson's disease, *Cochrane Database Syst Rev*, CD006504.

12. Birks, J. (2006) Cholinesterase inhibitors for Alzheimer's disease, *Cochrane Database Syst Rev*, CD005593.

13. Bodick, N. C., Offen, W. W., Levey, A. I., Cutler, N. R., Gauthier, S. G., Satlin, A., Shannon, H. E., Tollefson, G. D., Rasmussen, K., Bymaster, F. P., Hurley, D. J., Potter, W. Z. & Paul, S. M. (1997) Effects of xanomeline, a selective muscarinic receptor agonist, on cognitive function and behavioral symptoms in Alzheimer disease, *Arch Neurol.* **54**, 465-73.

14. Shekhar, A., Potter, W. Z., Lightfoot, J., Lienemann, J., Dube, S., Mallinckrodt, C., Bymaster, F. P., McKinzie, D. L. & Felder, C. C. (2008) Selective muscarinic receptor agonist xanomeline as a novel treatment approach for schizophrenia, *Am J Psychiatry.* **165**, 1033-9.

15. Levey, A. I. (1993) Immunological localization of m1-m5 muscarinic acetylcholine receptors in peripheral tissues and brain, *Life Sci.* **52**, 441-8.

16. Anagnostaras, S. G., Murphy, G. G., Hamilton, S. E., Mitchell, S. L., Rahnama, N. P., Nathanson, N. M. & Silva, A. J. (2003) Selective cognitive dysfunction in acetylcholine M1 muscarinic receptor mutant mice, *Nat Neurosci.* **6**, 51-8.

17. Gould, R. W., Dencker, D., Grannan, M., Bubser, M., Zhan, X., Wess, J., Xiang, Z., Locuson, C., Lindsley, C. W., Conn, P. J. & Jones, C. K. (2015) Role for the M1 Muscarinic Acetylcholine Receptor in Top-Down Cognitive Processing Using a Touchscreen Visual Discrimination Task in Mice, *ACS Chem Neurosci.* **6**, 1683-95.

18. Conn, P. J., Christopoulos, A. & Lindsley, C. W. (2009) Allosteric modulators of GPCRs: a novel approach for the treatment of CNS disorders, *Nat Rev Drug Discov.* **8**, 41-54.

19. Jones, C. K., Byun, N. & Bubser, M. (2012) Muscarinic and nicotinic acetylcholine receptor agonists and allosteric modulators for the treatment of schizophrenia, *Neuropsychopharmacology.* **37**, 16-42.

20. Inglis, F. (2002) The tolerability and safety of cholinesterase inhibitors in the treatment of dementia, *Int J Clin Pract Suppl*, 45-63.

21. Stinton, C., McKeith, I., Taylor, J. P., Lafortune, L., Mioshi, E., Mak, E., Cambridge, V., Mason, J., Thomas, A. & O'Brien, J. T. (2015) Pharmacological Management of Lewy

Body Dementia: A Systematic Review and Meta-Analysis, *Am J Psychiatry.* **172**, 731-42.
22. Hansen, R. A., Gartlehner, G., Webb, A. P., Morgan, L. C., Moore, C. G. & Jonas, D. E. (2008) Efficacy and safety of donepezil, galantamine, and rivastigmine for the treatment of Alzheimer's disease: a systematic review and meta-analysis, *Clin Interv Aging.* **3**, 211-25.
23. Ito, Y., Oyunzul, L., Seki, M., Fujino Oki, T., Matsui, M. & Yamada, S. (2009) Quantitative analysis of the loss of muscarinic receptors in various peripheral tissues in M1-M5 receptor single knockout mice, *Br J Pharmacol.* **156**, 1147-53.
24. Kurimoto, E., Matsuda, S., Shimizu, Y., Sako, Y., Mandai, T., Sugimoto, T., Sakamoto, H. & Kimura, H. (2018) An Approach to Discovering Novel Muscarinic M1 Receptor Positive Allosteric Modulators with Potent Cognitive Improvement and Minimized Gastrointestinal Dysfunction, *J Pharmacol Exp Ther.* **364**, 28-37.
25. Alt, A., Pendri, A., Bertekap, R. L., Jr., Li, G., Benitex, Y., Nophsker, M., Rockwell, K. L., Burford, N. T., Sum, C. S., Chen, J., Herbst, J. J., Ferrante, M., Hendricson, A., Cvijic, M. E., Westphal, R. S., O'Connell, J., Banks, M., Zhang, L., Gentles, R. G., Jenkins, S., Loy, J. & Macor, J. E. (2016) Evidence for Classical Cholinergic Toxicity Associated with Selective Activation of M1 Muscarinic Receptors, *J Pharmacol Exp Ther.* **356**, 293-304.
26. Davoren, J. E., Lee, C. W., Garnsey, M., Brodney, M. A., Cordes, J., Dlugolenski, K., Edgerton, J. R., Harris, A. R., Helal, C. J., Jenkinson, S., Kauffman, G. W., Kenakin, T. P., Lazzaro, J. T., Lotarski, S. M., Mao, Y., Nason, D. M., Northcott, C., Nottebaum, L., O'Neil, S. V., Pettersen, B., Popiolek, M., Reinhart, V., Salomon-Ferrer, R., Steyn, S. J., Webb, D., Zhang, L. & Grimwood, S. (2016) Discovery of the Potent and Selective M1 PAM-Agonist N-[(3R,4S)-3-Hydroxytetrahydro-2H-pyran-4-yl]-5-methyl-4-[4-(1,3-thiazol-4-yl)ben zyl]pyridine-2-carboxamide (PF-06767832): Evaluation of Efficacy and Cholinergic Side Effects, *J Med Chem.* **59**, 6313-28.
27. Rasmusson, D. D. (2000) The role of acetylcholine in cortical synaptic plasticity, *Behav Brain Res.* **115**, 205-18.
28. Blokland, A. (1995) Acetylcholine: a neurotransmitter for learning and memory?, *Brain Res Rev.* **21**, 285-300.
29. Lange, H. S., Cannon, C. E., Drott, J. T., Kuduk, S. D. & Uslaner, J. M. (2015) The M1 Muscarinic Positive Allosteric Modulator PQCA Improves Performance on

Translatable Tests of Memory and Attention in Rhesus Monkeys, *J Pharmacol Exp Ther.* **355**, 442-50.

30. Uslaner, J. M., Eddins, D., Puri, V., Cannon, C. E., Sutcliffe, J., Chew, C. S., Pearson, M., Vivian, J. A., Chang, R. K., Ray, W. J., Kuduk, S. D. & Wittmann, M. (2013) The muscarinic M1 receptor positive allosteric modulator PQCA improves cognitive measures in rat, cynomolgus macaque, and rhesus macaque, *Psychopharmacology (Berl).* **225**, 21-30.

31. Puri, V., Wang, X., Vardigan, J. D., Kuduk, S. D. & Uslaner, J. M. (2015) The selective positive allosteric M1 muscarinic receptor modulator PQCA attenuates learning and memory deficits in the Tg2576 Alzheimer's disease mouse model, *Behav Brain Res.* **287**, 96-9.

32. Bradley, S. J., Bourgognon, J. M., Sanger, H. E., Verity, N., Mogg, A. J., White, D. J., Butcher, A. J., Moreno, J. A., Molloy, C., Macedo-Hatch, T., Edwards, J. M., Wess, J., Pawlak, R., Read, D. J., Sexton, P. M., Broad, L. M., Steinert, J. R., Mallucci, G. R., Christopoulos, A., Felder, C. C. & Tobin, A. B. (2017) M1 muscarinic allosteric modulators slow prion neurodegeneration and restore memory loss, *J Clin Invest.* **127**, 487-499.

33. Sako, Y., Kurimoto, E., Mandai, T., Suzuki, A., Tanaka, M., Suzuki, M., Shimizu, Y., Yamada, M. & Kimura, H. (2019) TAK-071, a Novel M_1 Positive Allosteric Modulator with Low Cooperativity, Improves Cognitive Function in Rodents with Few Cholinergic Side Effects, *Neuropsychopharmacology.* **44**, 950-960.

34. Uslaner, J. M., Kuduk, S. D., Wittmann, M., Lange, H. S., Fox, S. V., Min, C., Pajkovic, N., Harris, D., Cilissen, C., Mahon, C., Mostoller, K., Warrington, S. & Beshore, D. C. (2018) Preclinical to Human Translational Pharmacology of the Novel M1 Positive Allosteric Modulator MK-7622, *J Pharmacol Exp Ther.* **365**, 556-566.

35. Beshore, D. C., C, N. D. M., Chang, R. K., Greshock, T. J., Ma, L., Wittmann, M., Seager, M. A., Koeplinger, K. A., Thompson, C. D., Fuerst, J., Hartman, G. D., Bilodeau, M. T., Ray, W. J. & Kuduk, S. D. (2018) MK-7622: A First-in-Class M1 Positive Allosteric Modulator Development Candidate, *ACS Med Chem Lett.* **9**, 652-656.

36. Voss, T., Li, J., Cummings, J., Farlow, M., Assaid, C., Froman, S., Leibensperger, H., Snow-Adami, L., McMahon, K. B., Egan, M. & Michelson, D. (2018) Randomized, controlled, proof-of-concept trial of MK-7622 in Alzheimer's disease, *Alzheimers Dement.*

4, 173-181.

37. Lim, Y., Kehm, V. M., Li, C., Trojanowski, J. Q. & Lee, V. M. (2010) Forebrain overexpression of alpha-synuclein leads to early postnatal hippocampal neuron loss and synaptic disruption, *Exp Neurol.* **221**, 86-97.

38. Lim, Y., Kehm, V. M., Lee, E. B., Soper, J. H., Li, C., Trojanowski, J. Q. & Lee, V. M. (2011) alpha-Syn suppression reverses synaptic and memory defects in a mouse model of dementia with Lewy bodies, *J Neurosci.* **31**, 10076-87.

39. Mayford, M., Bach, M. E., Huang, Y. Y., Wang, L., Hawkins, R. D. & Kandel, E. R. (1996) Control of memory formation through regulated expression of a CaMKII transgene, *Science.* **274**, 1678-83.

40. Sugimoto, T., Suzuki, S., Sakamoto, H., Yamada, M., Nakamura, M., Kamata, M., Shimokawa, K., Ogino, M., Kimura, E., Murakami, M., Yonemori, J. & Kojima, T. 2,3-dihydro-4h-1,3-benzoxazin-4-one derivatives as modulators of cholinergic muscarinic m1 receptor, *patent WO2016208775.* **2016 Dec 29**.

41. Lazareno, S. & Birdsall, N. J. (1995) Detection, quantitation, and verification of allosteric interactions of agents with labeled and unlabeled ligands at G protein-coupled receptors: interactions of strychnine and acetylcholine at muscarinic receptors, *Mol Pharmacol.* **48**, 362-78.

42. Hughes, R. N. (2004) The value of spontaneous alternation behavior (SAB) as a test of retention in pharmacological investigations of memory, *Neurosci Biobehav Rev.* **28**, 497-505.

43. Racine, R. J. (1972) Modification of seizure activity by electrical stimulation. II. Motor seizure, *Electroencephalogr Clin Neurophysiol.* **32**, 281-94.

44. Atack, J. R., Cook, S. M., Watt, A. P. & Ragan, C. I. (1992) Measurement of lithium-induced changes in mouse inositol(1)phosphate levels in vivo, *J Neurochem.* **59**, 1946-54.

45. Trinquet, E., Fink, M., Bazin, H., Grillet, F., Maurin, F., Bourrier, E., Ansanay, H., Leroy, C., Michaud, A., Durroux, T., Maurel, D., Malhaire, F., Goudet, C., Pin, J. P., Naval, M., Hernout, O., Chretien, F., Chapleur, Y. & Mathis, G. (2006) D-myo-inositol 1-phosphate as a surrogate of D-myo-inositol 1,4,5-tris phosphate to monitor G protein-coupled receptor activation, *Anal Biochem.* **358**, 126-35.

46. van Koppen, C. J. & Kaiser, B. (2003) Regulation of muscarinic acetylcholine

receptor signaling, *Pharmacol Ther.* **98**, 197-220.

47. Davis, A. A., Heilman, C. J., Brady, A. E., Miller, N. R., Fuerstenau-Sharp, M., Hanson, B. J., Lindsley, C. W., Conn, P. J., Lah, J. J. & Levey, A. I. (2010) Differential effects of allosteric M(1) muscarinic acetylcholine receptor agonists on receptor activation, arrestin 3 recruitment, and receptor downregulation, *ACS Chem Neurosci.* **1**, 542-551.

48. Thomas, R. L., Langmead, C. J., Wood, M. D. & Challiss, R. A. (2009) Contrasting effects of allosteric and orthosteric agonists on m1 muscarinic acetylcholine receptor internalization and down-regulation, *J Pharmacol Exp Ther.* **331**, 1086-95.

49. Vardigan, J. D., Cannon, C. E., Puri, V., Dancho, M., Koser, A., Wittmann, M., Kuduk, S. D., Renger, J. J. & Uslaner, J. M. (2015) Improved cognition without adverse effects: novel M1 muscarinic potentiator compares favorably to donepezil and xanomeline in rhesus monkey, *Psychopharmacology (Berl).* **232**, 1859-66.

50. Whitfield, D. R., Vallortigara, J., Alghamdi, A., Howlett, D., Hortobagyi, T., Johnson, M., Attems, J., Newhouse, S., Ballard, C., Thomas, A. J., O'Brien, J. T., Aarsland, D. & Francis, P. T. (2014) Assessment of ZnT3 and PSD95 protein levels in Lewy body dementias and Alzheimer's disease: association with cognitive impairment, *Neurobiol Aging.* **35**, 2836-2844.

51. Kramer, M. L. & Schulz-Schaeffer, W. J. (2007) Presynaptic alpha-synuclein aggregates, not Lewy bodies, cause neurodegeneration in dementia with Lewy bodies, *J Neurosci.* **27**, 1405-10.

52. Bereczki, E., Francis, P. T., Howlett, D., Pereira, J. B., Hoglund, K., Bogstedt, A., Cedazo-Minguez, A., Baek, J. H., Hortobagyi, T., Attems, J., Ballard, C. & Aarsland, D. (2016) Synaptic proteins predict cognitive decline in Alzheimer's disease and Lewy body dementia, *Alzheimers Dement.* **12**, 1149-1158.

53. Calderon, J., Perry, R. J., Erzinclioglu, S. W., Berrios, G. E., Dening, T. R. & Hodges, J. R. (2001) Perception, attention, and working memory are disproportionately impaired in dementia with Lewy bodies compared with Alzheimer's disease, *J Neurol Neurosurg Psychiatry.* **70**, 157-64.

54. Sahgal, A., Galloway, P. H., McKeith, I. G., Lloyd, S., Cook, J. H., Ferrier, I. N. & Edwardson, J. A. (1992) Matching-to-sample deficits in patients with senile dementias of the Alzheimer and Lewy body types, *Arch Neurol.* **49**, 1043-6.

55. Pagonabarraga, J., Kulisevsky, J., Llebaria, G., Garcia-Sanchez, C., Pascual-Sedano, B. & Gironell, A. (2008) Parkinson's disease-cognitive rating scale: a new cognitive scale specific for Parkinson's disease, *Mov Disord.* **23**, 998-1005.

56. Mori, E., Ikeda, M. & Kosaka, K. (2012) Donepezil for dementia with Lewy bodies: a randomized, placebo-controlled trial, *Ann Neurol.* **72**, 41-52.

57. Dubois, B., Tolosa, E., Katzenschlager, R., Emre, M., Lees, A. J., Schumann, G., Pourcher, E., Gray, J., Thomas, G., Swartz, J., Hsu, T. & Moline, M. L. (2012) Donepezil in Parkinson's disease dementia: a randomized, double-blind efficacy and safety study, *Mov Disord.* **27**, 1230-8.

58. Murakami, K., Watanabe, T., Koike, T., Kamata, M., Igari, T. & Kondo, S. (2016) Pharmacological properties of a novel and potent gamma-secretase modulator as a therapeutic option for the treatment of Alzheimer's disease, *Brain Res.* **1633**, 73-86.

59. Nagakura, A., Shitaka, Y., Yarimizu, J. & Matsuoka, N. (2013) Characterization of cognitive deficits in a transgenic mouse model of Alzheimer's disease and effects of donepezil and memantine, *Eur J Pharmacol.* **703**, 53-61.

60. Davie, B. J., Christopoulos, A. & Scammells, P. J. (2013) Development of M1 mAChR allosteric and bitopic ligands: prospective therapeutics for the treatment of cognitive deficits, *ACS Chem Neurosci.* **4**, 1026-48.

61. Teles-Grilo Ruivo, L. M., Baker, K. L., Conway, M. W., Kinsley, P. J., Gilmour, G., Phillips, K. G., Isaac, J. T. R., Lowry, J. P. & Mellor, J. R. (2017) Coordinated Acetylcholine Release in Prefrontal Cortex and Hippocampus Is Associated with Arousal and Reward on Distinct Timescales, *Cell Rep.* **18**, 905-917.

62. Howe, W. M., Gritton, H. J., Lusk, N. A., Roberts, E. A., Hetrick, V. L., Berke, J. D. & Sarter, M. (2017) Acetylcholine Release in Prefrontal Cortex Promotes Gamma Oscillations and Theta-Gamma Coupling during Cue Detection, *J Neurosci.* **37**, 3215-3230.

63. Moran, S. P., Dickerson, J. W., Cho, H. P., Xiang, Z., Maksymetz, J., Remke, D. H., Lv, X., Doyle, C. A., Rajan, D. H., Niswender, C. M., Engers, D. W., Lindsley, C. W., Rook, J. M. & Conn, P. J. (2018) M1-positive allosteric modulators lacking agonist activity provide the optimal profile for enhancing cognition, *Neuropsychopharmacology.* **43**, 1763-1771.

64. Bradley, S. J., Molloy, C., Bundgaard, C., Mogg, A. J., Thompson, K. J., Dwomoh,

L., Sanger, H. E., Crabtree, M. D., Brooke, S. M., Sexton, P. M., Felder, C. C., Christopoulos, A., Broad, L. M., Tobin, A. B. & Langmead, C. J. (2018) Bitopic Binding Mode of an M1 Muscarinic Acetylcholine Receptor Agonist Associated with Adverse Clinical Trial Outcomes, *Mol Pharmacol.* **93**, 645-656.

65. Moran, S. P., Cho, H. P., Maksymetz, J., Remke, D. H., Hanson, R. M., Niswender, C. M., Lindsley, C. W., Rook, J. M. & Conn, P. J. (2018) PF-06827443 Displays Robust Allosteric Agonist and Positive Allosteric Modulator Activity in High Receptor Reserve and Native Systems, *ACS Chem Neurosci.* **9**, 2218-2224.

66. Chesselet, M. F. & Richter, F. (2011) Modelling of Parkinson's disease in mice, *Lancet Neurol.* **10**, 1108-18.

67. Fibiger, H. C. (1991) Cholinergic mechanisms in learning, memory and dementia: a review of recent evidence, *Trends Neurosci.* **14**, 220-3.

68. Whitehouse, P. J., Price, D. L., Struble, R. G., Clark, A. W., Coyle, J. T. & Delon, M. R. (1982) Alzheimer's disease and senile dementia: loss of neurons in the basal forebrain, *Science.* **215**, 1237-9.

69. McKeith, I. G., Galasko, D., Kosaka, K., Perry, E. K., Dickson, D. W., Hansen, L. A., Salmon, D. P., Lowe, J., Mirra, S. S., Byrne, E. J., Lennox, G., Quinn, N. P., Edwardson, J. A., Ince, P. G., Bergeron, C., Burns, A., Miller, B. L., Lovestone, S., Collerton, D., Jansen, E. N., Ballard, C., de Vos, R. A., Wilcock, G. K., Jellinger, K. A. & Perry, R. H. (1996) Consensus guidelines for the clinical and pathologic diagnosis of dementia with Lewy bodies (DLB): report of the consortium on DLB international workshop, *Neurology.* **47**, 1113-24.

70. Crook, J. M., Tomaskovic-Crook, E., Copolov, D. L. & Dean, B. (2000) Decreased muscarinic receptor binding in subjects with schizophrenia: a study of the human hippocampal formation, *Biol Psychiatry.* **48**, 381-8.

71. Crook, J. M., Tomaskovic-Crook, E., Copolov, D. L. & Dean, B. (2001) Low muscarinic receptor binding in prefrontal cortex from subjects with schizophrenia: a study of Brodmann's areas 8, 9, 10, and 46 and the effects of neuroleptic drug treatment, *Am J Psychiatry.* **158**, 918-25.

72. el-Mallakh, R. S., Kirch, D. G., Shelton, R., Fan, K. J., Pezeshkpour, G., Kanhouwa, S., Wyatt, R. J. & Kleinman, J. E. (1991) The nucleus basalis of Meynert, senile plaques, and intellectual impairment in schizophrenia, *J Neuropsychiatry Clin Neurosci.* **3**, 383-6.

73. Domino, E. F., Krause, R. R. & Bowers, J. (1973) Various enzymes involved with putative neurotransmitters. Regional distribution in the brain of deceased mentally normal, chronic schizophrenics or organic brain syndrome patients, *Arch Gen Psychiatry.* **29**, 195-201.

74. Haroutunian, V., Davidson, M., Kanof, P. D., Perl, D. P., Powchik, P., Losonczy, M., McCrystal, J., Purohit, D. P., Bierer, L. M. & Davis, K. L. (1994) Cortical cholinergic markers in schizophrenia, *Schizophr Res.* **12**, 137-44.

75. Thal, L. J., Forrest, M., Loft, H. & Mengel, H. (2000) Lu 25-109, a muscarinic agonist, fails to improve cognition in Alzheimer's disease. Lu25-109 Study Group, *Neurology.* **54**, 421-6.

76. Wienrich, M., Ceci, A., Ensinger, H. A., Gaida, W., Mendla, K. D., Osugi, T., Raschig, A. & Weiser, T. (2002) Talsaclidine (WAL 2014 FU), a muscarinic M1 receptor agonist for the treatment of Alzheimer's disease, *Drug Dev Res.* **56**, 321-334.

77. Heidrich, A. & Rösler, M. (1999) Milameline: Nonselective, Partial Muscarinic Receptor Agonist for the Treatment of Alzheimer's Disease?, *Drug Dev Res.* **5**, 93-104.

78. Bymaster, F. P., Whitesitt, C. A., Shannon, H. E., DeLapp, N., Ward, J. S., Calligaro, D. O., Shipley, L. A., Buelke-Sam, J. L., Bodick, N. C., Farde, L., Sheardown, M. J., Olesen, P. H., Hansen, K. T., Suzdak, P. D., Swedberg, M. D., Sauerberg, P. & Mitch, C. H. (1997) Xanomeline: A selective muscarinic agonist for the treatment of Alzheimer's disease, *Drug Dev Res.* **40**, 158-170.

79. Watson, J., Brough, S., Coldwell, M. C., Gager, T., Ho, M., Hunter, A. J., Jerman, J., Middlemiss, D. N., Riley, G. J. & Brown, A. M. (1998) Functional effects of the muscarinic receptor agonist, xanomeline, at 5-HT1 and 5-HT2 receptors, *Br J Pharmacol.* **125**, 1413-20.

80. Woolley, M. L., Carter, H. J., Gartlon, J. E., Watson, J. M. & Dawson, L. A. (2009) Attenuation of amphetamine-induced activity by the non-selective muscarinic receptor agonist, xanomeline, is absent in muscarinic M4 receptor knockout mice and attenuated in muscarinic M1 receptor knockout mice, *Eur J Pharmacol.* **603**, 147-9.

81. Ghoshal, A., Rook, J. M., Dickerson, J. W., Roop, G. N., Morrison, R. D., Jalan-Sakrikar, N., Lamsal, A., Noetzel, M. J., Poslusney, M. S., Wood, M. R., Melancon, B. J., Stauffer, S. R., Xiang, Z., Daniels, J. S., Niswender, C. M., Jones, C. K., Lindsley, C. W. & Conn, P. J. (2016) Potentiation of M1 Muscarinic Receptor Reverses Plasticity Deficits

and Negative and Cognitive Symptoms in a Schizophrenia Mouse Model, *Neuropsychopharmacology.* **41**, 598-610.

82. Xiu, J., Zhang, Q., Zhou, T., Zhou, T. T., Chen, Y. & Hu, H. (2014) Visualizing an emotional valence map in the limbic forebrain by TAI-FISH, *Nat Neurosci.* **17**, 1552-9.

83. Clayton, D. F. (2000) The genomic action potential, *Neurobiol Learn Mem.* **74**, 185-216.

84. Lein, E. S.Hawrylycz, M. J.Ao, N.Ayres, M.Bensinger, A.Bernard, A.Boe, A. F.Boguski, M. S.Brockway, K. S.Byrnes, E. J.Chen, L.Chen, T. M.Chin, M. C.Chong, J.Crook, B. E.Czaplinska, A.Dang, C. N.Datta, S.Dee, N. R.Desaki, A. L.Desta, T.Diep, E.Dolbeare, T. A.Donelan, M. J.Dong, H. W.Dougherty, J. G.Duncan, B. J.Ebbert, A. J.Eichele, G.Estin, L. K.Faber, C.Facer, B. A.Fields, R.Fischer, S. R.Fliss, T. P.Frensley, C.Gates, S. N.Glattfelder, K. J.Halverson, K. R.Hart, M. R.Hohmann, J. G.Howell, M. P.Jeung, D. P.Johnson, R. A.Karr, P. T.Kawal, R.Kidney, J. M.Knapik, R. H.Kuan, C. L.Lake, J. H.Laramee, A. R.Larsen, K. D.Lau, C.Lemon, T. A.Liang, A. J.Liu, Y.Luong, L. T.Michaels, J.Morgan, J. J.Morgan, R. J.Mortrud, M. T.Mosqueda, N. F.Ng, L. L.Ng, R.Orta, G. J.Overly, C. C.Pak, T. H.Parry, S. E.Pathak, S. D.Pearson, O. C.Puchalski, R. B.Riley, Z. L.Rockett, H. R.Rowland, S. A.Royall, J. J.Ruiz, M. J.Sarno, N. R.Schaffnit, K.Shapovalova, N. V.Sivisay, T.Slaughterbeck, C. R.Smith, S. C.Smith, K. A.Smith, B. I.Sodt, A. J.Stewart, N. N.Stumpf, K. R.Sunkin, S. M.Sutram, M.Tam, A.Teemer, C. D.Thaller, C.Thompson, C. L.Varnam, L. R.Visel, A.Whitlock, R. M.Wohnoutka, P. E.Wolkey, C. K.Wong, V. Y.Wood, M., et al. (2007) Genome-wide atlas of gene expression in the adult mouse brain, *Nature.* **445**, 168-76.

85. Jones, C. A., Watson, D. J. & Fone, K. C. (2011) Animal models of schizophrenia, *Br J Pharmacol.* **164**, 1162-94.

86. Trinquet, E., Bouhelal, R. & Dietz, M. (2011) Monitoring Gq-coupled receptor response through inositol phosphate quantification with the IP-One assay, *Expert Opin Drug Discov.* **6**, 981-94.

87. Bartolomeo, A. C., Morris, H., Buccafusco, J. J., Kille, N., Rosenzweig-Lipson, S., Husbands, M. G., Sabb, A. L., Abou-Gharbia, M., Moyer, J. A. & Boast, C. A. (2000) The preclinical pharmacological profile of WAY-132983, a potent M1 preferring agonist, *J Pharmacol Exp Ther.* **292**, 584-96.

88. Abe, Y., Aoyagi, A., Hara, T., Abe, K., Yamazaki, R., Kumagae, Y., Naruto, S.,

Koyama, K., Marumoto, S., Tago, K., Toda, N., Takami, K., Yamada, N., Ori, M., Kogen, H. & Kaneko, T. (2003) Pharmacological characterization of RS-1259, an orally active dual inhibitor of acetylcholinesterase and serotonin transporter, in rodents: possible treatment of Alzheimer's disease, *J Pharmacol Sci.* **93**, 95-105.

89. Murai, T., Okuda, S., Tanaka, T. & Ohta, H. (2007) Characteristics of object location memory in mice: Behavioral and pharmacological studies, *Physiol Behav.* **90**, 116-24.

90. Kang, S. Y., Lee, K. Y., Koo, K. A., Yoon, J. S., Lim, S. W., Kim, Y. C. & Sung, S. H. (2005) ESP-102, a standardized combined extract of Angelica gigas, Saururus chinensis and Schizandra chinensis, significantly improved scopolamine-induced memory impairment in mice, *Life Sci.* **76**, 1691-705.

91. Mirza, N. R., Peters, D. & Sparks, R. G. (2003) Xanomeline and the antipsychotic potential of muscarinic receptor subtype selective agonists, *CNS Drug Rev.* **9**, 159-86.

92. Perry, K. W., Nisenbaum, L. K., George, C. A., Shannon, H. E., Felder, C. C. & Bymaster, F. P. (2001) The muscarinic agonist xanomeline increases monoamine release and immediate early gene expression in the rat prefrontal cortex, *Biol Psychiatry.* **49**, 716-25.

93. Byun, N. E., Grannan, M., Bubser, M., Barry, R. L., Thompson, A., Rosanelli, J., Gowrishankar, R., Kelm, N. D., Damon, S., Bridges, T. M., Melancon, B. J., Tarr, J. C., Brogan, J. T., Avison, M. J., Deutch, A. Y., Wess, J., Wood, M. R., Lindsley, C. W., Gore, J. C., Conn, P. J. & Jones, C. K. (2014) Antipsychotic drug-like effects of the selective M4 muscarinic acetylcholine receptor positive allosteric modulator VU0152100, *Neuropsychopharmacology.* **39**, 1578-93.

94. Poulin, S. P., Dautoff, R., Morris, J. C., Barrett, L. F. & Dickerson, B. C. (2011) Amygdala atrophy is prominent in early Alzheimer's disease and relates to symptom severity, *Psychiatry Res.* **194**, 7-13.

95. Du, A. T., Schuff, N., Amend, D., Laakso, M. P., Hsu, Y. Y., Jagust, W. J., Yaffe, K., Kramer, J. H., Reed, B., Norman, D., Chui, H. C. & Weiner, M. W. (2001) Magnetic resonance imaging of the entorhinal cortex and hippocampus in mild cognitive impairment and Alzheimer's disease, *J Neurol Neurosurg Psychiatry.* **71**, 441-7.

96. Mizuno, K., Wakai, M., Takeda, A. & Sobue, G. (2000) Medial temporal atrophy and memory impairment in early stage of Alzheimer's disease: an MRI volumetric and memory assessment study, *J Neurol Sci.* **173**, 18-24.

97. Mosconi, L., Pupi, A., De Cristofaro, M. T., Fayyaz, M., Sorbi, S. & Herholz, K. (2004) Functional interactions of the entorhinal cortex: an 18F-FDG PET study on normal aging and Alzheimer's disease, *J Nucl Med.* **45**, 382-92.

98. Nestor, P. J., Fryer, T. D., Smielewski, P. & Hodges, J. R. (2003) Limbic hypometabolism in Alzheimer's disease and mild cognitive impairment, *Ann Neurol.* **54**, 343-51.

99. Hazlett, E. A., Buchsbaum, M. S., Jeu, L. A., Nenadic, I., Fleischman, M. B., Shihabuddin, L., Haznedar, M. M. & Harvey, P. D. (2000) Hypofrontality in unmedicated schizophrenia patients studied with PET during performance of a serial verbal learning task, *Schizophr Res.* **43**, 33-46.

100. Millan, M. J., Agid, Y., Brune, M., Bullmore, E. T., Carter, C. S., Clayton, N. S., Connor, R., Davis, S., Deakin, B., DeRubeis, R. J., Dubois, B., Geyer, M. A., Goodwin, G. M., Gorwood, P., Jay, T. M., Joels, M., Mansuy, I. M., Meyer-Lindenberg, A., Murphy, D., Rolls, E., Saletu, B., Spedding, M., Sweeney, J., Whittington, M. & Young, L. J. (2012) Cognitive dysfunction in psychiatric disorders: characteristics, causes and the quest for improved therapy, *Nat Rev Drug Discov.* **11**, 141-68.

101. Grannan, M. D., Mielnik, C. A., Moran, S. P., Gould, R. W., Ball, J., Lu, Z., Bubser, M., Ramsey, A. J., Abe, M., Cho, H. P., Nance, K. D., Blobaum, A. L., Niswender, C. M., Conn, P. J., Lindsley, C. W. & Jones, C. K. (2016) Prefrontal Cortex-Mediated Impairments in a Genetic Model of NMDA Receptor Hypofunction Are Reversed by the Novel M1 PAM VU6004256, *ACS Chem Neurosci.* **7**, 1706-1716.

102. Arnt, J. & Skarsfeldt, T. (1998) Do novel antipsychotics have similar pharmacological characteristics? A review of the evidence, *Neuropsychopharmacology.* **18**, 63-101.

103. Stanhope, K. J., Mirza, N. R., Bickerdike, M. J., Bright, J. L., Harrington, N. R., Hesselink, M. B., Kennett, G. A., Lightowler, S., Sheardown, M. J., Syed, R., Upton, R. L., Wadsworth, G., Weiss, S. M. & Wyatt, A. (2001) The muscarinic receptor agonist xanomeline has an antipsychotic-like profile in the rat, *J Pharmacol Exp Ther.* **299**, 782-92.

104. Shannon, H. E., Rasmussen, K., Bymaster, F. P., Hart, J. C., Peters, S. C., Swedberg, M. D., Jeppesen, L., Sheardown, M. J., Sauerberg, P. & Fink-Jensen, A. (2000) Xanomeline, an M(1)/M(4) preferring muscarinic cholinergic receptor agonist, produces

antipsychotic-like activity in rats and mice, *Schizophr Res.* **42**, 249-59.

105. Wikenheiser, A. M. & Schoenbaum, G. (2016) Over the river, through the woods: cognitive maps in the hippocampus and orbitofrontal cortex, *Nat Rev Neurosci.* **17**, 513-23.

106. Schobel, S. A., Kelly, M. A., Corcoran, C. M., Van Heertum, K., Seckinger, R., Goetz, R., Harkavy-Friedman, J. & Malaspina, D. (2009) Anterior hippocampal and orbitofrontal cortical structural brain abnormalities in association with cognitive deficits in schizophrenia, *Schizophr Res.* **114**, 110-8.

107. Pantelis, C., Velakoulis, D., McGorry, P. D., Wood, S. J., Suckling, J., Phillips, L. J., Yung, A. R., Bullmore, E. T., Brewer, W., Soulsby, B., Desmond, P. & McGuire, P. K. (2003) Neuroanatomical abnormalities before and after onset of psychosis: a cross-sectional and longitudinal MRI comparison, *Lancet.* **361**, 281-8.

108. Crick, F. C. & Koch, C. (2005) What is the function of the claustrum?, *Philos Trans R Soc Lond B Biol Sci.* **360**, 1271-9.

109. Morys, J., Bobinski, M., Wegiel, J., Wisniewski, H. M. & Narkiewicz, O. (1996) Alzheimer's disease severely affects areas of the claustrum connected with the entorhinal cortex, *J Hirnforsch.* **37**, 173-80.

110. Girard-Joyal, O., Faragher, A., Bradley, K., Kane, L., Hrycyk, L. & Ismail, N. (2015) Age and sex differences in c-Fos expression and serum corticosterone concentration following LPS treatment, *Neuroscience.* **305**, 293-301.

111. Procaccini, C., Maksimovic, M., Aitta-Aho, T., Korpi, E. R. & Linden, A. M. (2013) Reversal of novelty-induced hyperlocomotion and hippocampal c-Fos expression in GluA1 knockout male mice by the mGluR2/3 agonist LY354740, *Neuroscience.* **250**, 189-200.

112. Stanisavljevic, A., Peric, I., Gass, P., Inta, D., Lang, U. E., Borgwardt, S. & Filipovic, D. (2019) Brain Sub/Region-Specific Effects of Olanzapine on c-Fos Expression of Chronically Socially Isolated Rats, *Neuroscience.* **396**, 46-65.

113. Filipovic, D., Stanisavljevic, A., Jasnic, N., Bernardi, R. E., Inta, D., Peric, I. & Gass, P. (2018) Chronic Treatment with Fluoxetine or Clozapine of Socially Isolated Rats Prevents Subsector-Specific Reduction of Parvalbumin Immunoreactive Cells in the Hippocampus, *Neuroscience.* **371**, 384-394.

114. Hitti, F. L. & Siegelbaum, S. A. (2014) The hippocampal CA2 region is essential

for social memory, *Nature.* **508**, 88-92.

115. Benes, F. M., Kwok, E. W., Vincent, S. L. & Todtenkopf, M. S. (1998) A reduction of nonpyramidal cells in sector CA2 of schizophrenics and manic depressives, *Biol Psychiatry.* **44**, 88-97.

116. Kim, Y., Venkataraju, K. U., Pradhan, K., Mende, C., Taranda, J., Turaga, S. C., Arganda-Carreras, I., Ng, L., Hawrylycz, M. J., Rockland, K. S., Seung, H. S. & Osten, P. (2015) Mapping social behavior-induced brain activation at cellular resolution in the mouse, *Cell Rep.* **10**, 292-305.

117. Paxinos, G. & Franklin, K. B. J. (2001) The Mouse Brain in Stereotactic Coordinates (2 nd Edition), *Academic Press, Inc: San Diego*.

118. Maeda, S., Xu, J., FM, N. K., Clark, M. J., Zhao, J., Tsutsumi, N., Aoki, J., Sunahara, R. K., Inoue, A., Garcia, K. C. & Kobilka, B. K. (2020) Structure and selectivity engineering of the M1 muscarinic receptor toxin complex, *Science.* **369**, 161-167.

119. Maeda, S., Qu, Q., Robertson, M. J., Skiniotis, G. & Kobilka, B. K. (2019) Structures of the M1 and M2 muscarinic acetylcholine receptor/G-protein complexes, *Science.* **364**, 552-557.

120. Bakker, G., Vingerhoets, C., Boucherie, D., Caan, M., Bloemen, O., Eersels, J., Booij, J. & van Amelsvoort, T. (2018) Relationship between muscarinic M1 receptor binding and cognition in medication-free subjects with psychosis, *Neuroimage Clin.* **18**, 713-719.

121. Marino, M. J., Rouse, S. T., Levey, A. I., Potter, L. T. & Conn, P. J. (1998) Activation of the genetically defined m1 muscarinic receptor potentiates N-methyl-D-aspartate (NMDA) receptor currents in hippocampal pyramidal cells, *Proc Natl Acad Sci U S A.* **95**, 11465-70.

122. Davoren, J. E., Garnsey, M., Pettersen, B., Brodney, M. A., Edgerton, J. R., Fortin, J. P., Grimwood, S., Harris, A. R., Jenkinson, S., Kenakin, T., Lazzaro, J. T., Lee, C. W., Lotarski, S. M., Nottebaum, L., O'Neil, S. V., Popiolek, M., Ramsey, S., Steyn, S. J., Thorn, C. A., Zhang, L. & Webb, D. (2017) Design and Synthesis of gamma- and delta-Lactam M1 Positive Allosteric Modulators (PAMs): Convulsion and Cholinergic Toxicity of an M1-Selective PAM with Weak Agonist Activity, *J Med Chem.* **60**, 6649-6663.

123. Gautam, D., Heard, T. S., Cui, Y., Miller, G., Bloodworth, L. & Wess, J. (2004)

Cholinergic stimulation of salivary secretion studied with M1 and M3 muscarinic receptor single- and double-knockout mice, *Mol Pharmacol.* **66**, 260-7.